TÉCNICO
LISBOA

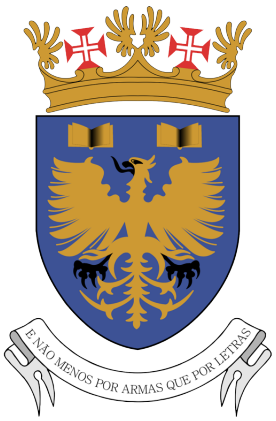

Efficient Evidence Accumulation Clustering for large datasets/big data

Diogo Alexandre Oliveira Silva

Thesis to obtain the Master of Science Degree in

Electrical and Computer Engineering

Supervisors: Dra. Ana Luísa Nobre Fred
Dra. Helena Isabel Aidos Lopes

Examination Committee

Chairperson: Prof. Dr. João Fernando Cardoso Silva Sequeira
Supervisor: Dra. Ana Luísa Nobre Fred
Members of the Committee: Dr. Pedro Filipe Zeferino Tomás
BGEN ENGEL José Manuel dos Santos Vicêncio
TCOR ENGEL Ana Paula da Silva Jorge

December 2015

Acknowledgments

It would come as a great oversight if I was not aware of the help and contribution I received for the completion of this undertaking.

I should start by expressing deep appreciation to my supervisors, Dr. Ana Fred and Dr. Helena Lopes. The freedom I was allowed was crucial for keeping my motivation up for such a long period. When that was lacking, their guidance and encouragement quickly put me back on track.

I leave my warmest regards to the family I built throughout my military and academic career, during these last years. Your camaraderie has shaped where I stand and who I am today. Your support throughout these long months was invaluable.

To my loving girlfriend, who would always hear my boundless enthusiasm or disheartening frustrations, whichever was the case, and who followed me closest in the last months, I am deeply grateful. You motivated me most of all, and that was no small task.

And to my parents, thank you for all your support and motivation during all these years. You were always caring and encouraging and I am forever grateful for that.

Last, but not least, thank you to all my friends and family for understanding my absence during these challenging months.

Resumo

Avanços na tecnologia permitem a recolha e armazenamento de quantidades e variedades de dados sem precedente. A maior parte destes dados são armazenados eletrónicamente e existe interesse em realizar análise automática dos mesmos. As técnicas de *clustering* estão entre as mais populares para essa tarefa porque não assumem nada sobre a estrutura dos dados *a priori*. Muitas técnicas existem, mas, típicamente, não têm um bom desempenho em todos os conjuntos de dados devido às especifidades de cada um. Técnicas de *ensemble clustering* tentam responder a esse desafio ao combinar outros algoritmos. Esta dissertação foca-se numa em particular, o *Evidence Accumulation Clustering* (EAC). O EAC é uma algorithm robusto que tem demonstrado bons desempenhos na literatura numa variedade de conjuntos de dados. No entanto, esta robustez vem com um maior custo computacional associado. A sua aplicação não só é mais lenta como está restrita a conjuntos de dados pequenos. Assim, o objetivo desta dissertação é escalar o EAC, possibilitando a sua a aplicação a conjuntos de dados grandes, com tecnologia disponivel numa típica estação de trabalho. Com isto em mente, várias abordagens foram exploradas: acelerar processamento com outros algoritmos (*quantum clustering*), através de processamento paralelo (com GPU), escalar com algoritmos de memória externa (disco rígido) e explorando a natureza esparsa do EAC. Além disto, foi desenvolvido um método eficiente para construir uma matriz esparsa específico ao EAC. A solução proposta é aplicável a conjuntos de dados grandes e é entre 6 a 200 vezes mais rápida que a original para conjuntos pequenos.

Palavras-chave: Métodos de agrupamento, EAC, K-Means, MST, GPGPU, CUDA, Matrizes esparsas, Single-Link

Abstract

Advances in technology allow for the collection and storage of an unprecedent amount and variety of data. Most of this data is stored electronically and there is an interest in automated analysis for generation of knowledge and new insights. Since the structure of the data is unknown, clustering techniques become particularly interesting for knowledge discovery and data mining, as they make as few assumptions on the data as possible. A vast body of work on these algorithms exist, yet, typically, no single algorithm is able to respond to the specificities of all data. Ensemble clustering algorithm address this problem by combining other algorithms. Evidence Accumulation Clustering (EAC) is a robust ensemble algorithm that has shown good results and is the focus of this dissertation. However, this robustness comes with higher computational cost. Its application is slower and restricted to smaller datasets. Thus, the objective of this dissertation is to scale EAC, allowing its applicability to big datasets, with technology available at a typical workstation. Accordingly, several approaches were explored: speed-up with other algorithms (*quantum clustering*) or parallel computing (with GPU) and reducing space complexity by using external memory (hard drive) algorithms and exploiting the sparse nature of EAC. A relevant contribution is a novel method to build a sparse matrix specialized in EAC. Results show that the proposed solution is applicable to large datasets and presents speed-ups between 6 and 200 over the original implementation on different phases of EAC for small datasets.

Key words: Clustering methods, EAC, K-Means, MST, GPGPU, CUDA, Sparse matrices, Single-Link

Contents

List of Tables

List of Figures

Glossary

API	Application Programming Interface
CPU	Central Processing Unit
EAC	Evidence Accumulation Clustering
FCM	Fuzzy C-Means
GPGPU	General Purpose computing in Graphics Processing Units
GPU	Graphics Processing Unit
HAC	Hierarchical Agglomeration Clustering
MST	Minimum Spanning Tree
PCA	Principal Component Analysis
PC	Principal Component
QC	Quantum clustering
QK-Means	Quantum K-Means
Qubit	Quantum bit
SL-MST	Single-Link based on Minimum Spanning Tree
SL	Single Link
WEAC	Weighted Evidence Accumulation Clustering

Chapter 1

Introduction

1.1 Challenges and Motivation

Advances in technology allow for the collection and storage of unprecedented amount and variety of data, a concept commonly designated by *Big Data*. Most of this data is stored electronically and there is an interest in automated analysis for generation of knowledge and new insights. The applications of such analysis are abundant and across many fields, ranging from recommender systems and customer segmentation in business, to predicting when a jet engine is likely to fail using sensor data, or even the study of gene expression in biomedics, to name a few.

A growing body of formal methods aiming to model, structure and/or classify data already exist, e.g. linear regression, principal component analysis, cluster analysis, support vector machines, neural networks. Cluster analysis is an interesting tool because it typically does not make assumptions on the structure of the data. Since, often, the structure of the data is unknown, clustering techniques become particularly interesting for transforming this data into knowledge and discovering its underlying structure and patterns. Clustering is a hard problem and a vast body of work on these algorithms exist. Yet, typically, no single algorithm is able to respond to the specificities of all data. Different methods are suited to datasets of different characteristics and, often, the challenge of the researcher is to find the right algorithm for the task.

Currently, there are state of the art algorithms that are more robust than ”traditional” algorithms by having a wider applicability or being less dependent on input parameters, e.g. algorithms that do not take any parameters for performing an analysis. One such approach is Evidence Accumulation Clustering (EAC), belonging to the wider class of ensemble methods. EAC is a state-of-the art clustering method that addresses the robustness challenge. However, the current reality of capturing massive amounts of data rises new challenges. Two important challenges are efficiency and scalability, which translate on how fast the algorithms are and how well they scale when the input data multiplies in size, dimensionality and variety. The algorithms themselves are no longer the only focus of research. Much effort is being put into the scalability and performance of algorithms, which usually translates in addressing their computational complexity with parallelized computation and distributed memory being

some of the proposed solutions. Cluster analysis with EAC should be fast and able to scale to larger datasets as well as robust, so as to address the reality of big data.

This dissertation is concerned with pushing the current limits of the EAC to large datasets by addressing the problems of scalability and efficiency without compromising robustness, using technology available in a workstations. Processing of huge amounts of data has been out of the range of capability of the traditional workstations. This sprouted the rise of new uses of existing computing architectures (e.g. Graphic Processing Units) and development of new programming models (e.g. Hadoop, shared and distributed memory). The problem at hand is, then, to optimize the algorithm regarding both speed and memory usage. This, of course, comes with challenges. How can one keep the original accuracy while significantly increase efficiency? Is there an exploitable trade-off between the three main characteristics: speed, memory and accuracy? These are guiding questions that this dissertation addresses.

1.2 Goals

This dissertation aims to research and extend the state of the art of ensemble clustering, in what concerns the EAC method and its application to large datasets, while also assessing algorithmic solutions and parallelization techniques. The goal is to understand EAC's suitability for large datasets and find ways to respond to the stated challenges, in terms of speed and memory. The main objectives for this work are:

- Study the integration of quantum inspired methods in EAC.
- Study the integration of the General Purpose computing in a Graphics Processing Unit (GPGPU) paradigm in EAC.
- Devise strategies to reduce computation and memory complexities of EAC.
- Application of Evidence Accumulation Clustering to Big Data.
- Validation of Big Data EAC on real data.
- Application of EAC to real-world large datasets.

1.3 Contributions

The main contributions are the adaptation of the three distinct stages of the EAC framework to larger datasets. In particular, an efficient parallel version for Graphics Processing Units (GPU) of the K-Means clustering algorithm is implemented for the first stage of EAC. Still in this stage, two clustering algorithms in the young field of Quantum Clustering were reviewed, tested and evaluated having EAC in mind. Different methods for the second stage were tested, using complete matrices and sparse matrices.Worthy of mention is a novel and specialized method for building a sparse matrix in the second stage. A GPU parallel version of a MST (Minimum Spanning Tree) solver algorithm was reviewed and tested for the

last stage, a co-product of which was an algorithm to find the connected components of a MST. A hard disk solution was implemented for dealing with large datasets whose space complexity in the final stage exceeded the available memory.

Selected work from the present dissertation was compiled into a conference paper and submitted to the 5^{th} The International Conference on Pattern Recognition Applications and Methods.

1.4 Outline

Chapter 2 provides an introduction to clustering nomenclature and concepts, as well as some ”traditional” clustering algorithms. Chapter 3 starts by reviewing the Evidence Accumulation Clustering algorithm in detail. It goes on to review possible approaches to the problem of scaling EAC. Based on an algorithmic approach, a review of the young field of quantum clustering is presented, with a more in-depth emphasis on two algorithms. With a parallelization approach in mind, a programming model for the GPU (CUDA) is reviewed, followed by some parallelized versions of relevant algorithms to the problem of this dissertation. The following chapter, 4, presents the approach that was actually taken to scale EAC. It presents the steps taken on each part of the algorithm, the underlying difficulties and what was done to address them. It also includes the reference of approaches that were developed but were not deemed suited to integrate the EAC toolchain. Chapter 5 presents the results of the different approaches for optimizing the EAC method and critical discussion of those results. Finally, chapter 6 concludes the dissertation. It also offers recommendations for future work.

Chapter 2

Clustering: basic concepts, definitions and algorithms

Hundreds of methods for data analysis exist. Many of these methods fall into the realm of machine learning, which is usually divided into 2 major groups: *supervised* and *unsupervised* learning. Supervised learning deals with labeled data, i.e. data for which the ground truth is known, and tries to solve the problem of classification. Examples of supervised learning algorithms are Neural Networks, Decision Trees, Linear Regression and Support Vector Machines. Unsupervised learning deals with unlabeled data for which no extra information is known. Clustering methods are an example of unsupervised methods and are the focus of this chapter.

This chapter will serve as an introduction to clustering. It starts by defining the problem of clustering in section 2.1, goes on to provide useful definitions and notation in section 2.2 and briefly addresses different properties of clustering algorithms in section 2.3. Two very well known algorithms are presented: K-Means in section 2.4 and Single-Link in section 2.5. Evidence Accumulation Clustering is a state of the art ensemble clustering algorithm and the focus of this dissertation. Section 2.6 will explain briefly the concept of ensemble clustering followed by an overview and application examples of the EAC algorithm in section 2.7.

2.1 The problem of clustering

Cluster analysis methods are unsupervised and the backbone of the present work. The goal of data clustering, as defined by [1], is the discovery of the *natural grouping(s)* of a set of patterns, points or objects. In other words, the goal of data clustering is to discover structure on data. The methodology used is to group patterns (usually represented as a vector of measurements or a point in space [2]) based on some similarity, such that patterns belonging to the same cluster are typically more similar to each other than to patterns of other clusters. Clustering is a strictly data-driven method, in contrast with classification techniques which have a training set with the desired labels for a limited collection of patterns. Because there is very little information, as few assumptions as possible should be made

about the structure of the data (e.g. number of clusters). Also, because clustering typically makes as few assumptions on the data as possible, it is appropriate to use it on exploratory data analysis. The process of clustering data has three main aspects [2]:

- **Pattern representation** refers to the choice of representation of the input data in terms of size, scale and type of features. The input patterns may be fed directly to the algorithms or undergo *feature selection* and/or *feature extraction*. The former is simply the selection of which features should be used. The latter deals with the transformation of the original feature space such that the resulting space will produce more accurate and insightful clusterings, e.g. by applying Principal Component Analysis.
- **Pattern similarity** refers to the definition of a measure for computing the similarity between two patterns.
- **Grouping** refers to the algorithm that will perform the actual clustering on the dataset with the defined pattern representation, using the appropriate similarity measure.

As an example, Figure 2.1a shows the plot of the Iris dataset [3, 4], a small well-known Machine Learning dataset. This dataset has 4 features, of which only 2 are represented, and 3 classes, of which 2 are overlapping. A class is overlapping another if they share part of the feature space, i.e. there is a region in the feature space whose patterns might belong to either class. Figure 2.1b presents the desired clustering for this dataset.

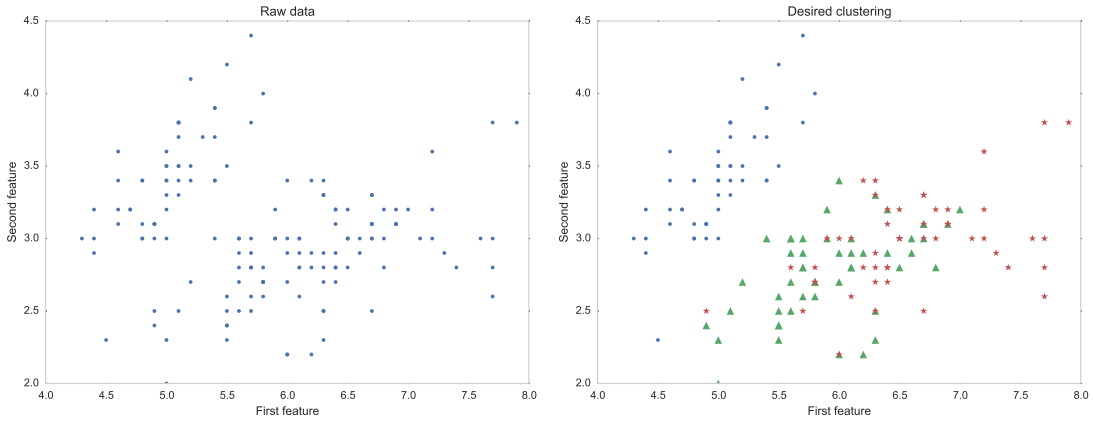

(a) Input data, unlabeled. (b) Desired labels.

Figure 2.1: First and second features of the Iris dataset. Fig. 2.1a shows the scatter plot of the raw input data, i.e. how the algorithms ”see” the data. Fig. 2.1b shows the desired labels for each point, where each color and symbol are coded to a class.

2.2 Definitions and Notation

This section will introduce relevant definitions and notation within the clustering context that will be used throughout the rest of this document and were largely adopted from [2].

A *pattern* $\mathbf{x}$ is a single data item and, without loss of generality, can be represented as a vector of d *features* x_i that characterize that data item, $\mathbf{x} = (x_1, \ldots, x_d)$, where d is referred to as the dimensionality of the pattern. A *pattern set* (or dataset) $\mathcal{X}$ is then the collection of all n patterns $\mathcal{X} = \{\mathbf{x}_1, \ldots, \mathbf{x}_n\}$. The number of features is usually the same for all patterns in a given pattern set.

In cluster analysis, the desired clustering, typically, is one that reflects the natural structure of the data, i.e. the original ground truth labeling. In other words, one wants to group the patterns that came from the same state of nature when they were generated, the same *class*. A class, then, can be viewed as a source of patterns and the effort of the clustering algorithm is to group patterns from the same source. Throughout this work, these classes will also be referred to as the "natural" or "true" clusterings. *Hard* clustering (or partitional) techniques assign a class label l_i to each pattern $\mathbf{x}_i$. The whole set of labels corresponding to a pattern set $\mathcal{X}$ is given by $\mathcal{L} = \{l_1, \ldots, l_n\}$, where l_i is the label of pattern $\mathbf{x}_i$. Closely related to the whole set of labels is the concept of a *partition*, which completely describes a clustering. A partition P is a collection of k *clusters*. A cluster C is a subset of nc patterns $\mathbf{x}_i$ taken from the pattern set, where the patterns belonging to one subset do not belong to any other in the same partition. A clustering *ensemble* $\mathbb{P}$ is a set of N partitions P^j of a given pattern set, each composed of a set of k_j clusters C_i^j, where $j = 1, \ldots, N$, $i = 1, \ldots, k_j$. Each cluster is composed of a set of nc_i^j patterns that does not intercept any other cluster of the same partition. The relationship between the above concepts is condensed in the following expressions:

$$\begin{aligned} ensemble \quad & \mathbb{P} = \left\{P^1, P^2, \ldots P^N\right\} \\ partition \quad & P^j = \left\{C_1^j, C_2^j, \ldots C_{k_j}^j\right\} \\ cluster \quad & C_i^j = \left\{x_1, x_2, \ldots x_{nc_i^j}\right\} \end{aligned}$$

Typically, a clustering algorithm will use a *proximity* measure for determining how alike are two patterns. A proximity measure can either be a *similarity* or a *dissimilarity* measure, as one can easily be converted to the other. The main difference is that the former increases in value as patterns are more alike, while the latter decreases in value. A *distance* is a dissimilarity function *d* which yields non-negative real values and is also a *metric*, which means it obeys the following three properties:

$$\begin{aligned} identity \quad & d(\mathbf{x}_i, \mathbf{x}_i) = 0 \\ symmetry \quad & d(\mathbf{x}_i, \mathbf{x}_j) = d(\mathbf{x}_j, \mathbf{x}_i), i \neq j \\ triangle\ inequality \quad & d(\mathbf{x}_i, \mathbf{x}_j) + d(\mathbf{x}_j, \mathbf{x}_z) \geq d(\mathbf{x}_x, \mathbf{x}_z) \end{aligned}$$

where $\mathbf{x}_i$, $\mathbf{x}_j$ and $\mathbf{x}_z$ are 3 distinct patterns belonging to the pattern set $\mathcal{X}$. Examples of proximity measures include the Euclidean distance, the Pearson's correlation coefficient and Mutual Shared Neighbors [5]. It should be noted that different proximity measures may be more appropriate in different contexts, such as document, biological or time-series clustering. Furthermore, data can come in different

types such as numerical (discrete or continuous) or categorical (binary or multinomial) attributes. The researcher should take these factors into account as different proximity measures are more appropriate for some type or even heterogeneous type data.

An introduction of clustering would be incomplete without a discussion on how good is a partition after clustering. Several *validity measures* exist and they can placed in two main categories [6]. *External* measures use *a priori* information about the data to evaluate the clustering against some external structure. An application of an external measure could be to test how accurate a clustering algorithm is for a particular dataset by matching the output partition against the ground truth. The *Consistency Index* [7] and the H-index [8] are examples of such measures that will be used in this work. Both of them are based on giving a score to each pair of clusters from two different partitions and then choosing the pairs that produce the best overall score. *Internal* measures, on the other hand, determine the quality of the clustering without the use of external information about the data. The Davies-Bouldin index [9] is such a measure. This index outputs a high score to partitions with high inter-cluster distance and low intra-cluster distance, and vice versa.

2.3 Characteristics of clustering techniques

Clustering algorithms may be categorized and described according to different properties. For the sake of completeness, a brief discussion of some of their properties will be layed out in this section.

It is common to organize cluster algorithms into two distinct types: *partitional* and *hierarchical*. A partitional algorithm, such as K-Means, is a hard clustering algorithm that will output a partiton where each pattern belongs exclusively to one cluster. A hierarchical algorithm produces a tree-based data structure called *dendrogram*. A dendrogram contains different partitions at different levels of the tree which means that the user can easily change the desired number of clusters by simply traversing the different levels. This is an advantage over a partitional algorithm since a user can analyze different partitions with different numbers of clusters without having to rerun the algorithm. Hierarchical algorithms can be further split into two approaches: bottom-up (or *agglomerative*) and top-down (or *divisive*). The former starts with all patterns as distinct clusters and will group them together according to some dissimilarity measure, building the dendrogram from the ground up; examples of algorithms that take this approach are Single-Link and Average-Link. The latter will start will all patterns in the same cluster and continuously split it until all patterns are separated, building the dendrogram from the top level to the bottom; this approach is taken by the Principal Directon Divisive Partitioning [10] and Bisecting K-Means [11] algorithms.

Another characteristic relates to how algorithms use the features for computing similarities. If all features are used simultaneously the algorithm is called *polithetic*, e.g. K-Means. Otherwise, if the features are used sequentially, it is called *monothetic*, e.g. [12].

Contrasting with *hard* clustering algorithms, are the *fuzzy* algorithms. A fuzzy algorithm will attribute to each pattern a degree of membership to each cluster. A partition can still be extracted from this output by choosing, for each pattern, the cluster with higher degree of membership. An example of a

fuzzy algorithm is the Fuzzy C-Means [13].

Another characteristic is an algorithm's stochasticity. A *stochastic* algorithm uses a probabilistic process at some point in the algorithm, possibly yielding different results in each run. As an example, the K-Means algorithm typically picks the initialization centroids randomly. A *deterministic* algorithm, on the other hand, will always produce the same result for a given input, e.g. Single-Link.

Finally, the last characteristic discussed is how an algorithm processes the input data. An algorithm is said to be *incremental* if it processes the input incrementally, i.e. taking part of the data, processing it and then doing the same for the remaining parts, e.g. PEGASUS [14]. A *non-incremental* algorithm, on the other hand, will process the whole input in each run, e.g. K-Means. This discussion is specially relevant when considering large datasets that may not fit in memory or whose processing would take too long for a single run and is therefore done in parallel.

2.4 K-Means

One of the most famous non-optimal solutions for the problem of partitional clustering is the K-Means algorithm [15]. The K-Means algorithm uses K *centroid* representatives, c_k, for K clusters. Patterns are assigned to a cluster such that the squared error (or, more accurately, squared dissimilarity measure) between the cluster representatives and the patterns is minimized. In essence, K-Means is a solution (although not necessarily an optimal one) to an optimization problem having the Sum of Squared Errors as its objective function, which is known to be a computationally NP hard problem [1]. It can be mathematically demonstrated that the optimal representatives for the clusters are the means of the patterns of each cluster [6]. K-Means, then, minimizes the following expression, where the proximity measure used is the Euclidean distance:

$$\sum_{k=1}^{K} \sum_{\mathbf{x}_i \in C_k} \|\mathbf{x}_i - c_k\|^2 \tag{2.1}$$

K-Means needs two initialization parameters: the number of clusters and the centroid initializations. It starts by assigning each pattern to its closer cluster based on the cluster's centroid. This is called the **labeling** step since one usually uses cluster labels for this assignment. The centroids are then recomputed based on this assignment, in the **update** step. The new centroids are the mean of all the patterns belonging to the clusters, hence the name of the algorithm. These two steps are executed iteratively until a stopping condition is met, usually the number of iterations, a convergence criteria or both. The initial centroids are usually chosen randomly, but other schemes exist to improve the overall accuracy of the algorithm, e.g. K-Means++ [16]. There are also methods to automatically choose the number of clusters [6].

The proximity measure used is typically the Euclidean distance. This tends to produce hyperspherical clusters [2]. Still, according to [1], other measures have been used such as the L1 norm, Mahalanobis distance, as well as the cosine similarity [6]. The choice of similarity measure must be made carefully

as it may not guarantee that the algorithm will converge.

A detail of implementation is what to do with clusters that have no patterns assigned to them. One approach to this situation is to drop the empty clusters in further iterations. However, allowing the existence of empty clusters or dropping empty clusters is undesirable since the number of clusters is an input parameter and it is expected that the output contains the specified number of clusters. Other approaches exist dealing with this problem, such as equaling the centroid of an empty cluster to the pattern furthest away from its assigned centroid or reusing the old centroids as in [17].

K-Means is a simple algorithm with reduced complexity $O(ntk)$, where n is the number of patterns in the pattern set, k is the number of clusters and t is the number of iterations that it executes. Accordingly, K-Means is often used as a foundational step of more complex and robust algorithms, such as the EAC algorithm.

As an example, the evolution and output of the K-means algorithm to the data presented in Fig. 2.1 is represented in Fig. 2.2. The algorithm was executed with 3 random centroids.

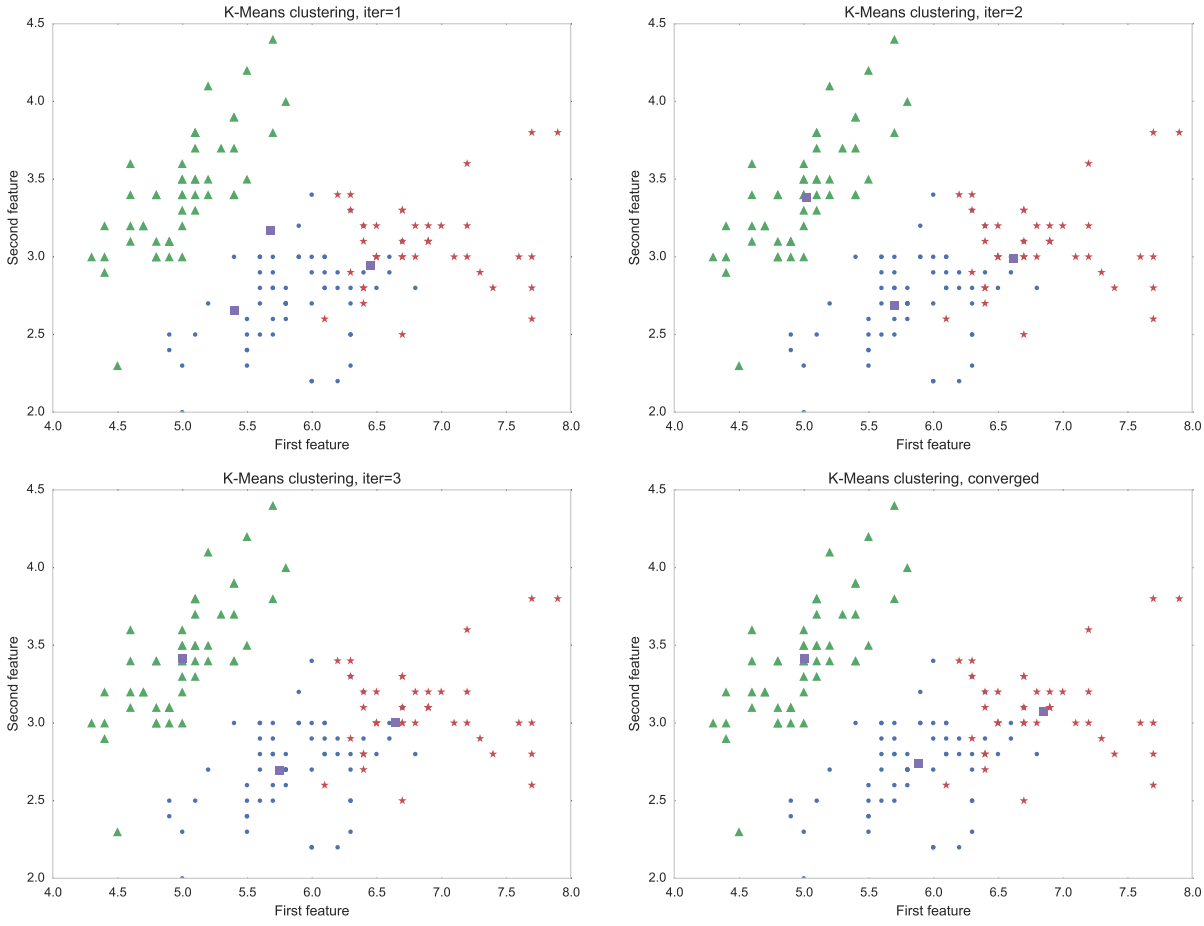

Figure 2.2: The output labels of the K-Means algorithm with the number of clusters (input parameter) set to 3. The different plots show the centroids (squares) evolution on each iteration. Between iteration 3 and the converged state 2 more iterations were executed.

Even with the correct number of clusters, the clustering results do not match 100% the natural clusters. The accuracy relative to the natural clusters of Fig. 2.1b is 88% as measured by the Consistency Index (CI) [7]. In this example, the problem is the two overlapping clusters. It is hard for an algorithm to

discriminate between two clusters when they have similar patterns. When no prior information about the dataset is given, the number of clusters can be hard to discover. This is why, when available, a domain expert may provide valuable insight on tuning the initialization parameters.

2.5 Single-Link

Single-Link [18] is one of the most popular hierarchical agglomerative clustering (HAC) algorithms. HAC algorithms operate over a pair-wise dissimilarity matrix and output a dendrogram (e.g. Fig 2.4a). The main steps of an agglomerative hierarchical clustering algorithm are the following [2]:

1. Create a pair-wise dissimilarity matrix of all patterns, where each pattern is a distinct cluster singleton;

2. Find the closest clusters, merge them and update the matrix to reflect this change. The rows and columns of the two merged clusters are deleted and a new row and column are created to store the new cluster.

3. Stop if all patterns belong to a single cluster, otherwise continue to step 2.

The algorithm stops when $n-1$ merges have been performed, which is when all patterns have been connected in the same cluster. Just like in the K-Means algorithm, different similarity measures can be used between pairs of objects.

The proximity measure between clusters in the second step distinguishes between the different HAC linkage algorithms, such as Single-Link , Average-Link, Complete-Link, among others. In Single-Link (SL), the proximity between any two clusters is the the dissimilarity between their closest patterns. On the other hand, in Complete-Link, it is the proximity between their most distant patterns and, in Average-Link, is the proximity between the average point of each cluster. In SL, because the algorithm connects first clusters that are more similar, it naturally gives more importance to regions of higher density [6].

The total time complexity of a naive implementation is $O(n^3)$ since it performs a $O(n^2)$ search in step two and it does it $n-1$ times. Over time, more efficient implementations have been proposed, such as SLINK [19]. SLINK needs no working copy of the $O(n^2)$ pair-wise similarity matrix (if the original can be modified), has a working memory of $O(n^2)$ and time complexity of $O(n^2)$. This increase in performance comes from the observation that the $O(n^2)$ search can be transformed in a $O(n)$ search at the expense of keeping two arrays of length n that will store the most similar cluster for each pattern and the corresponding similarity measure. This way, to find the two closest clusters, the algorithm will not search the entire similarity matrix, but only the new similarity array since this array keeps the closest cluster of each cluster. Naturally these arrays must be updated upon a cluster merge.

An interesting property of the SL algorithm is its equivalence with a Minimum Spanning Tree (MST), an observation first made by [20]. In graph theory, a MST is a tree that connects all vertices together while minimizing the sum of all the distance between them. An example of a graph and its corresponding MST can be seen in Fig. 2.3. In this context, the edges of the MST are the distances between the

patterns and the vertices are the patterns themselves. A MST contains all the information necessary to build a Single-Link dendrogram. To walk down through the levels of the dendrogram from the MST, one cuts the least similar edges. Furthermore, this approach can be used to apply Single-Link clustering to graphs-encoded problems in a straight-forward way. Furthermore, the performance properties of this method are roughly the same as SLINK [21].

The true advantage of using an MST based approach comes when the number of edges (similarities) m of the MST is less than $\frac{n(n-1)}{2}$, where n is the number of nodes (patterns) [22]. This is because SLINK works over a inter pattern similarity matrix, meaning that the similarity between every pair of patterns must be explicitly represented. The minimum number of similarities is $\frac{n(n-1)}{2}$, which is equivalent to the upper or lower half triangular matrices of the similarity matrix. The MST, on the other hand, works over a graph that may or may not have edges between every pair of nodes. Fast MST algorithms have a time complexity of $O(m \log n)$, which is a significant improvement over $O(n^2)$ when $m << \frac{n(n-1)}{2}$.

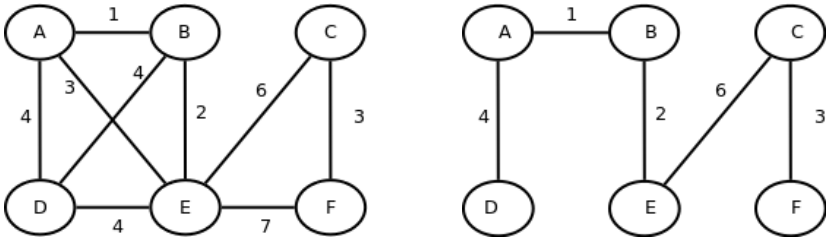

(a) Example of a graph. (b) MST of the graph to the left.

Figure 2.3: The above figures show an example of a graph (left) and its corresponding Minimum Spanning Tree (right). The circles are vertices and the edges are the lines linking the vertices.

An example of a Single-Link dendrogram and resulting cluster can be observed in Fig. 2.4. The dendrogram in Fig. 2.4a has been truncated to 25 clusters in the bottom level for the sake of readability. The clustering presented on Fig. 2.4b is the result of cutting the dendrogram such that only 3 clusters exist (the number of classes). The accuracy, as measured by the CI, is of 58%.

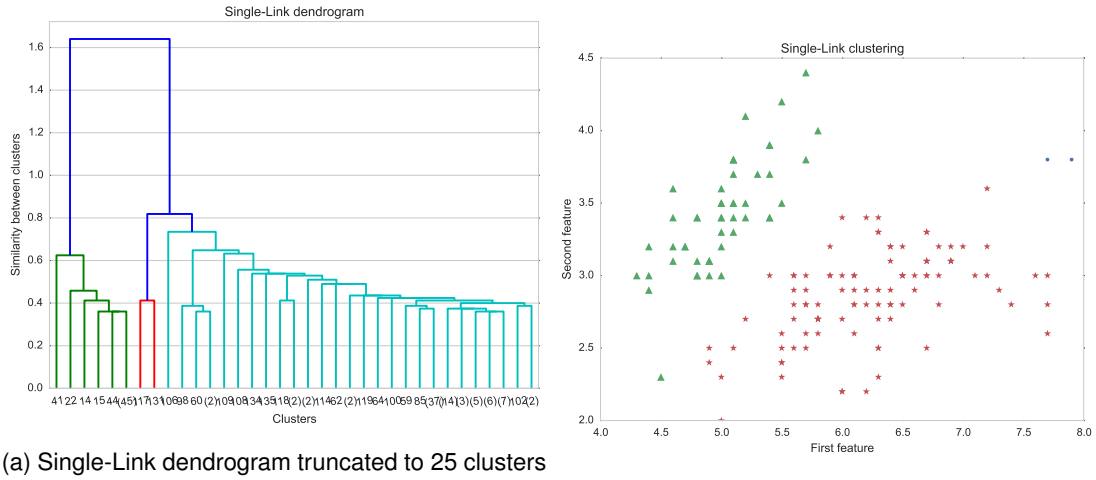

(a) Single-Link dendrogram truncated to 25 clusters in the bottom level.

(b) Clustering with 3 clusters.

Figure 2.4: The above plots show the dendrogram and a possible clustering taken from a Single-Link run over the Iris dataset. Fig. 2.4b was obtained by performing a cut on a level that would yield a partition of 3 clusters.

2.6 Ensemble Clustering

The underlying idea behind ensemble clustering is to take a collection of partitions, a *clustering ensemble*, and combine it into a single partition. There are several motivations for ensemble clustering. Data from real world problems appear in different configurations regarding shape, cardinality, dimensionality, sparsity, etc. Different clustering algorithms are appropriate for different data configurations, e.g. K-Means tends to group patterns in hyperspheres [2] so it is more appropriate for data whose structure is formed by hypershere like clusters. If the true structure of the data at hand is heterogeneous in its configuration, a single clustering algorithm might perform well for some part of the data while other performs better for some other part. Since different partitions are used, one can use a mix of algorithms to address different properties of the data such that the combination is more **robust** to noise and outliers [23] and the final clustering has a **better quality** [6]. Even using several partitions from different initializations of the same algorithm may also allow retrieving complex shaped structures from otherwise simple methods. Ensemble clustering can also be useful in situations where one does not have direct access to all the features of a given dataset but can have access to partitions from different subsets and later combining with an ensemble algorithm. Furthermore, the generation of the clustering ensemble can be **parallelized and distributed** since each partition is independent from every other partition.

A clustering ensemble, according to [24], can be produced from (1) different data representations, e.g. choice of preprocessing, feature selection and extraction, sampling; or (2) different partitions of the data, e.g. output of different algorithms, varying the initialization parameters on the same algorithm.

Ensemble clustering algorithms can take three main distinct approaches [6]: based on pair-wise similarities, probabilistic or direct. EAC [24] and CSPA [25] are examples of pair-wise similarity based approach, where the algorithms use a co-associations matrix. The MMCE [23] and BCE [26] are examples of a probabilistic approach. This approach will be further clarified when the EAC algorithm is explained. HGPA [25], MCLA [25] and bagging [27] are examples of a direct approach to combining the ensemble clusterings, where the algorithms work directly with the labels without creating a co-association matrix. A detailed and thorough review of the similarity measures that can be used on with clustering ensembles and the state of the art algorithms can be consulted in [6].

2.7 Evidence Accumulation Clustering

2.7.1 Overview

The goal of EAC is to find an optimal partition P^* containing k^* clusters, from the clustering ensemble $\mathbb{P}$. The optimal partition should have the following properties [24]:

- **Consistency** with the clustering ensemble;
- **Robustness** to small variations in the ensemble; and,
- **Goodness** of fit with ground truth information, when available.

Ground truth is the true labels of each sample of the dataset, when such exists, and is used for validation purposes. Since EAC is an unsupervised method, this typically will not be available. EAC makes no assumption on the number of clusters in each data partition. Its approach is divided in 3 steps:

1. **Production** of a clustering ensemble $\mathbb{P}$ (the evidence);
2. **Combination** of the ensemble into a co-association matrix;
3. **Recovery** of the natural clusters of the data.

In the first step, a clustering ensemble is produced. Within the context of EAC, it is of interest to have variety in the ensemble with the intention of better capturing the underlying structure of the data. One such parameter to measure that variety is the number of clusters in the partitions of the ensemble. Typically, the number of clusters in each partition is drawn from an interval $[K_{min}, K_{max}]$ with uniform probability. This influences other properties of other parts of the algorithm such as the sparsity of the co-association matrix as will become clearer in future chapters. Reviewing the literature [28, 24, 29, 30], it is clear the ensemble is usually produced by random initialization of K-Means (specifying only the number of centroids within the above interval). Still, other clustering algorithms have been used for the production of the ensemble [31] such as Single-Link, Average-Link and CLARANS.

The ensemble of partitions is combined in the second step, where a non-linear transformation turns the ensemble into a co-association matrix [24], i.e. a matrix $\mathcal{C}$ where each of its elements n_{ij} is the association value between the pattern pair (i, j). The association between any pair of patterns is given by the number of times those two patterns appear clustered together in any cluster of any partition of the ensemble, i.e. the number of co-occurrences in the same cluster. The rationale is that pairs that are frequently clustered together are more likely to be representative of a true link between the patterns [28], revealing the underlying structure of the data. In other words, a high association n_{ij} means it is more likely that patterns i and j belong to the same class. The construction of the co-association matrix is at the very core of this method.

The co-association matrix itself is not the output of EAC. Instead, it is used as input to other methods to obtain the final partition. The co-association between any two patterns can be interpreted as a similarity measure. Thus, since this matrix is a similarity matrix it's appropriate to use algorithms that take this type of matrices as input, e.g. K-Medoids or hierarchical algorithms such as Single-Link or Average-Link, to name a few. Typically, algorithms use a distance as the dissimilarity, which means that they minimize the distance to obtain the highest similarity between objects. However, a low value on the co-association matrix translates in a low similarity between a pair of objects, which means that the co-association matrix requires prior transformation for accurate clustering results, e.g. replace every similarity value n_{ij} between every pair of object (i, j) by $max\{\mathcal{C}\} - n_{ij}$.

Although any algorithm can be used, the final clustering is usually done using SL or AL. Each of these algorithms will take as input the transformed co-association matrix as the dissimilarity matrix. Furthermore, not knowing the "natural" number of clusters one can use the lifetime criteria. The k-cluster lifetime is defined by Fred and Jain [24] as the range of threshold values on the dendrogram that

lead to the identification of k clusters. The lifetime criteria chooses the longest lifetime as the threshold interval where a cut in the dendrogram should be made so as to produce a partition. In other words, the number of clusters k should be such that it maximizes the cost of cutting the dendrogram from $k-1$ clusters to k.

Related work to EAC has been developed. The Weighted EAC (WEAC) algorithm [31] and a study on the sparsity of the co-association matrix [32] should be mentioned. The latter is discussed in more depth in chapter 3. The former introduces the novelty of having weights associated to each partition such that good quality partitions are more relevant than their counterparts. These weights are based on internal validity measures. Weighing the partitions in terms of quality has shown to improve the original algorithm, accuracy wise.

EAC has been used with success in several areas. To name a few, it was used for the automatic identification of chronic lymphocyt leukemia [33], for the unsupervised analysis of ECG-based biometric database to highlight natural groups and gain further insight [**?**] and as a solution to the problem of clustering of contour images (from hardware tools) [29].

Chapter 3

State of the art

Scalability of EAC to large datasets is the concern of this work and, because of that, this chapter starts by reviewing what has been done in terms of scaling EAC in section 3.1. EAC is a method of three parts and this dissertation is concerned with the scalability of the whole algorithm which means that each step must be optimized. Scaling an algorithm means one has to take into account both speed of execution and memory requirements. Increasing speed can be attained with either faster algorithms and/or faster computation of existing algorithms. This chapter reflects research done within both approaches.

Although research on the application of EAC to large datasets has not been pursued before, cluster analysis of large datasets has. Since EAC uses traditional clustering algorithms (e.g. K-Means, Single-Link) in its approach, it is useful to understand how scalable the individual algorithms are as they will have a big impact in the scalability of EAC. Furthermore, valuable insights may be taken from the techniques used in the scalability of other algorithms. To this end, section 3.2 presents a brief review on cluster analysis of large datasets, with a focus on parallelization with GPUs. Furthermore, it offers a more detailed description of a GPU parallel version of K-Means and an approach for parallelizing Single-Link with the GPU.

An alternative approach on clustering for scaling with faster algorithms, the still young field of quantum clustering, was reviewed in section 3.3. This line of research was taken mostly with the first step of EAC in mind.

3.1 Scalability of EAC

The quadratic space and time complexity of processing the $n \times n$ co-association matrix is an obstacle to an efficient scaling of EAC. Two approaches have been proposed to address this obstacle: one dealing with reducing the co-association matrix by considering only the distances of patterns to their p neighbors and the other by using a sparse co-association matrix and maximizing its sparsity.

3.1.1 p neighbors approach

The first approach, [24], proposes an alternative $n \times p$ co-association matrix, where only the p nearest neighbors of each pattern are considered in the evidence combination step. This comes at the cost of having to keep track of the neighbors of each pattern in a separate data structure of $O(np)$ memory complexity and also of pre-computing the p neighbors, which has a time complexity of $O(n^2)$ to compute the proximity measure from each pattern to every other pattern. The quadratic space complexity of the co-association matrix is then transformed to $O(2np)$: $O(np)$ for the actual co-association matrix and $O(np)$ for keeping track of the neighbors. Since usually one has $p < \frac{n}{2}$ (value for which both this approach and the original $n \times p$ matrix would take the same space), the cost of storing the extra data structure is lower than that of storing an $n \times n$ matrix, e.g. for a dataset with 10^6 patterns and $p = \sqrt{10^6}$ (a value much higher than the 20 neighbors used in [24]), the total memory required for the co-association matrix would decrease from $3725.29GB$ to $7.45GB$ (0.18% of the memory occupied by the complete matrix).

3.1.2 Increased sparsity approach

The second approach, presented in [32], exploits the sparse nature of the co-association matrix. The co-association matrix is symmetric and with a varying degree of sparsity. The former property translates in the ability of storing only the upper triangular of the matrix without any loss on the quality of the results. The latter property is further studied with regards to its relationship with the minimum K_{min} and maximum K_{max} number of clusters in the partitions of the input ensemble. The core of this approach is to only store the non-zero values of the upper triangular of the co-association matrix. The authors study 3 models for the choice of these parameters:

- choice of K_{min} based on the minimum number of gaussians in a gaussian mixture decomposition of the data;
- based on the square root of the number of patterns ($\{K_{min}, K_{max}\} = \{\frac{\sqrt{n}}{2}, \sqrt{n}\}$);
- or based on a linear transformation of the number of patterns ($\{K_{min}, K_{max}\} = \{\frac{n}{A}, \frac{n}{B}\}, A < B$).

where A and B are two suitable constants chosen by the researcher. The study compared the impact of each model in the sparsity of the co-association matrix (and, thus, the space complexity) and in the relative accuracy of the final clusterings. Both theoretical predictions and results revealed that the linear model produces the highest sparsity in the co-association matrix, under a dataset consisting of a mixture of Gaussians. Furthermore, it is true for both linear and square root models that the sparsity increases as the number of samples increases.

For real datasets, the performance of the three models became increasingly similar with the increase of the cardinality of the problem. It was found that the chosen granularity of the input partitions (K_{min}) is the variable with most impact, affecting both accuracy and sparsity. The authors reported this technique has linear space and time complexity on benchmark data.

The number of samples of the datasets analysed in [32] was under 10^4. Furthermore, it should be noted that the remarks concerning the sparsity of the co-association matrix in the aforementioned study refer to the number of non-zero elements in the matrix and does not take into account extra data structures that accompany real sparse matrices implementations.

3.2 Clustering with large datasets

When large datasets, and big data, is in discussion, two perspectives should be taken into account [6]. The first deals with the applications where data is too large to be stored efficiently. This is the problem that streaming algorithms such as LOCALSEARCH [34] try to solve by analyzing data as it is produced, close to real-time processing. The other perspective is data that is actually stored for later processing which is the perspective relevant to the present work and will be further discussed below.

The flow of clustering algorithms typically involves some initialization step (e.g. choosing the number of centroids in K-Means) followed by an iterative process until some stopping criteria is met, where each iteration updates the clustering of the data [6]. In light of this, to speed up and/or scale up an algorithm, three approaches are available: (1) reduce the number of iterations, (2) reduce the number of patterns and/or features to process or (3) parallelizing and distributing the computation. The solutions for each of these approaches are, respectively, one-pass algorithms (e.g. CLARANS [35], BIRCH [36], CURE [37]), randomized techniques that reduce the input space complexity (e.g. PCA, CX/CUR [38]) and parallel algorithms (parallel K-Means [39], parallel spectral clustering [40]).

Parallelization can be attained by adapting algorithms to multi core CPU, GPU, distributed over several machines (a *cluster*) or a combination of the former, e.g. parallel and distributed processing using GPU in a cluster of hybrid workstations. Each approach has its advantages and disadvantages. The CPU approach has access to a larger memory but the number of computation units is reduced when compared with the GPU or cluster approach. Furthermore, CPUs have advanced techniques such as branch prediction, multiple level caching and out of order execution - techniques for optimized sequential computation. GPU have hundreds or thousands of computing units but typically the available device memory is reduced which entails an increased overhead of memory transfer between host (workstation) and device (GPU) for computation of large datasets. In addition, it is harder to scale the above solutions for even bigger datasets. On the other hand, GPUs can be found on a large variety of computing platforms, from mobile devices to workstations and datacenters. A cluster offers a parallelized and distributed solution, which is easier to scale. According to [6], the two algorithmic approaches for cluster solutions are (1) memory-based, where the problem data fits in the main memory of the machines of the cluster and each machine loads part of the data; or (2) disk-based, comprising the widely used MapReduce framework capable of processing massive amounts of data in a distributed way. The main disadvantage is that there is a high communication and memory I/O cost to pay. Communication is usually done over the network with TCP/IP, which is several orders of magnitude slower than the direct access of the CPU or GPU to memory (host or device).

The present work is oriented towards GPU based parallelization, since GPUs are an easily accessible

commodity and the goals of the dissertation are oriented towards computation on a single machine. Taking that into consideration, this section reviews a GPU parallel version of the K-Means algorithm and goes on to describe a GPU parallel approach for performing Single-Link clustering. For an overview of General Purpose computing in GPUs (GPGPU), the reader is referred to Appendix A.

3.2.1 Parallel K-Means

K-Means is an obvious candidate to generate the ensemble of the first step of EAC because it uses different initializations and parameters and due to its simplicity. Besides, K-Means is a very good candidate for parallelization. Still, other algorithms can be used to produce ensembles.

Several parallel implementations of this algorithm for the GPU exist [41, 42, 43, 44, 45] and all report significant speed-ups relative to their sequential counterparts in certain conditions, usually after the input dataset goes above a certain cardinality, dimensionality or number of clusters threshold. The first step is inherently parallel as the computation of the label of the i-th pattern is not dependent on any other pattern, but only on the centroids. Two approaches to parallelize this step on the GPU are possible, a centroid-centric or a data-centric [41]. In the former each thread is responsible for a centroid and will compute the distance from its centroid to every pattern. These distances must be stored and, in the end, the patterns are assigned to the closest centroid. In the latter, each thread will compute the distance from one or more data points to every centroid and determines to which centroid they are closest. This strategy has the advantage of using less memory since it does not need to store all the pair-wise distances to perform the labeling - it only needs to store the best distance for each pattern. According to [41], the former approach is suitable for devices with a low number of cores so as to stream the data to each one, while the latter is better suited to devices with more cores.

The approach taken in [39] only parallelizes the labeling stage and takes a data-centric approach to the problem. Each thread computes the distance from a set of data points to every centroid and determines the labels. The remaining steps are performed by the host CPU. This study reported speed-ups up to 14, for input datasets of $500\,000$ points. Furthermore, it should be noted that the speed up was measured against a sequential version with all C++ compiler optimizations turned on, including vector operations (which, by themselves, are a way of parallelizing computation). The parallelized algorithm's flow can be observed in Figure 3.1.

The implementation of Zechner and Granitzer [39] uses one thread per data point. Each centroid is transfered to shared memory and each thread will compute the distance from its data point to the centroid. Moreover, the data point is fetched from global memory in a coalesced manner.

It should be noted that the literature reports that the performance of K-Means using Dynamic Parallelism is slightly worse than its standard GPU counterpart [46].

3.2.2 Parallel Single-Link Clustering

Single-Link (SL) is an important step in the EAC chain. Given the new similarity metric (how many times a pair of patterns are clustered together in the ensemble), SL provides an intuitive way of obtaining

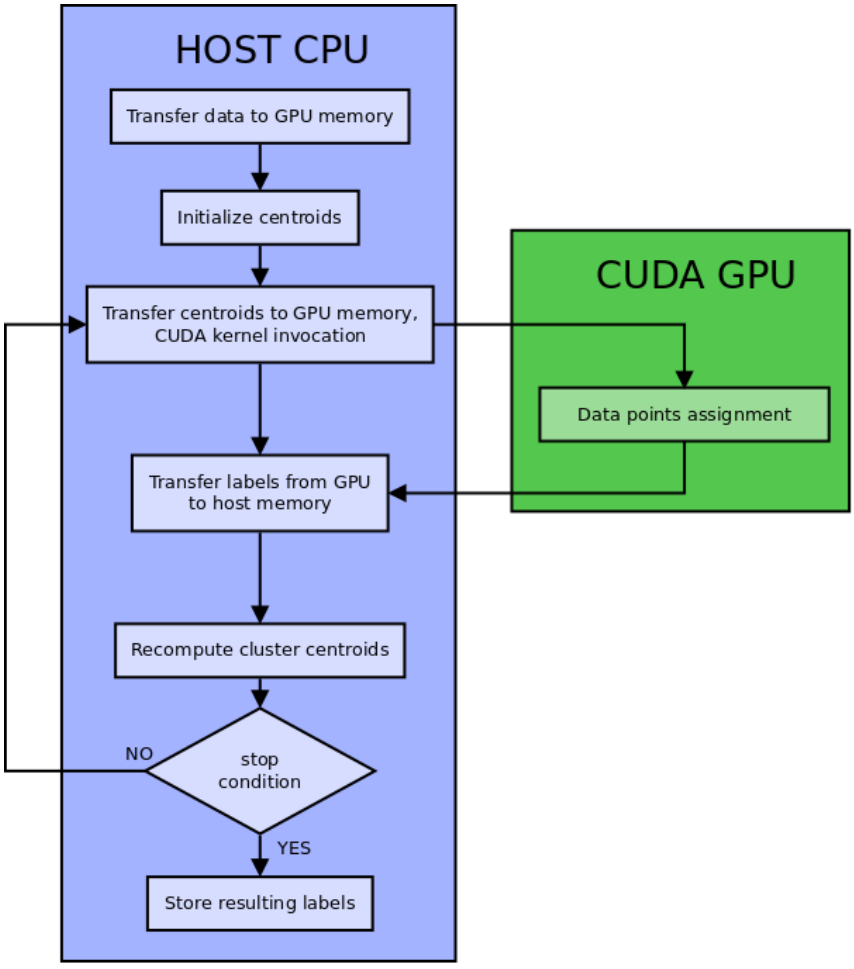

Figure 3.1: Flow execution of the GPU parallel K-Means algorithm.

the final partition: patterns that are clustered together often in the ensemble should remain clustered together in the final solution.

SL is not easily parallelized since a new cluster generated at each step may include the one generated in the previous iteration. The most parallelizable part is the computation of the pair-wise similarity matrix, which is only useful if the input is raw data instead of a similarity matrix as in the case of EAC. The relationship between SL and the Minimum Spanning Tree, explained in chapter 2, is the key to parallelize it. If one takes this approach for solving the SL problem, it becomes easier to parallelize it since parallel MST algorithms are abundant in literature [47, 48, 49]. The same approach for extracting the final clustering in EAC was used in [28].

Algorithm for finding Minimum Spanning Trees

There are several algorithms for computing an MST. The most famous are Kruskal [50], Prim [51] and Borůvka [52]. Borůvka's algorithm is also known as Sollin's algorithm. The first two are mostly sequential, while the latter has the highest potential for parallelization, specially in the first iterations. As such, even though GPU parallel variants of Kruskal's [48] and Prim's [53] algorithms exist, the focus will be on Borůvka's.

Several parallel implementations of this algorithm for the GPU exist, e.g. [47], [54] and [49]. Da Silva Sousa et al. [49] provides a more in-depth review over the current state of the art of MST solvers for the GPU and proposes an algorithm reported to be the fastest. This section will review the algorithm proposed in [49], referred to as *Sousa2015* from henceforth.

Since this algorithm operates over graphs, relevant graph notation is introduced here. In graph theory, a graph $G = (V, E)$ is composed by a set of vertices V and a set of edges E connecting those vertices. Furthermore, if G is a connected graph, then there is a path between any $s, t \in V$. An example of a graph can be observed in Fig. 2.3 of chapter 2, where the MST was first introduced. A $|V| \times |V|$ matrix can fully represent a graph if one takes each element (i, j) of the matrix to be the weight of the edge connecting vertices i and j. Typically, a graphs is not fully connected (vertices connected to all the other vertices), which means that the matrix is often sparse.

CSR format

Sousa2015 takes in a graph as input, represented in the CSR format (a format used for sparse matrices). This representation is equivalent to having a square matrix G with zeroed diagonal where the g_{ij} element of the matrix is the weight of the link connecting the node i with the node j. This format is represented in Fig. 3.2. It requires three arrays to fully describe the graph:

- a *data* array containing all the non-zero values, where values from the same row appear sequentially from left to right and top to bottom, i.e. in *row-major* order, e.g. if the first row has 20 non-zero values, then the first 20 elements from this array belong to the first row;
- an *indices* array of the same size as *data* containing the column index of each non-zero value;

- an *indptr* array of the size of the number of rows containing a pointer to the first element in the *data* and *indices* arrays that belongs to each row, e.g. if the $i-th$ element (row) of *indptr* is k and it has 10 values, then all the elements from k to $k+10$ in *data* belong to the $i-th$ row.

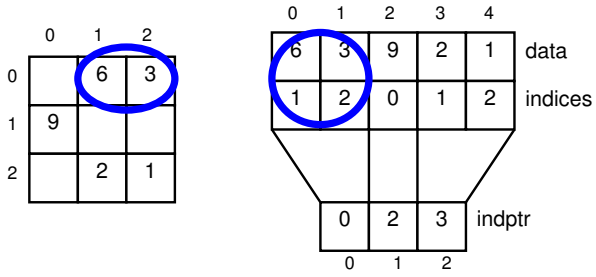

Figure 3.2: Correspondence between a sparse matrix and its CSR counterpart.

Within the algorithm's context, these three arrays are denominated as *first_edge*, *destination* and *weight*, respectively. There change in denomination is for making their purposes clearer. Although these three arrays can completely describe a graph, the algorithm uses an extra array *outdegree* that stores the number of non-zero values of each row and can be deduced from the *first_edge* array.

The length and purpose of each of these arrays are:

- *first_edge* is an array of size $|V|$, where the *i-th* element points to the first edge corresponding to the *i-th* vertex.
- *outdegree* is an array of size $|V|$, where the *i-th* element contains the number of edges attached to the *i-th* vertex.
- *destination* is an array of size $|E|$, where the *j-th* element points to the destination vertex of the *j-th* edge.
- *weight* is an array of size $|E|$, where the *j-th* element contains the weight of the *j-th* edge.

$|V|$ is the number of vertices and $|E|$ is the number of edges. The number of edges is duplicated to cover both directions, since the algorithm works with undirected graphs. This basically means that instead of using the the upper (or lower) triangular matrix (which can also completely describe the graph), it uses a complete matrix resulting in double redundancy of each edge. The edges in the *destination* array are grouped together by the vertex they originate from, e.g. if edge j is the first edge of vertex i and this vertex has 3 edges, then edges $\{j, j+1, j+2\}$ are the outgoing edges of vertex i and are stored sequentially in the *destination* array.

Steps of the algorithm

Within the context of the algorithm the *id* of a vertex is its index in the *first_edge* array, the *color* represents a component and is the *id* of the component representative and the *successor* of a vertex is the destination vertex of one of its edges. One should keep in mind this is a parallel algorithm and each of its steps is computed concurrently. Except for the *exclusive prefix sum*, each thread processes a

single vertex and each computation is usually independent. In some steps, however, threads need to access the same resource and it is important the state of the resource does not change in the middle of the operation that accesses it. In these cases, atomic operations (operation that are guaranteed to be isolated and, thus, not interruptible) are used. The algorithm's flow is presented in Figure 3.3 and its main steps are explained below.

1. *Find minimum edge per vertex*: select and store the minimum weighted edge for each vertex and resolve same weight conflict by picking the edge with lower destination vertex id.

2. *Remove mirrored edges*: an edge is mirrored if the successor of its the destination vertex is the origin vertex, e.g. if vertex 1 points to vertex 2 and vertex 2 points back to vertex 1. All mirrored edges are removed from the selected edges in the first step. All edges that are not removed are added to the resulting MST.

3. *Initialize and propagate colors*: this step is responsible for identifying connected components so the graph may be contracted. Each connected component will be a super-vertex in the contracted graph, which means it will be a single vertex representing a subgraph. Each vertex is initialized with the same color of its successor's id. If a vertex has no successor because that edge was removed in the previous step, then it will be the representative vertex of the component and its color is initialized with its own id. The colors are then propagated by setting each vertex's color to the color of its successor, until convergence.

4. *Create new vertex ids*: only the super-vertices will be propagated to the next iteration but they will have new ids for building the new contracted graph. The new ids will range from 0 to s, where s is the number of super-vertices. The vertices representing a super-vertex (component) will take the new ids in increasing order according to their own ids in increasing order, e.g. vertex 2 is the representative with lowest id so it will have the id 0 in the contracted graph. This step relied on the *exclusive scan* operation, which is explained in section 3.2.2.

5. *Count, assign, and insert new edges*: the final step consists in building the contracted graph. The algorithm will count the number of edges connecting each super-vertex to other super-vertices, i.e. the connections between subgraphs. This is simply accomplished by selecting every edge whose origin and destination colors are distinct. For each such edge the corresponding positions of the origin and destination super-vertices in a new *outdegree* array are incremented with an atomic operation. The new *first_edge* array is obtained from performing an exclusive scan over *outdegree*. The next step is to assign and insert edges in the contracted graph. Once again, the algorithm will determine which edges will be in the contracted graph by checking the origin and destination colors. A copy, called *top_edge*, of the new *first_edge* array will track of where to insert the new edges. When an edge is assigned to a super-vertex it is inserted in the new *weight* and *destination* arrays composing the contracted graph. The position of insertion is specified by *top_edge* and the algorithm increments *top_edge* atomically so the next edge will not overwrite the previous one. The increment is done with an atomic operation since multiple edges can be

assigned to the same super-vertex and the insertion of all edges is being done in parallel. It should be noted that duplicated edges are not removed, i.e. several distinct connections between two super-vertices can be kept, since the author considers that the benefit of doing so does not outweigh the computational overhead.

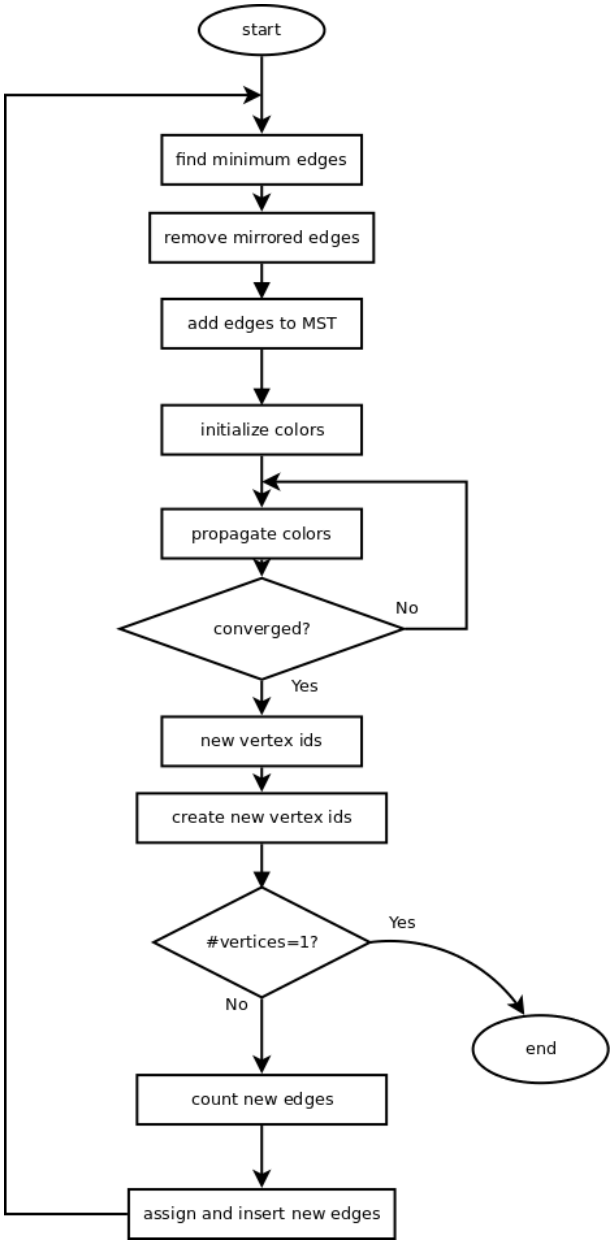

Figure 3.3: Flow execution of Sousa2015.

It should be noted, however, that this algorithm does not support unconnected graphs, i.e., it is not able to output a forest of MSTs. A solution to that problem is, on the step of building the flag array, only mark a vertex if it is both the representative of its supervertex and has at least one neighbour.

Exclusive scan

The *scan* operation is one of the fundamental building blocks of parallel computing. Furthermore, two of the steps of the Borůvka variant of [49] are performed with an exclusive scan where the operation is a sum. To illustrate the functioning of the exclusive scan, let us consider the particular case where the operation of the scan is the sum and the identity (the value for which the operation produces the same output as the input) is naturally 0. An example of this operation is presented in Fig. 3.4.

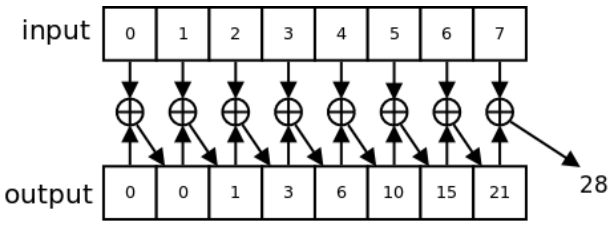

Figure 3.4: Example of the exprefix sum operation.

The first element of the output will be the identity (if it were an inclusive scan, it would be the first element itself). The second element is the sum between the first element of the input array and the first element of the output array, etc. The nature of this algorithm seems highly sequential, since each element of the output array depends on the previous one, but two main parallel versions can be found in literature: Hillis and Steele [55] and Blelloch [56]. The two approaches focus on distinct efforts. The former focuses on optimizing the number of steps [55], has a work complexity of $O(nlogn)$ and a step complexity of $O(logn)$. The latter focuses on optimizing the amount of work done [56], has a work complexity of $O(n)$ and a step complexity of $O(2logn)$. The focus of this dissertation will be on the Blelloch's algorithm. The reason for this is that the main objective is to deal with very large datasets which guarantees that there will be more work to be done (operations on the data) than there will be available computing resources (streaming processors in the GPU in this case). When there is more work than processors, one wants to minimize the total amount of work. On the other hand, when there is more processors than work, one wants to minimize the amount of steps of the algorithm as this translates in the biggest increase in speed.

Blelloch's algorithm is comprised by two main phases: the *reduce phase* (or *up-sweep*) and the *down-sweep phase*. The algorithm is based on the concept of *balanced binary trees* [57], but it should be noted that no such data structure is actually used. An in-depth explanation of this concept and how it relates to the algorithm falls outside the scope of the present work and it is recommended that the reader consult [57] or [56] for such details.

During the reduce phase (see Figure 3.5), the algorithm traverses the tree and computes partial sums at the internal nodes of the tree. This operation is also known as a parallel reduction due to the fact that the total sum is stored in the root node (last node) of the tree [57].

In the down-sweep phase (see Figure 3.6) the algorithm traverses back the tree. During the traversal, and using the partial sums calculated in the reduce phase, it builds the scan in place (overwriting the result of the reduce phase).

The computational complexity of this algorithm is higher than that of its sequential counterpart. The

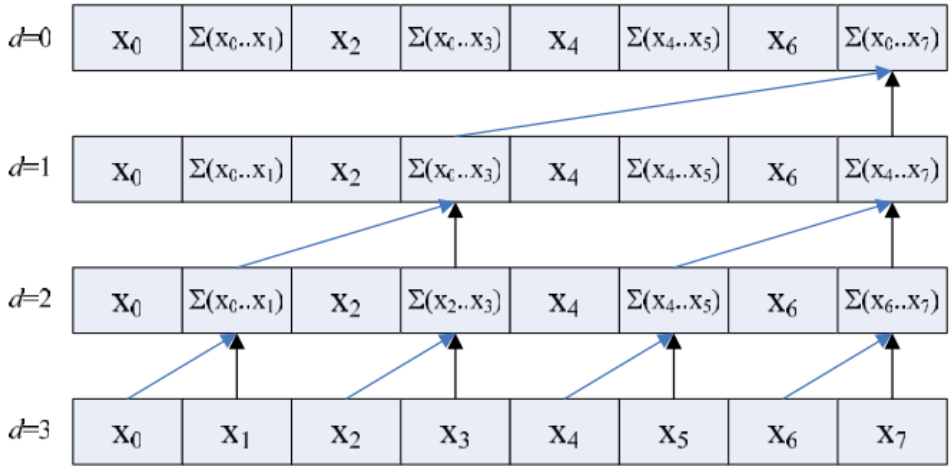

Figure 3.5: Representation of the reduce phase of Blelloch's algorithm [57]. *d* is the level of the tree and the input array can be observed at $d = 0$.

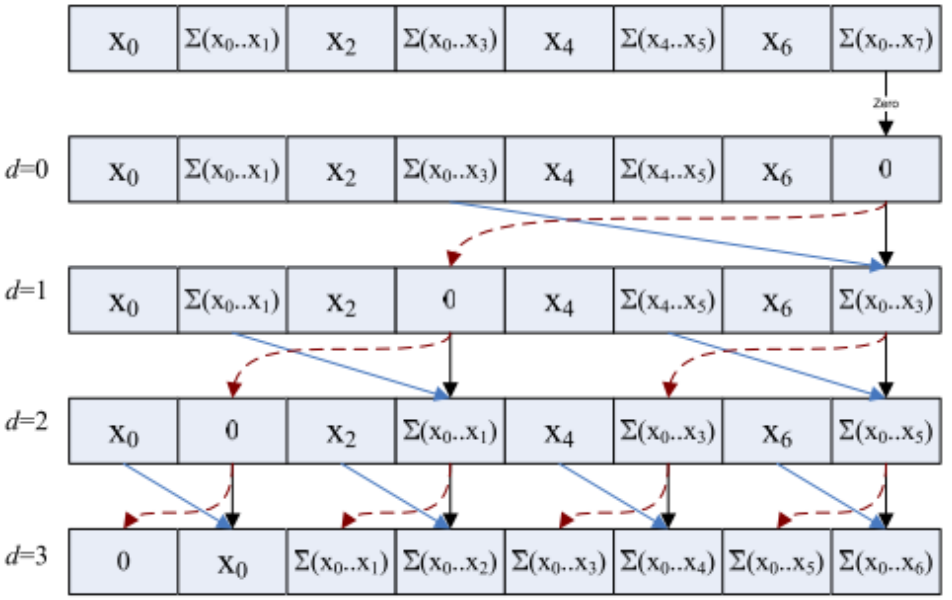

Figure 3.6: Representation of the down-sweep phase of Blelloch's algorithm [57]. *d* is the level of the tree.

sequential version has a $O(n)$ computational complexity, since it only goes through the input array once and performs exactly n additions. Blelloch's algorithm, on the other hand, performs $n-1$ additions in the reduce phase and $n-1$ in the down-sweep phase, but still keeps the linear work complexity of the sequential version. Since it is a parallel algorithm and the computation will be distributed across several processing units, its performance is significantly better. It should be noted that, as described, the algorithm supports input arrays of a size that is a power of 2. However, Harris et al. [57] explains how to overcome this limitation and also offers the description of an implementation for CUDA along with hardware specific optimizations, which presented a speed-up as high as 6.

3.3 Quantum clustering

The field of quantum clustering has shown promising results regarding potential speed-ups in several tasks over their classical counterparts. Currently, two major approaches for the concept of quantum clustering were found in the literature: quantization of clustering methods to work in quantum computers or algorithms inspired by quantum physics.

The former approach translates in converting algorithms to work partially or totally on a different computing paradigm, with support of quantum circuits or quantum computers. Both Aïmeur et al. [58] and Lloyd et al. [59] show how the quantum paradigm can be used for speed-ups in machine learning algorithms, with the possibility of obtaining exponential speed-ups. Many of these quantizations make use of Groover's database search algorithm [60], or a variant of it, e.g. Wiebe et al. [61]. Most literature on this approach is also mostly theoretical, since the physical requirements still do not exist for testing these methods. This approach can be seen as part of the bigger problem of quantum computing and quantum information processing. An alternative to using real quantum systems would be to simulate them. However, simulating quantum systems in classical computers is a very hard task by itself and literature suggest that it is not feasible [62]. The quantization approach falls outside the scope of this dissertation, but Wittek [63] offers a thorough review on the state of the art of machine learning in the quantum paradigm.

The second approach is part of the wider field of Computational Intelligence. A study of the literature reveals that it typically further divides itself into two categories [64]. One comprises the algorithms based on the concept of the qubit, the quantum analogue of a classical bit with interesting properties found in quantum objects. Several algorithms have been modeled after this concept, often also gathering inspiration from evolutionary genetic algorithms, which were successfully applied in several areas:

- tackling the Knapsack problem as described in Han and Kim [65] and its improved version [66];
- solving the traveling salesman problem [67];
- two implementations of a Quantum K-Means algorithm [68, 69];
- a Quantum Artificial Bee Colony algorithm [70, 64];

- two approaches for Fuzzy C-Means (FCM), namely Quantum New Weighted Fuzzy C-Means (QNW-FCM) [64] and Quantum Fuzzy C-Means (QFCM) [71, 64];
- a novel quantum inspired clustering technique based on manifold distance [72];
- a Quantum-inspired immune clonal clustering algorithm based on watershed [73].

The other approach models data as a quantum system and uses Schrödinger's equation in some way. Often, the data is modeled as a quantum system, where each pattern is a particle, and Schrödinger's equation is used to evolve the particle system into a solution. This has been applied in an optimization problem for electromagnetics using a quantum particle swarm [74] and also on several clustering algorithms:

- the Quantum Clustering [75] algorithm treats patterns as quantum particles whose potential is computed with Schrödinger's equation and the system is evolved with the Gradient Descent method;
- Dynamic Quantum Clustering [76] is a variation of Horn and Gottlieb [75] that uses Schrödinger's equation to evolve the system;
- a Fuzzy C-Means approach [77] based on Quantum Clustering [75];
- QPSO+FCM, a Fuzzy C-means [78] based on Quantum-behaved Particle Swarm Optimization (QPSO) [79].

For more information on quantum inspired algorithms, the reader is referred to Manju and Nigam [80] which offers a thorough survey on the state of the art of quantum inspired computation intelligence algorithms. The following two sections contain a brief overview of the concept of the qubit and the description of an algorithm that uses this approach. Afterwards, an algorithm that follows the Schrödinger's equation approach is reviewed.

3.3.1 The quantum bit approach

The quantum bit

To understand the algorithms based on the concept of the qubit, it is useful to cast some insight about its properties and functioning. This section has the purpose to provide a brief introduction to this topic. An extended and in-depth review of this and related topics can be found in Lanzagorta and Uhlmann [81]. The qubit is a quantum object with certain quantum properties such as entanglement and superposition. Within the context of the studied algorithm, the only property used is superposition. A qubit can have any value between 0 and 1 (superposition property) until it is observed, which is when the system collapses to either state. However, the probability with which the system collapses to either state may be different. The superposition property or linear combination of states can be expressed [68] as

$$|\psi\rangle = \alpha|0\rangle + \beta|1\rangle$$

where ψ is an arbitrary state vector and α, β are the the probability amplitude coefficients of basis states $|0\rangle$ and $|1\rangle$, respectively. The Dirac bra ket notation is employed, where the *ket* $|.\rangle$ corresponds to a column vector. The basis states correspond to the spin of the modeled particle (in this case, a ferminion, e.g. electron). The coefficients are subjected to the following normalization:

$$|\alpha|^2 + |\beta|^2 = 1$$

where $|\alpha|^2$, $|\beta|^2$ are the probabilities of observing states $[0]$ and $[1]$, respectively, and α and β are complex quantities that represent a qubit:

$$\begin{bmatrix} \alpha \\ \beta \end{bmatrix}$$

Moreover, a qubit string may be represented by:

$$\left[\begin{array}{c|c|c} \alpha_1 & \alpha_2 & \alpha_3 \\ \beta_1 & \beta_2 & \beta_3 \end{array}\right]$$

The probability of observing the state $|000\rangle$ will be $|\alpha_1|^2 \times |\alpha_2|^2 \times |\alpha_3|^2$. To use this model for computing purposes, black-box objects called *oracles* are used. Oracles are important to understand quantum speed-ups. They can be understood as subroutines that cannot be usefully examined or as unknown physical systems that perform a quantum operation on a qubit string [82] and with properties one would like to estimate. Within the context of the present work an oracle is an abstraction for the programmer. It is an object which can be called and changes state (which can be observed) as a consequence. For the purpose of the following sections, the concept of the oracle is more related to *oracles with internal randomness* [82] or, more simply, a probabilistic Turing machine, as in the case of [70].

Quantum K-Means

The Quantum K-Means (QK-Means) algorithm, as described in [68], is based on the classical K-Means algorithm. It extends the basic K-Means with concepts from quantum mechanics (the qubit) and evolutionary genetic algorithms.

Within the context of this algorithm, oracles contain strings of qubits and generate their own input by observing the state of the qubits. After collapsing, the qubit value corresponds to a classical bit, with a binary value.

Ideally, oracles would contain actual quantum systems or simulate them - this would correctly account for the desirable quantum properties. As it stands, oracles are not quantum systems or even simulate them and can be more appropriately described as random number generators. Each string of qubits represents a number, so the number of qubits in each string will define its precision. The number of strings chosen for the oracles depends on the number of clusters and dimensionality of the problem (e.g. for 3 centroids of 2 dimensions, 6 strings will be used since 6 numbers are required). Each oracle will represent a possible solution.

The algorithm has the following steps:

1. Initialize population of oracles
2. Collapse oracles
3. K-Means
4. Compute cluster fitness
5. Store
6. Quantum Rotation Gate
7. Collapse oracles
8. Quantum cross-over and mutation
9. Repeat 3-7 until generation (iteration) limit is reached

Initialize population of oracles The oracles are created in this step and all qubit coefficients are initialized with $\frac{1}{\sqrt{2}}$, so that the system will observe either state of the qubit with equal probability. This value is chosen taken into account the necessary normalization of the coefficients, as described in the previous section.

Collapse oracles Collapsing the oracles implies making an observation of every qubit of each string in all oracles. This is done by first choosing a coefficient to use (either can be used), e.g. α. Then, a random value r between 0 and 1 is generated. If $\alpha \geq r$ then the system collapses to $[0]$, otherwise to $[1]$.

K-Means In this step we convert the binary representation of the qubit strings to base 10 and use those values as initial centroids for K-Means. For each oracle, classical K-Means is then executed until it stabilizes or reaches the iteration limit. The solution centroids are returned to the oracles in binary representation.

Compute cluster fitness Cluster fitness is computed using the Davies-Bouldin index for each oracle. The score of each oracle is stored in the oracle itself.

Store The best scoring oracle is stored.

Quantum Rotation Gate So far, the algorithm consisted of the classical K-Means with a complex random number generation for the centroids and complicated data structures, namely the oracles. This is the step that fundamentally differs from the classical version. In this step, a quantum gate (in this case a rotation gate) is applied to all oracles except the best one. The basic idea is to shift the qubit coefficients of the least scoring oracles in the direction of the best scoring one. These oracles will have a higher probability of collapsing into initial centroid values closer to the best solution so far. This way, in

future generations, the oracles do not initiate with the best centroids so far (which would not converge into a better solution) but we they are close while still ensuring diversity (which is also a desired property in the genetic computing paradigm). In other words, we look for better solutions than the one we got before in each oracle while moving in the direction of the best we found so far.

The genetic operations of cross-over and mutation are both part of the genetic algorithms toolbox. Literature suggests that this operations may not be required to produce variability in the population of qubit strings [66]. The reason for this is that enough variability is produced with the use of the angle-distance rotation method [66] in the quantum rotation operation, with a careful choice of the rotation angle. Still, when used, the goal of these operations is to produce further variability into the population of qubit strings.

3.3.2 Schrödinger's equation approach

The other approach to clustering that gathers inspiration from quantum mechanical concepts is to use the Schrödinger equation. The algorithm under study was created by Horn and Gottlieb [83] and was later extended by Weinstein and Horn [76].

The first step in this methodology is to compute a probability density function of the input data. This is done with a Parzen-window estimator in [84, 76]. The Parzen-window density estimation of the input data is done by associating a Gaussian with each point, such that

$$\psi(\mathbf{x}) = \sum_{i=1}^{N} e^{-\frac{\|\mathbf{x}-\mathbf{x}_i\|^2}{2\sigma^2}}$$

where N is the total number of points in the dataset, σ is the variance and ψ is the probability density estimation. ψ is chosen to be the wave function in Schrödinger's equation. Further details can be found in Weinstein and Horn [76], Horn and Gottlieb [84, 75].

With this information, one will compute the potential function $V(x)$ that corresponds to the state of minimum energy (ground state = eigenstate with minimum eigenvalue) [84], by solving the Schrödinger's equation in order of $V(x)$:

$$V(\mathbf{x}) = E + \frac{\frac{\sigma^2}{2}\nabla^2\psi}{\psi} = E - \frac{d}{2} + \frac{1}{2\sigma^2\psi}\sum_{i=1}^{N}\|\mathbf{x}-\mathbf{x}_i\|^2 e^{-\frac{\|\mathbf{x}-\mathbf{x}_i\|^2}{2\sigma^2}} \tag{3.1}$$

And since the energy should be chosen such that ψ is the groundstate (i.e. eigenstate corresponding to minimum eigenvalue) of the Hamiltonian operator associated with Schrödinger's equation (not represented above), the following is true

$$E = -min\frac{\frac{\sigma^2}{2}\nabla^2\psi}{\psi} \tag{3.2}$$

From equations 3.1 and 3.2, $V(x)$ can be computed. This potential function is related to the inverse of

a probability density function. Minima of the potential correspond to intervals in space where points are together. So minima will naturally correspond to cluster centers [84]. However, it is very computationally intensive to compute $V(x)$ to the whole space, so the compututation of the potential function is only done at the data points. This should not be problematic since clusters' centers are generally close to the data points themselves. Even so, the minima may not lie on the data points themselves. One method to address this problem is to compute the potential on the input data and converge these points toward some minima of the potential function. This is done with the gradient descent method in [84].

Another method [76] is to think of the input data as particles and use the Hamiltonian operator to evolve the quantum system in the time-dependent Schrödinger's equation. Given enough time steps, the particles will converge to and oscillate around potential minima. This method makes the Dynamic Quantum Clustering algorithm. The nature of the computations involved in this algorithm make it a good candidate for parallelization techniques. Wittek [85] parallelized this algorithm to the GPU obtaining speed-ups of up to two magnitudes relative to an optimized multicore CPU implementation.

Chapter 4

EAC for large datasets: proposed solutions

The aim of this thesis is the optimization and scalability of EAC, with a focus for large datasets. EAC is divided in three steps and each has to be considered for optimization. This chapter will present the considered solutions for each step, which are also visually summarized in Fig. 4.1.

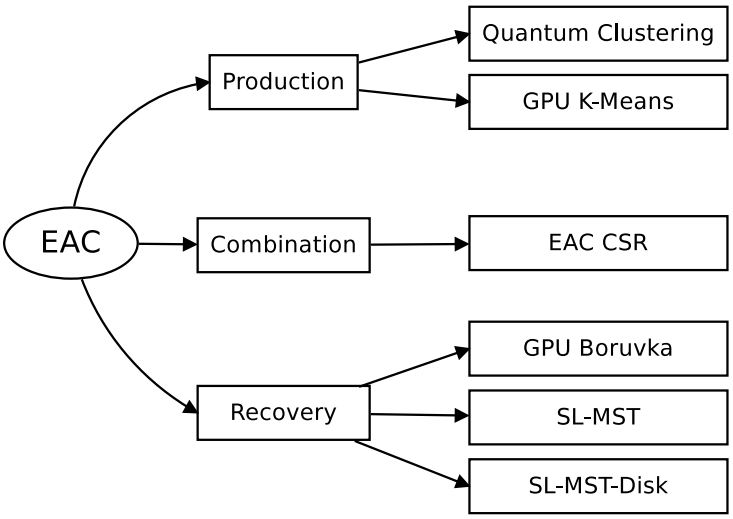

Figure 4.1: Diagram of proposed solution in each phase of EAC.

The first step is the gathering of evidence, i.e. generating an ensemble of partitions. The main objective for the optimization of this step is speed. Using fast clustering methods for generating partitions is an obvious solution, as is the optimization of particular algorithms aiming for the same objective. Since each partition is independent from every other partition, parallel computing over a cluster of computing units would result in a fast ensemble generation. Using either or any combination of these strategies will guarantee a speed-up.

Initial research was under the field of quantum clustering. After this pursuit proved fruitless for being slow, the focus of research shifted to parallel computing, more specifically a K-Means parallel version within the GPGPU paradigm.

The second step is mostly bound by memory. The complete co-association matrix has a space complexity of $\mathcal{O}(n^2)$. Such complexity becomes prohibitive for big data, e.g. a dataset of 2×10^6 patterns will result in a complete co-association matrix of $14901\ GB$ if values are stored in single precision floating-point format. This problem is addressed by exploring the inherent sparse nature of the co-association matrix.

The last step has to take into account both memory and speed requirements. The final clustering must be able to produce good results and be fast while not exploding the already big space complexity from the co-association matrix. The work in this last step was initially directed towards parallelization and afterwards out-of-core processing using a disk stored co-association matrix.

The methodology for optimizing for speed is relevant and permeates the approach taken to every problem faced in the present work. For optimizing the speed of an algorithm, one starts by first profiling that algorithm and analyze which parts take the longest to compute. These parts are the focus of optimization as any change on them will have the greatest effect on the overall algorithm. To further illustrate this point, let us consider an algorithm that spends 75% of its time on a section of the code to which a speed-up of 2 is possible and 25% on a part to which an infinite speed-up is possible (this translates in its execution time being negligible). Let us further assume that only one part of the algorithm may be optimized. If one optimizes the first part, the local speed-up is 2 and the overall speed-up is 1.6. On the other hand, if one optimizes the second part, the local speed-up is infinite but the overall speed-up is only $1.333(3)$.

All the algorithms were implemented in Python with high reliance on numerical and scientific modules, namely NumPy [86] and SciPy [87, 88, 89]. The main reason for using Python on all implementations was to use the same technology everywhere and have a high interoperability between modules. Important modules for visualizing and processing statistical results were MatplotLib [90] and Pandas [91], respectively. The SciKit-Learn [92] machine learning library has a plethora of implemented algorithms which were used for benchmarking as well as integration in the devised solutions. The iPython [93] module was used for interactive computing which allowed for accelerated prototyping and testing of algorithms. Python is an interpreted language which translates in its performance being worse than a compiled language such as C or Java. To address this problem, the open-source Numba [94] module from Continuum Analytics was used to allow for writing code in native Python and have it converted to fast compiled code. Furthermore, this module provides a pure Python interface for the CUDA API. The proprietary NumbaPro module was used for two high level CUDA functions, namely *argsort* and *max*.

4.1 Quantum Clustering

Research under this paradigm aimed to find a candidate for the first phase of EAC. Two candidates were considered: Quantum K-Means (QK-Means) and Horn and Gottlieb's quantum clustering (QC) algorithm. These algorithms were chosen so as to have a representative from both approaches of quantum inspired algorithms identified in chapter 3.

The implementation of QK-Means followed the description presented in section 3.3.1, with the excep-

tion of the removal of the genetic operations *cross-over* and *mutation*. The main goal for the first phase of EAC is speed but these operations aim at improving the quality of the solution by producing variability in the oracles. Furthermore, literature [66] suggests that enough variability is produced in the quantum rotation step with the angle-distance rotation method. As such, it was an implementation decision to cut the overhead of these operations for the sake of time optimization.

An implementation of QC was already available in Matlab. Accordingly, implementing this algorithm translated into porting the code from Matlab to Python.

4.2 Speeding up Ensemble Generation with Parallel K-Means

K-Means is an obvious candidate for the generation of partitions since it is simple, fast and partitions do not need to be accurate - variability in the partitions is a desirable property. This relaxation on the accuracy of the partitions already allows for a faster generation of partitions since fewer iterations of the algorithm need to be executed for a partition to be generated - typically 3 iterations suffice. Further gains are possible with a parallel GPU version of K-Means. The overview of the algorithm used is presented in section 3.2.1, but some implementation differences exist, namely the lack of some optimizations used in the original source. The choice to only parallelize the labeling phase was motivated by the maximum potential speed-ups presented below. Afterwards, the implementation is described.

4.2.1 Maximum potential speed-up

Previously, it was mentioned that the methodology followed for speeding up an application was to first profile the code and identify the portions of code that can be optimized and what fraction of the total computational time they take. Table 4.1 presents statistical results on the theoretical maximum speed-up for the two K-Means phases. These results came from the same experiment as that presented in section 5.3. The sequential version of K-Means was executed over a wide spectrum of datasets varying the number of patterns, dimensions and centroids. The theoretical maximum speed-up is considered to be the overall speed-up of the algorithm if one of its phases had infinite speed-up, i.e. when its time is negligible relative to the other phases. Analyzing these results it is clear that the labeling phase holds the most potential for optimizations. Furthermore, the theoretical speed-up also increases with the problem complexity (number of patterns, dimensions and centroids), since, the execution time for the labeling phase with more complex datasets is higher compared to the update phase. The theoretical speed-up of the update phase is almost negligible when compared to the labeling phase. This illustrates the importance of profiling the code before proceeding with optimizations, since effort invested in the update phase would yield little effect.

4.2.2 Implementation details

The implementation gives as much freedom as possible to the user regarding CUDA parameter choices, such as the threads per block, blocks per grid or number of patterns to process per thread. By default,

Table 4.1: Maximum theoretical speed-up for the labeling and update phases of K-Means based on experimental data. The datasets used range from 1000 to $500\,000$ patterns, from 2 to 1000 dimensions and from 2 to 2048 centroids.

	Labeling phase	Update phase
mean	540.8308	1.0468
std	879.9143	0.0836
min	2.9983	1.0002
25% percentile	18.6578	1.0015
50% percentile	99.8681	1.0101
75% percentile	681.2509	1.0567
max	5026.9722	1.5199

each thread will compute the label of one pattern and the blocks are unidimensional and composed by 512 threads, which maximizes GPU occupancy since no shared memory is used. The number of blocks, then, is the number of patterns divided by the number of threads per block. If the number of blocks exceeds the maximum allowed for one dimension (65535), the grid configuration automatically uses other dimensions. The other parameter that the user can choose deals with how data is transfered back and forward between host and device. The user can choose to allow the Numba CUDA API to handle all the memory transfers or to allow the implementation to optimize those. The latter will minimize the amount of data transfers and memory allocations and is the default option. Furthermore, it also allows for the algorithm to be executed multiple times without redundant transfer of the pattern set. This permits the production of an entire ensemble with a single transfer of the pattern set. These parameters (number of patterns per thread, number of threads per block and memory transfer mode) may be configured at runtime. Still, a typical user does not need to be knowledgeable about CUDA to be able to use this implementation, since the tuning of these parameters is optional.

The CUDA implementation of the label computation part of the algorithm starts by transferring the data to global memory (pattern set and initial centroids) and allocates space for the labels and corresponding distances, also in global memory. Both data and centroids are transfered and stored in a row-major order and all memory transfers are synchronous. The computation of a label for one pattern is done by iteratively computing the distance from the pattern to each centroid and storing the label and the distance corresponding to the closest centroid. Finally, the labels and distances are sent back to the host for computation of the centroids. This procedure is available as a CUDA kernel or as three different sequential versions: pure Python, based on NumPy or compiled code with Numba. These same sequential versions exist for the recomputation of the centroids. The fastest of CPU versions is the Numba based, followed by the one based on NumPy and finally pure Python. The implementation of the centroid computation starts by counting the number of patterns attributed to each centroid. Afterwards, it checks if there are any ”empty” clusters, i.e. if there are centroids that are not the closest ones to any pattern. Dealing with empty clusters is important because, although empty clusters may be desirable in some situations, the target use expects that the output number of clusters to be the same as defined in the input parameter. Centroids corresponding to empty clusters will be the patterns that are furthest away from their centroids, which is the reason why the distances to the centroids are kept and transfered. Any

other centroid c_i will be the mean of the patterns that were labeled i.

At the end of each iteration, a stopping criteria is checked: either the difference between the centroids of two consecutive iterations reached an user supplied threshold (default of 0.0001) or the maximum number of iterations was reached (default of 300). In EAC, the number of iterations is the stopping criteria used with a low number of iterations (e.g. 3 in the present work).

4.3 Dealing with the space complexity of the co-association matrix

In chapter 3, two approaches to the space complexity of the co-association matrix in the second phase of EAC are presented: one dealing with p prototypes and the other with the inherent sparsity of the matrix.

The results presented in the sparsity study of EAC [32] show that it is possible to obtain a high sparsity in the co-association matrix. In some cases the density of the matrix was as low as 1%. This motivated the focus of the work on exploiting the inherent sparsity of the matrix. A discussion on using sparse matrices and a novel solution for building the co-association matrix is presented in section 4.4.

As stated before, the focus of the work is on sparse matrices. Still, for the sake of completeness, the different strategies considered for the prototypes approach are discussed here. One strategy is to use the **p-Nearest Neighbors** as prototypes, as already presented in chapter 3. Before building the co-association matrix, the p closest patterns to each pattern are computed and stored in the $n \times p$ neighbor matrix. During the voting mechanism of EAC only the neighbors of each pattern are considered. This strategy has a space complexity of $O(2nk)$ and requires the computation of the k-Nearest Neighbors. A second strategy is to use **p random prototypes**, which will be a set of unique p patterns. This will be the same for every pattern. Here the voting mechanism is altered so that if a pattern is clustered with any of the prototypes, the correspondent element in the co-association matrix is incremented. This has the advantage that only a $n \times p$ matrix needs to be stored along with a p array for the chosen prototypes. Furthermore, if p is high enough to provide a representative pattern of the dataset the results can be as good as the full matrix. The third, and final, possible strategy identified is similar to the random prototypes. The difference is that instead of choosing p random patterns from the dataset, the prototypes will be the representatives of the dataset from another algorithm, e.g. K-Medoids, K-Means.

It would be ideal to combine both approaches (sparsity and neighbors) to further reduce space complexity, but they are not necessarily compatible. This is specially true for the p-Nearest Neighbors strategy since it is unlikely that a pattern will never be clustered with its closest p neighbors. This means that the $n \times p$ co-association matrix may not have many zeros which translates in little advantage for using the sparsity augmentation approach the matrix of co-associations.

4.4 Building the sparse matrix

Building a non-sparse matrix is easy and fast since the memory for the whole matrix is allocated and indexing the matrix is direct. When using sparse matrices, neither is true. In the specific case of EAC, there is no way to know what is the number of associations the co-association matrix will have which means it is not possible to pre-allocate the memory to the correct size of the matrix. This translates in allocating the memory gradually which may result in fragmentation, depending on the implementation, and more complex data structures, which incurs overhead.

Documentation of the SciPy library recommends different sparse formats for either building a matrix or operating over it. For building a matrix, the COO (COOrdinate), DOK (Dictionary of Keys) and LIL (List of Lists) formats are recommended. All of these formats rely on extra data structures such as lists as dictionaries to efficiently build the matrices incrementally, i.e. allocating memory as it is required. For operating over a matrix, the documentation recommends converting from one of the previous formats to either CSR (Compressed Sparse Row) or CSC (Compressed Sparse Column).

As observed before, the sparsity study of EAC [32] did not account for the overhead of using the data structures supporting sparse matrices. However, scaling to very large datasets must take this into account. Exploratory testing revealed that using one of the recommended matrices, allowed for building the matrix took around two orders of magnitude as long as using a full allocated matrix. Furthermore, because of the extra data structures, the implementations from SciPy would saturate the main memory from datasets with less than 1 million patterns. Using the CSR format did not saturate memory but it took a completely unacceptable amount of time, many orders of magnitude above any of the formats recommended for building the matrix.

After a search in the literature for efficient and scalable ways to build a sparse matrix proved fruitless, these problems motivated the design of a new method for building the matrix specialized for the characteristics of EAC. The solution devised is based on the CSR format (described previously in section 3.2.2), which has the desired properties of having a low memory trace and allows for fast computations.

4.4.1 EAC CSR

The first step is making an initial assumption on the maximum number of associations *max_assocs* that each pattern can have. A possible rule is

$$max\_assocs = 3 \times bgs$$

where bgs is the biggest cluster size in the ensemble. The biggest cluster size is a good heuristic for trying to predict the number of associations a pattern will have since it is the limit of how many associations each pattern will have in any partition. Furthermore, one would expect that the neighbors of each pattern will not vary significantly, i.e. the same neighbors will be clustered together with a pattern repeatedly in many partitions. This rule was motivated by the relationship between the maximum number of associations and the biggest cluster size, which will be presented in the results. This scheme

for building the matrix uses 4 supporting arrays, 3 of which (*indices*, *data* and *indptr*) are part of the standard CSR format. The arrays are:

- **indices** - an array of $n \times max\_assocs$ size that stores the columns of each non-zero value of the matrix, i.e. the destination pattern to which each pattern associates with;
- **data** - an array of $n \times max\_assocs$ size that stores all the non-zero values;
- **indptr** - an array of n size where the *i-th* element is the index of the *indices* and *data* arrays that holds the value and column of the first non-zero value in the *i-th* row.
- **degree** - an array of n size that stores the number of non-zero values of each row.

Each pattern (row) has a maximum of *max_assocs* pre-allocated that it can use to fill with new associations. New associations that exceed this pre-allocated maximum are discarded. The *degree* array is the one keeping track of the number of associations of each pattern. The data types used are picked to be smallest necessary for the problem at hand. The *data* array is usually composed of singly Byte unsigned integer values since the ensemble size is typically less than 255. The *indices* array stores unsigned integers of the smallest size possible to store the number of patterns of the dataset. The data type of *indptr* is an 8 Byte integer, since the number of associations of large problems are usually often bigger than 2^{32}. Lastly, the *degree* array stores 4 Byte unsigned integers. The last two data types never change, since the size of the *indptr* and *degree* arrays is usually negligible compared to the combined size of the *data* and *indices* arrays. Throughout this section, the interval of the *indices* array corresponding to a specific pattern (row) is referred to as that pattern's *indices* interval. If it is said that an association is added to the end of the *indices* interval, this refers to the beginning of the part of the interval that is free for new associations. The term indices is used either in the context of the array, in which case it will appear as *indices*, or as the plural of index, in which case it will appear as indices. Furthermore, it should be noted that this method assumes that the clusters received come sorted in a increasing order.

The first partition is inserted in a special way. Since it is the first and the clusters are sorted, it is a matter of copying the cluster to the *indices* array in the positions of each pattern, with the exclusion of the pattern itself. The data array (containing the co-association score) is set to 1 on the relevant positions. This process can be observed clearly in Fig. 4.2. Because it is the fastest partition to be inserted, it is picked to be the one with the least amount of clusters (more patterns per cluster) so that each pattern gets the most amount of associations in the beginning (on average). This is only applicable if the whole ensemble is provided, otherwise there is no way to know what is the biggest cluster of the whole ensemble. This increases the probability that any new cluster will have more patterns that correspond to already established associations. Because the clusters are sorted and only a copy of each cluster was made, it is not necessary to sort each row of the matrix by column index.

For the remaining partitions, the process is different. Now, it is necessary to check if an association already exists. For each pattern in a cluster it is necessary to add or increment the association to every other pattern in the cluster. This is described in Algorithm 1.

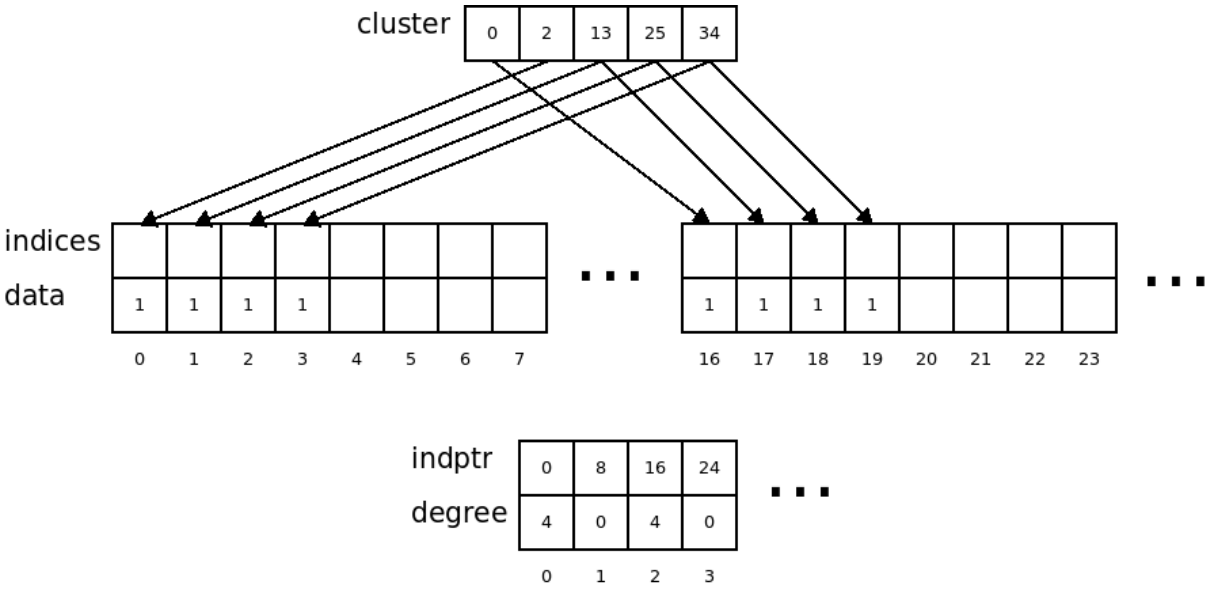

Figure 4.2: Inserting a cluster of the first partition in the co-association matrix.

Algorithm 1 Update matrix with cluster.

```
1: procedure UPDATE_CLUSTER(indices, data, indptr, degree, cluster, max_assocs)
2:     for pattern n in cluster do
3:         for every other pattern na in cluster do
4:             ind = binary_search(na, indices,interval of n in indices)
5:             if ind ≥ 0 then
6:                 increment data[ind]
7:             else
8:                 if maximum assocs not reached then
9:                     add new assoc. with weight 1
```

Binary search is used to search for the association in the *indices* array in the interval corresponding to a specific row (or pattern). This is necessary because it is not possible to index directly a specific position of a row in the CSR format. Since a binary search is performed $(ns-1)^2$ times for each cluster, where ns is the number of patterns in any given cluster, the indices of each pattern must be in a sorted state at the beginning of each partition insertion. Two strategies for sorting were devised. The first strategy is to just insert the new associations at the end of the *indices* array (in the correct interval for each pattern) and then, at the end of processing each partition, use a sorting algorithm to sort all the patterns' intervals in the *indices* array. This was easily implemented with existing code, namely using *NumPy*'s *quicksort* implementation, which has an average time complexity of $O(n \log n)$

The second strategy is more complex. It results from the observation that, if one could know in which position each new association should be inserted, it would be possible to move all old associations to their final sorted positions and insert the new ones. Furthermore, this would be done in an efficient manner with minimum number of comparisons (and thus branches in the execution of the code). For this end, the implemented binary search returns the index of the searched value (key) if it is found or the position for a sorted insertion of the key in the array, if it is not found. In reality, it returns $-ind-1$ if it is not found, where ind is the index for sorted insertion. This means that the position where each new association should be inserted is now available. New associations are stored in two auxiliary arrays of size max_assocs: one (*new_assoc_ids*) for storing the patterns of the associations and the other (*new_assoc_idx*) to store the indices where the new associations should be inserted (the result of the binary search). The process is illustrated with an example in Fig. 4.3, detailed in Algorithm 2 and explained in the following paragraph.

After each pass on a cluster (adding or incrementing all associations to a pattern in the cluster), the new associations have to be added to the pattern's *indices* interval in a sorted manner. The number of associations corresponding to the i-th pattern (*degree[i]*) is incremented by the amount of new associations to be added. An element is added to the end of the *new_assoc_idx* array with the value of *degree[i]* so that the last new association can be included in the general cycle. During the sorting process a pointer to the current index to add associations o_ptr is kept (it is initialized to the new total number of associations of a pattern). The sorting mechanism looks at two consecutive elements in the *new_assoc_idx* array, starting from the end. If the i-th element of the *new_assoc_idx* array is greater or equal than the $(i-1)$-th element, then all the associations in the *indices* array between them (including the first element) are shifted to the right by i positions. Then, or in case the comparison fails, the $(i-1)$-th element of the *new_assoc_ids* is copied to the *indices* array in the position specified by *o_ptr*. The *o_ptr* pointer is decremented anytime an association is written in the *indices* array.

4.4.2 EAC CSR Condensed

The co-association matrix is symmetric, which means that only half is necessary to describe the whole matrix. That fact has consequences on both memory usage and computational effort on building the matrix. It translates in a asymptotical reduction to 50% of the original required memory. Furthermore,

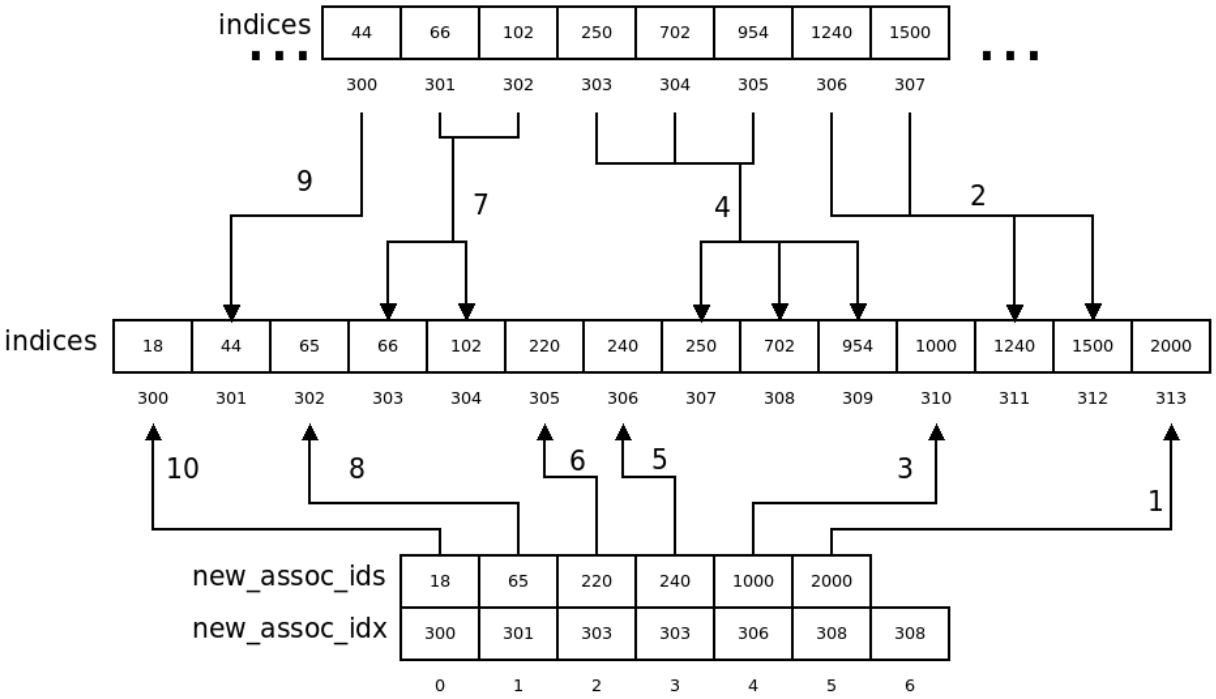

Figure 4.3: Inserting a cluster from a partition in the co-association matrix. The arrows indicate to where the indices are moved. The numbers indicate the order of the operation.

Algorithm 2 Sort the *indices* array in the interval of a pattern n.

procedure SORT_INDICES($indices, data, indptr, degree, n, new\_assocs\_ptr, new\_assocs\_ids, new\_assocs\_idx$)
    $new\_assocs\_idx[new\_assocs\_ptr] = indptr[n] + degree[n]$
    $i = new\_assocs\_ptr$
    $o\_ptr = indptr[n] + new\_assocs\_ptr + degree[n] - 1$
    while $i \geq 1$ **do**
        $start\_idx = new\_assocs\_idx[i-1]$
        $end\_idx = new\_assocs\_idx[i] - 1$
        while $end\_idx >= start\_idx$ **do**
            $indices[o\_ptr] = indices[end\_idx]$
            $data[o\_ptr] = data[end\_idx]$
            $end\_idx- = 1$
            $o\_ptr- = 1$
        $indices[o\_ptr] = new\_assocs\_ids[i-1]$
        $data[o\_ptr] = 1$
        $o\_ptr- = 1$
        $i- = 1$

only half the operations are made since only half the matrix is accessed, which also accelerates the building of the matrix. There is, however, a small overhead for translating the two dimensional index to the single dimensional index of the upper triangle matrix. When using a sparse matrix according to the EAC CSR scheme described above, there is no direct memory usage reduction. However, the number of binary searches performed by inserting new associations is half which has a significant impact on the computation time relative to the complete matrix.

Even though there is no direct memory reduction for switching to the condensed matrix form, this scheme does open possibilities for it. Previously, the number of associations for each pattern (number of non zero values in each row) remained constant throughout the whole set of patterns. However, using a condensed scheme means that the number of associations decreases as one steps further to the end of the set. An example of this can be seen in the plot of the number of associations per pattern in a complete and condensed matrix of Fig. 4.4. It is clear that, since the number of associations that is actually stored in the matrix decreases throughout the matrix, the pre-allocated memory for each pattern can decrease accordingly. One possible strategy, illustrated in Fig. 4.4, is to decrease the maximum number of associations linearly. In the example, the first 5% of patterns have the 100% of the maximum number of associations and it decreases linearly until 5% of the maximum number of associations for the last pattern.

Table 4.2 shows the memory usage of the different co-association matrix strategies in the general case and for an example of 100000 patterns. The memory consumption for the *sparse condensed linear* type of matrix if given for the parameters presented above for Fig. 4.4.

Table 4.2: Memory used for different matrix types for the generic case and a real example of 100000 patterns. The relative reduction (R.R.) refers to the memory reduction relative to the type of matrix above, the absolute reduction (A.R.) refers to the reduction relative to the full complete matrix.

Type of matrix	**Generic**	**Memory [MBytes]**	**R.R.**	**A.R.**
Full complete	N^2	9536.7431	-	-
Full condensed	$\frac{N(N-1)}{2}$	4768.3238	0.4999	0.4999
Sparse constant	$N \times max\_assocs$	678.8253	0.1423	0.0711
Sparse condensed linear	$0.54 \times N \times max\_assocs$	372.8497	0.5492	0.0390

4.5 Final partition recovery

This section will present the considered candidates for the final step of EAC. A GPU version of SL is described in section 4.5.1. External algorithms are a candidate solution and this approach is presented in section 4.5.2. This solution is based on storing the co-association matrix on disk, performing the expensive computation (memory and speed wise) of *argsort* and then processing the matrix in batches until the final MST is extracted.

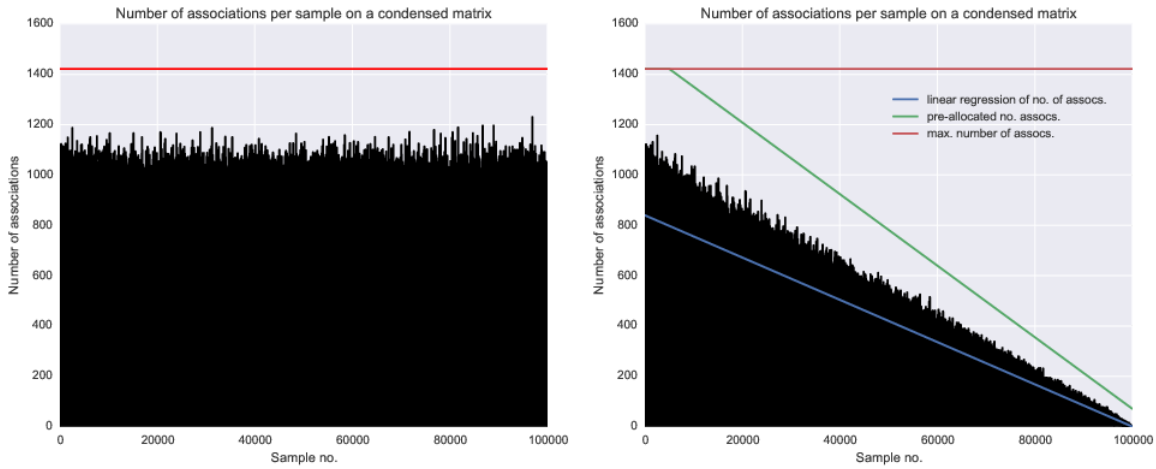

Figure 4.4: The left figure shows the number of associations per pattern in a complete matrix; the right figure shows the number of associations per pattern in a condensed matrix. Dataset used is a bidimensional mixture of 6 Gaussians with a total of $100\,000$ patterns.

4.5.1 Single-Link and GPGPU

Single-Link is an inherently sequential algorithm which means an efficient GPU version is hard to implement. However, SL can be performed by computing the MST and cutting edges until we have the desired number of clusters, as described in chapter 3. Considerable speed-ups are reported in the literature for MST solvers in the GPGPU paradigm. The considered solution uses the efficient parallel variant of Borůvka's algorithm [49]. After the necessary pruning of the MST edges has been performed to achieve the desired number of clusters, the output MST is fed to the labeling algorithm which will provide the final clustering.

Generating the MST

The output of the Borůvka's algorithm is a list of the indices of the edges constituting the MST. These indices point to the *destination* of the original graph. The original algorithm [49] assumes connected graphs, but this is not guaranteed in EAC's co-association matrix. In graph theory, given a connected graph $G = (V, E)$, there is a path between any $s, t \in V$, where V is the set of vertices in G and E is the set of edges that connects the vertices. In an unconnected graph, this is not the case and unconnected subsets are called components, i.e. a connected component $C \subset V$ ensures that for each $u, v \in C$ there is a path between u and v. The present implementation follows the original literature [49] for the exception of a modification that allows it to process unconnected graphs. The issue of unconnected graphs was solved in the first step (finding the minimum edge connected to each vertex or supervertex). If a vertex has no edges connected to it (an outdegree of 0 since all edges are duplicated to cover both directions) then it is marked as a mirrored edge. This means that the independent components will be marked as supervertices in all subsequent iterations of the algorithm. The overhead of having these redundant vertices is low since the number of independent components is typically low compared to the number of vertices in the graph and the processing of such vertices is very fast. As a consequence, the stopping criteria becomes the lack of edges connected to the remaining vertices, which is the same as

saying that all elements of the *outdegree* array are zero. This condition can be checked as a secondary result of the computation of the new *first_edge* array. This step is performed by applying an exclusive prefix sum over the *outdegree*. The prefix sum was implemented in such a way that it returns the sum of all elements, which translates in very low overhead to check this condition. The final output is the MST array and the number of edges in the array. The later is necessary because the number of edges will be less than $|V| - 1$ when independent components exist, and also because the MST array is pre-allocated in the beginning of the algorithm when the number of edges is not yet known.

Number of clusters and pruning the MST

The number of clusters can be automatically computed with the lifetime technique or be supplied. Either way, a list (*mst_weights*) with the weights of each edge of the MST is compiled and ordered. The list of edges is also ordered according to the order of the *mst_weights*. If the number of clusters k was given, the algorithm removes the $k - 1$ heaviest edges. If there are independent components inside the MST those are taken into consideration before removing any edges. If the number of clusters k is higher than the number of independent components the final number of clusters will be the number of independent components.

To compute the number of clusters (which results in a truly unsupervised method) the lifetimes are computed. In the traditional EAC, lifetimes are computed on the weights of the clusters by the order they are formed. With the MST, the lifetimes are computed over the ordered *mst_weights* array, which is equivalent. If there are independent components, an extra lifetime is computed from the representative weight connecting independent components. This lifetime will serve as the threshold between choosing the number of independent components as the number of clusters or looking into the lifetimes within the MST. This is because links between independent vertices are not included in the MST. For this reason, the lifetime for going from independent edges to the heaviest link in the MST (where the first cut would be performed) is computed separately. If the maximum lifetime within the MST is bigger than the threshold, than the number of clusters is computed as in traditional EAC plus the number of independent components. Otherwise, the independent components will be the final clusters. Most of this process can be done by the GPU. Library kernels were used to sort the array and compute the $argmax$, and a simple kernel was used to compute the lifetimes.

Building the new graph

The final MST (after performing the pruning) is then converted into a new, reduced graph. The function responsible for this produces a graph in CSR format from the original graph and the final selection of edges composing the MST. The function has to count the number of edges for each vertex, compute the origin vertex of each edge (the original *destination* array only contains the destination vertices) and, with that information, build the final graph. This process can be done by the GPU with simple mapping kernels and a modified binary search for determining the origin vertex.

Final clustering

The last step is computing the final clusters. Any incision in the MST translates in independent components in the constructed graph. This means that the problem of computing the clusters translates into a problem of finding independent connected components in a graph, a problem that usually goes by the name of Connected Component Labeling. To implement this part in the GPU, the aforementioned Borůvka algorithm was modified to output an array *labels* of length $|V|$ such that the $i-th$ position contains the label of the $i-th$ vertex. To this effect, the flow of the algorithm was slightly altered as shown in Figure 4.5. The kernel dealing with the MST was removed and a kernel to update the labels at each iteration, shown in Algorithm 3, was implemented. In the first iteration of the algorithm the converged colors are copied to the labels array. In every iteration the kernel to update the labels takes in the propagated colors and the array with the new vertex IDs. For each vertex in the array, the kernel first takes in the color of the current vertex and maps it to the new color (one should notice that the color is actually a vertex ID and that that vertex has had its color updated). Afterwards, the kernel maps the new color with the new vertex ID that color will take, to keep consistency with future iterations.

Algorithm 3 Update component labels kernel

1: **procedure** UPDATE_LABELS($vertex\_id, labels, colors, new\_vertex$)
2: $curr\_color \leftarrow labels[vertex\_id]$
3: $new\_color \leftarrow colors[curr\_color]$
4: $new\_color\_id \leftarrow new\_vertex[new\_color]$
5: $labels[vertex\_id] \leftarrow new\_color\_id$

Memory transfer with the GPU

The whole algorithm of computing the SL clustering has been implemented in the GPU, having the optimization of memory utilization in mind. The control logic is the only thing that is processed by the host. Transferring the initial graph is the most relevant memory transfer. It has to be transfered twice: first for computing the MST and then to build the processed MST graph. This happens because the initial device arrays used for the graph are deallocated to give space for the arrays of subsequent iterations of the MST algorithm. This implementation design had in mind memory consumption and could easily be avoided with the cost of having to store the bigger initial graph for the entire duration of the MST computation, which might be worthwhile if the GPU memory is abundant. The final labels array is transfered back to the host in the end of computation, but its size is small relative to the size of the original graph. Furthermore, because the control logic is processed by the host and it is dependent on some values computed by the device, extra memory transfers of single values (e.g. number of vertices and number of edges on each iteration) are necessary. These, however, may be safely dismissed since they are of little consequence in the overall computation time.

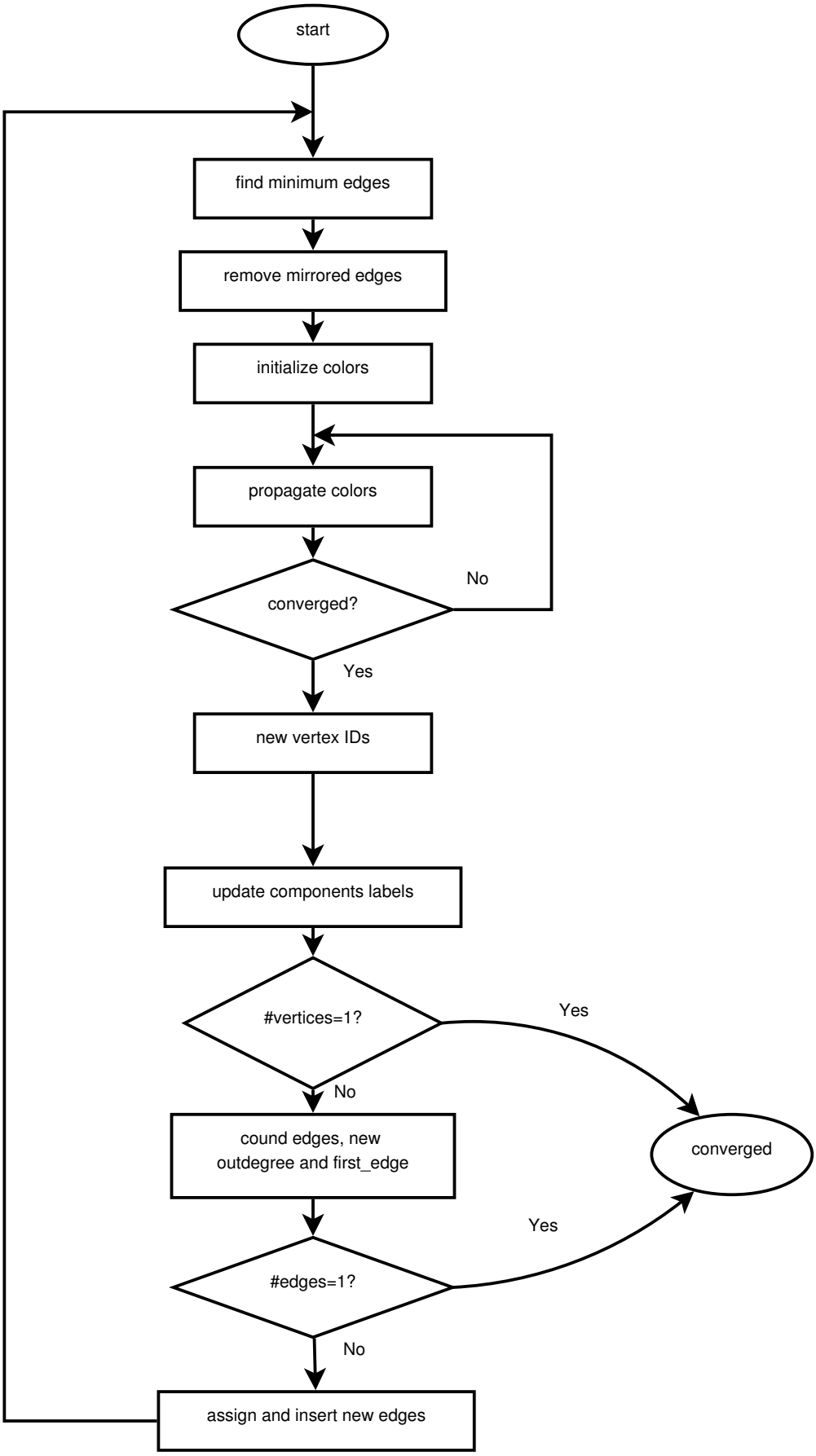

Figure 4.5: Diagram of the connected components labeling algorithm used.

Contrast between implementations

At this point it should be noted, for future reference, the contrast between the technology stack used by Da Silva Sousa et al. [49] and the one used here. Da Silva Sousa et al. [49] used the native CUDA language to program the GPUs and highly optimized libraries. The implementation in the present work used none of the above. Accordingly, some performance may be lost. This if specially true for some highly optimized operations that can be found in some libraries, since those use optimization mechanisms that are not available in the used CUDA API offered by the Numba package. An evaluation of the interoperability between the technology stacks was made but, currently, this does not seem feasible. Nevertheless, and whenever possible, we tried to close the gap so that these shortcomings become less noticeable in the overall performance.

4.5.2 Single-Link and external memory algorithms

The co-association matrix can become very large for large datasets. Even using the EAC CSR method to reduce memory usage, it occupies a significant portion of main memory. Furthermore, the algorithm to compute a MST brings additional space complexity that make it infeasible to perform the final partition recovery on a large co-association matrix in main memory. External memory algorithms address this issue. External memory algorithms (or out-of-core algorithms) refers to algorithms that are based on disk (or other large capacity but typically low latency storage technology), usually by loading small batches to main memory, processing them, saving the results and repeating until the whole computation is done. This section describes the process of building the MST with low memory usage. The details of converting the MST in a Single-Link clustering are described in chapter 3 and omitted here.

Kruskal's algorithm and implementation

The sequential MST algorithm used was Kruskal [50], which describes three approaches for finding a MST. The SciPy library offers an efficient implementation for the following construct (taken directly from the original paper of Kruskal's algorithm):

> CONSTRUCTION A. Perform the following step as many times as possible: Among the edges of G not yet chosen, choose the shortest edge which does not form any loops with those edges already chosen. Clearly the set of edges eventually chosen must form a spanning tree of G, and in fact it forms a shortest spanning tree.

If the graph is connected, the algorithm will stop before processing all edges when $|V| - 1$ edges are added to the MST. Within the EAC context, it is very common for the co-association graph to have independent components which translates in every edge being processed. It should be noted that this implementation works on a sparse matrix in the CSR format.

One of the main steps of the implementation is computing the order of the edges of the graph without sorting the edges themselves, an operation called *argsort*. To illustrate this, the *argsort* operation on the array $[4, 5, 2, 1, 3]$ would yield $[3, 2, 4, 0, 1]$ since the smallest element is at position 3 (starting from 0), the

second smallest at position 2, etc. This operation is useful to avoid computing the shortest edge in every iteration. Doing so would increase time complexity since a sorting algorithm may have an average time complexity to $O(nlogn)$ (QuickSort algorithm) while a single minimum has a time complexity of $O(n)$. Computing the minimum at every iteration when every edge must be processed means that there will be $|E|$ iterations and so the total time complexity for the minimum operation alone will be $O(E^E)$ if processed edges are not removed or $O(E!)$ if they are. These are much higher than Kruskal's time complexity of $O(ElogE)$. The result of this operation is an array of length $|E|$ (i.e. the number of associations in EAC), which means it will occupy at least the same size as the array containing the weights of the edges. However, the total size is typically 8 times larger for EAC since the data type of the weights uses only one byte and the number of associations is very large, forcing the use a 8 byte integer for the *argsort* output array. This is the real motivation to store the co-association matrix in disk and use an external sorting algorithm.

Kruskal's implementation with an external sorting algorithm

The *PyTables* library [95], which is built on top of the *HDF5* format [96], was used for storing the graph, performing the external sorting for the *argsort* operation and loading the graph in batches for processing. This implementation starts by storing the CSR graph to disk. However, instead of saving the *indptr* array directly, an expanded version is stored instead. The expanded version will be of the same length as the *indices* array and the i-th element contains the origin vertex (or row) of the i-th edge. This way, a binary search for discovering the origin vertex becomes unnecessary.

Afterwards, the *argsort* operation is performed by building a completely sorted index (CSI) of the *data* array of the CSR matrix. The details of CSI implementation fall outside the scope of this dissertation but are explained in further detail in [97]. It should be noted that the arrays themselves are not sorted. Instead, the CSI allows for a fast indexing of the arrays in a sorted manner (according to the order of the edges). The process of building the CSI has a very low main memory usage that can be disregarded.

The SciPy implementation of Kruskal's algorithm was modified to work with batches of the graph. This was easily implemented just by making the additional data structures used in the building of MST persistent between calls of the function. The new implementation loads the graph in batches and in a sorted manner, e.g. first load a batch of the 1000 smallest edges, then a batch of the next 1000 smalled edges, etc. Each batch must be processed sequentially since the edges must be processed in a sorted manner, which means that there is no possibility for parallelism in this process. Typically, the batch size is a very small fraction of the size of the edges, which means that the total memory usage for building the MST is overshadowed by the size of the co-association matrix. The time complexity for building the CSI is higher than computing the *argsort* operation, but the formal time complexity is not reported in the source [97]. As an example, for a $500\,000$ pattern set the SL-MST approach took 54.9 seconds while the external memory approach took 2613.5 seconds - two orders of magnitude higher.

4.6 Overview of the developed work

This chapter exposed a great deal of the actual developed work. It covered solutions and implementations related to the three phases of EAC. For the production of the ensemble, two quantum clustering algorithms and a GPU parallel K-Means variant were implemented. These are algorithms existing in the literature (presented in chapter 3) and implementation details were presented when relevant. For addressing the computation complexity of the second phase of EAC, a novel method **EAC CSR** for building the co-association matrix was designed and implemented. Finally, three approaches are presented for the last phase of EAC. An implementation of a parallel GPU MST algorithm based on Borůvka's algorithm was presented along with a labeling algorithm for a forest of MSTs. Also, an implementation of SL-MST based on Kruskal's algorithm and an external memory variant of it were presented. The core of the external memory variant is based on using an external algorithm for sorting a very big array stored in disk and, although this is not something new, its application within the SL clustering framework was not found in literature.

4.7 Guidelines for using the different solutions

The final proposed solution is composed by the parallel K-Means implementation described, the EAC CSR method and the external memory variant for performing Single-Link. The implementations have several parameters available for tinkering. A general guideline of what is available and when should it be used is presented in this chapter.

It is recommended that the execution of the parallel K-Means algorithm be done with the optimized memory transfer, so as to minimize communication between GPU and host. When the combined size of the dataset, centroid set, labels and distance arrays exceed the available device memory, the pure sequential version of K-Means should be used. An optimized sequential version is offered alongside the implementation of its parallel counterpart.

The choice of parameters of the method for building the co-association matrix is a simple one to make. The available choices are:

- if the matrix should be condensed (filling only the upper triangular) or not,
- if the matrix should be sparse or not;
- within the sparse matrices, if a constant or linear memory allocation should be used.

The condensed version of the matrix is always preferred. Not only does it occupy less than half of the memory, it takes less time to build and completely describes the co-association matrix. Furthermore, when this is paired with a sparse strategy, the final clustering is also nearly twice as fast. A sparse representation should be chosen whenever $n(n-1)/2$ times the size of the data type used (typically unsigned 1 byte integer) exceeds the available memory, where n is the number of patterns in the dataset. The linear memory allocation is the ideal choice when a sparse representation of the condensed matrix is used, since half the memory is saved.

For the final clustering, the SLINK algorithm must be paired with a fully allocated matrix while the SL-MST strategy must be paired with a sparse representation. Then, the final choice to make is if one should use the main memory approach for the final Single-Link clustering or the external memory approach. Here, again, the decision is straightforward. Typically if the sparse co-association matrix exceeds half of the available main memory, a external memory approach should be chosen. The reason for this is that one of the crucial steps of the final clustering will almost double the memory used.

Chapter 5

Results and Discussion

The present chapter is dedicated to the results relevant to the work produced and their associated interpretation and subsequent discussion. Results include the reviewed quantum clustering algorithms, the parallel GPU K-Means, a brief analysis of sparse matrix building performance, performance analysis of GPU Borůvka, validation of the proposed solution against the original implementation, a thorough study on different properties of EAC and performance of the proposed solution in several large real world data sets.

5.1 Experimental environment

All experiments were carried out in one of three distinct machines that will be referred to as **Alpha**, **Bravo** and **Charlie**. Their CPU and GPU hardware configurations are described in Tables 5.1, 5.2 and 5.3, respectively. Besides, Charlie has a *Seagate ST2000DM001* 7200 RPM spinning disk and a *Samsung 840 EVO* Solid State Drive, informations relevant for the third phase of EAC.

Software wise, all machines are running Linux based operating systems. Alpha and Bravo are using the Ubuntu 14.04 and 12.04, respectively, with a graphical interface. Whether the machine is running a graphical interface or not is important because the amount of time a GPU kernel can take when the GPU is being used as a display device is severely constrained. Charlie is running Fedora 21 without a graphical interface.

Table 5.1: **Alpha** machine specifications.

	CPU	**GPU**
# Devices	1	1
Manufacturer	Intel	NVIDIA
Model	i3-2310M	GT 520M
Launch date	Q1'11	Q1'2011
Architecture	Sandy Bridge	Fermi
# Cores	2	48
Clock frequency [Mhz]	2100	1480
L1 Cache	64KB IC [a] + 64KB DC [b]	16/48 KB/SM [c]
L2 Cache	512KB	n/a
L3 Cache	3 MB	n/a
Memory [GB]	4	1
Max. memory bandwidth [Gbps]	21.3	12.8

[a]Instruction Cache (IC)
[b]Data Cache (IC)
[c]Each Streaming Multiprocessor has 64 KB of on-chip memory that can be configured as either 16KB of L1 cache and 48 KB of shared memory, or vice versa.

Table 5.2: **Bravo** machine specifications.

	CPU	**GPU**
# Devices	1	1
Manufacturer	Intel	NVIDIA
Model	i7-4930K	Quadro K600
Launch date	Q3'13	Q1'2013
Architecture	Ivy Bridge	
# Cores	6	192
Clock frequency [Mhz]	3400	876
L1 Cache	192 KB IC [a] + 192 KB DC [b]	16/48 KB/SM [c] + 48KB DC [d]
L2 Cache	1,5 MB	1.5 MB
L3 Cache	12 MB	n/a
Memory [GB]	32	1
Max. memory bandwidth [Gbps]	59,6	28,5

[a]Instruction Cache (IC)
[b]Data Cache (IC)
[c]Each Streaming Multiprocessor has 64 KB of on-chip memory that can be configured as either 16KB of L1 cache and 48 KB of shared memory, or vice versa.
[d]The Kepler architecture has an extra read-only 48KB of Data Cache at the same level of the L1 cache.

Table 5.3: **Charlie** machine specifications.

	CPU	GPU
# Devices	1	1
Manufacturer	Intel	NVIDIA
Model	i7 4770K	K40c
Launch date	Q2'13	Q4'13
Architecture	Haswell	Kepler
# Cores	4	2880
Clock frequency [Mhz]	3500	745
L1 Cache	128 KB IC [a] + 128 KB DC [b]	16/48 KB/SM [c] + 48KB DC [d]
L2 Cache	1 MB	1.5 MB
L3 Cache	8 MB	n/a
Memory [GB]	32	12
Max. memory bandwidth [Gbps]	25,6	288

[a] Instruction Cache (IC)
[b] Data Cache (IC)
[c] Each Streaming Multiprocessor has 64 KB of on-chip memory that can be configured as either 16KB of L1 cache and 48 KB of shared memory, or vice versa.
[d] The Kepler architecture has an extra read-only 48KB of Data Cache at the same level of the L1 cache.

5.2 Quantum Clustering

This section presents performance and validity results of Quantum K-Means and Horn and Gottlieb's algorithm. All results were obtained using machine Alpha.

5.2.1 Quantum K-Means

The testing was aimed at benchmarking both accuracy and speed. The input used was synthetic data, namely, Gaussian mixtures with variable number of clusters and features.

The tests were performed using 10 oracles, a qubit string length of 8 and 100 generations per round. The classical K-Means was executed using the *k-means++* centroid initialization method to make for a fairer comparison, since QK-Means performs several operations (initialization and collapse of oracles) at the beginning of the algorithm. Furthermore, the performance results for K-Means alone refer to $num.oracles \times num.generations \times factor$ runs, where $factor$ is an adjustable multiplier. Each test had 20 rounds to allow for statistical analysis of the results. The stopping criteria for all classical K-Means runs was the error between the centroids of two subsequent iterations, more specifically, when the centroids of two iterations differed by less than 0.001.

All tests were done with 6 clusters (natural number of clusters). Two tests were done with the two dimensional dataset: one with a $factor = 1.10$ (increase initializations by 10%) and another with $factor =$

1. These tests will be called T1 and T2, respectively. The test was done with the six dimensional dataset (T3) using $factor = 1.10$.

Performance results are presented in Table 5.4. The mean computation time of classical K-Means is an order of magnitude lower than that of QK-Means. However, the solution chosen in classical K-Means was the one with lowest sum of squared euclidean distances of points to their attributed centroid. To analyze the influence of the Davies-Bouldin (DB) index, it was computed on all classical K-Means solutions and used as the criteria to choose the best solution. When this is done, we can see in Table 5.4 that the total time of classical K-Means is actually higher that that of QK-Means in T1 and T3, but this is only due to the 1.10 multiplier on the number of initializations. In T2, the computation times become very similar with only a 2% difference between these two variants. Results show that most computational cost (88% on T2) lies on the evaluation of the solutions obtained from each oracle, i.e. computing the DB index. This is a costly but necessary step in this algorithm.

Table 5.4: Timing results for the different algorithms in the different tests. Fitness time refers to the time that took to compute the DB index of each solution of classical K-Means. All time values are the average over 20 rounds and are displayed in seconds.

Dataset	Algorithm	Mean	Variance	Best	Worst
T1	QK-Means	62.02642975	0.077065212	61.620424	62.579969
bi36	K-Means	6.4774672	0.002501651	6.352554	6.585451
	K-Means + fitness	70.2238286	0.022223755	69.889105	70.548572
	fitness	63.7463614	0.019722105	63.536551	63.963121
T2	QK-Means	64.22347165	0.056559152	63.807367	64.807373
bi36 noFactor	K-Means	5.71167475	0.004903253	5.581391	5.877091
	K-Means + fitness	62.7021533	0.066919692	63.417207	62.180021
	fitness	56.99047855	0.062016439	56.59863	57.540116
T3	QK-Means	74.4917966	0.067688312	74.12105	74.976446
sex36	K-Means	8.291648	0.007015777	8.160859	8.426203
	K-Means + fitness	72.36315915	0.05727269	71.856457	73.031841
	fitness	64.07151115	0.050256913	63.695598	64.605638

DB index results are presented in Table 5.5. These results show that the quality of the solutions from K-Means and QK-Means do not differ significantly on these datasets. The results presented before steered the direction of the analysis to a ”fairer” comparison. Yet, the main requirement for the target application of this algorithm is speed. In this regard, it is several orders of magnitude slower than the classical K-Means, since the K-Means performance results refer to many runs. This, allied with the fact that the quality of the solutions does not differ much in the two algorithms and the fact that good quality is not necessary in the target application, makes the use of this algorithm prohibitive in the EAC context.

5.2.2 Horn and Gottlieb's algorithm

For measuring the performance of Horn and Gottlieb's algorithm, several mixtures of 4 Gaussians with different number of patterns and dimensions were produced. Table 5.6 presents the execution times for each of these datasets. It can be seen that the execution time of this algorithm is rather high even for small datasets as the ones presented, since this algorithm is being analyzed with the goal of speed

Table 5.5: All values displayed are the average over 20 rounds, except for the Overall best which shows the best result in any round. The values represent the Davies-Bouldin fitness index (low is better).

Dataset	Algorithm	Best	Worst	Mean	Variance
T1	QK-Means	15.42531927	32.29577426	19.94704511	21.23544567
	K-Means	15.42531927	25.44913817	16.25013365	1.216919278
T3	QK-Means	22.72836641	65.19984617	36.10699242	78.14043743
	K-Means	22.71934191	46.72231967	26.18440481	22.96730826

optimization. More than 1 hour for a small dataset such as $10\,000$ patterns is prohibitive for application in the EAC context.

Table 5.6: Time of computation of Horn and Gottlieb [75] algorithm for a mixture of 4 Gaussians of different cardinality and dimensionality.

Cardinality	Dimensionality	Time [s]
10	2	0.035382
10	3	0.411391
10	4	0.385114
10	5	0.429747
100	2	2.954650
100	3	3.322593
100	4	3.743720
100	5	4.143823
1000	2	52.840666
1000	3	60.293262
1000	4	68.225671
1000	5	81.523212
10000	2	3009.678259
10000	3	3418.342830
10000	4	3956.289064
10000	5	4918.185844

In spite of its computational complexity, the accuracy of the algorithm was tested on the Iris and Crab datasets, taken from the UCI Machine Learning repository [98]. The Iris dataset has 150 patterns, 4 features and 3 classes where 2 are overlapping. The Crab dataset has 200 patterns, 5 features and 4 classes where 2 pairs of classes are overlapping. Principal Component Analysis (PCA) was applied to both datasets before clustering. An accuracy as high as 86% was obtained for the Iris dataset when using the first and second principal components (PC), and as high as 82% when using all PCs. For the Crab dataset an accuracy of 81.5% was obtained for the second and third PCs (PCs chosen to reproduce the results of the original source of the algorithm), 63% when using all PCs. However, when applied to the unprocessed data the accuracy was only 34% .

5.3 Parallel K-Means

This section will present results relevant to the GPU parallel K-Means. Its purpose is to understand how dataset complexity (number of patterns, features and centroids) affect the speed-up of the GPU version over the CPU. All tests were executed on machine Charlie and the block size was maintained constant

at 512.

5.3.1 Analysis of speed-up

Observing Figures 5.1 and 5.2, it is clear that the number of patterns, dimensions and centroids influence the speed-up. It should be noted that whenever the number of centroids was superior to 70% of the number of patterns, that particular test case was not executed. For the simple case of 2 dimensions (Fig 5.1), the speed-up increases with the number of patterns. However, there is no speed-up when the overall complexity of the datasets is low. For 2 clusters, there is no speed-up before of $100\,000$ patterns. And even after that mark, the speed-up is not significant relative to higher number of clusters. The reason for this is that the benefits from the parallelization of such simple problems does not outweigh the cost of the memory transfers. On the other hand, for a large number of clusters, there is speed-up for any number of patterns processed. Not only that, that speed-up is highest of any other case with inferior number of clusters. The reason for this is that the total amount of work increases linearly with the number of clusters but is diluted by the number of threads that can execute simultaneously.

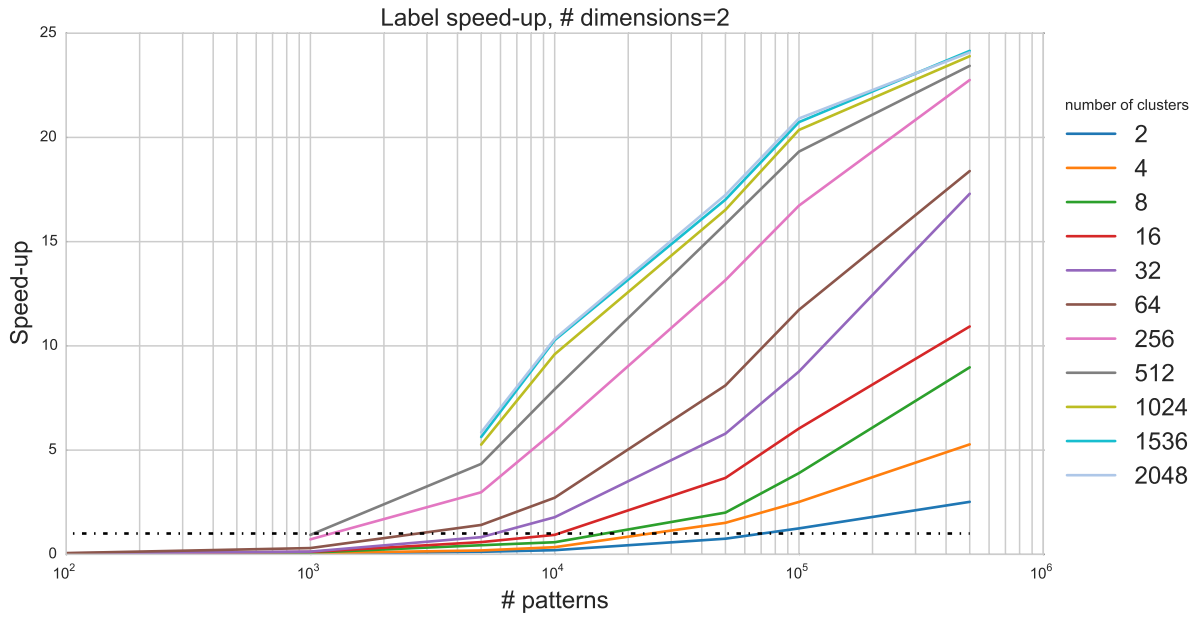

Figure 5.1: Speed-up of the labeling phase for datasets of 2 dimensions and varying cardinality and number of clusters. The dotted black line represents a speed-up of one.

However, as the number of dimensions increases (observe Fig. 5.2), the speed-up increases until a certain number of patterns and then decreases. Here, the initial number of patterns for which there is a speed-up is lower than in the low dimensionality case and the number of clusters plays less an influence on the speed-up. It is believed that the reason for this is related to the implementation itself. The current parallel implementation does not use shared memory, which is fast. As such, for every computation, each thread fetches the relevant data from global memory which is significantly slower. As the number of dimensions increases, the amount of data that each thread must fetch also increases. Furthermore, since the number of dimensions affects both data points and centroids, if the number of dimensions

increases by 2 the number of fetches to memory increases by 4. So, the speed-up increases with the dataset complexity until a point where the number of fetches to memory starts having a very significant effect on the execution time, decreasing the speed-up close to 50%.

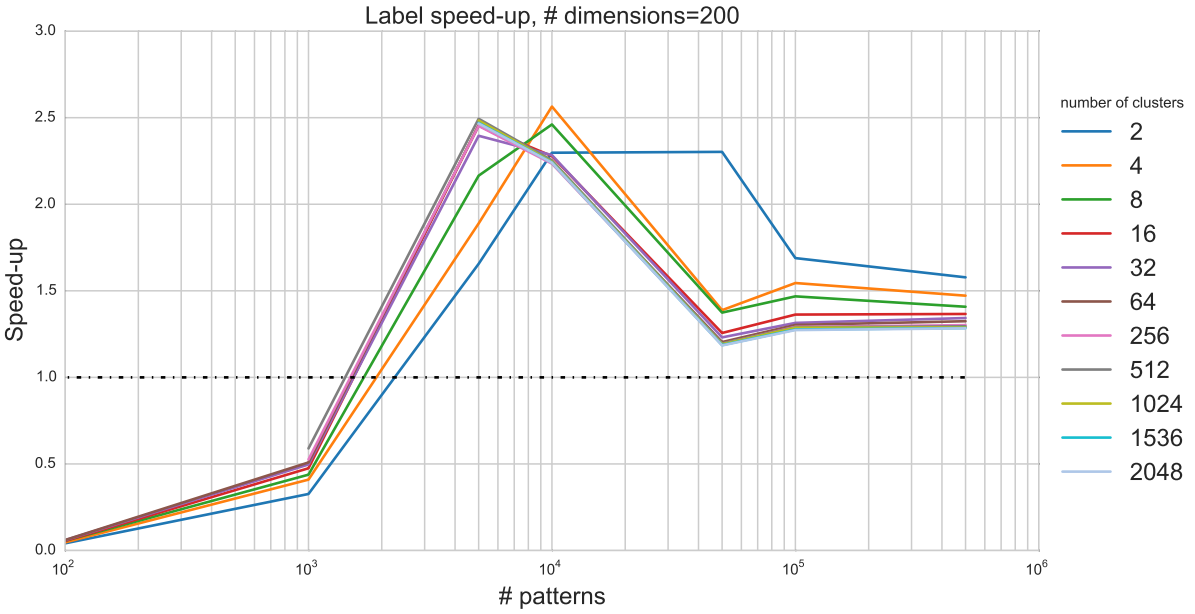

Figure 5.2: Speed-up of the labeling phase for datasets of 200 dimensions and varying cardinality and number of clusters. The dotted black line represents a speed-up of one.

5.3.2 Effective bandwidth and computational throughput

Effective bandwidth and throughput are two useful metrics to measure the efficiency of CUDA programs. The effective bandwidth was computed by summing the times of transferring data to and fro the device divided by the total amount of data transfered and is usually represented in GBytes/s. The computational throughput is usually represented in GFLOP/s (Giga-FLoating-point OPerations per second). These metrics were computed from the results and a statistical overview is presented in Table 5.7. The results refer only to the labeling phase to make a fair comparison between CPU and GPU, although considering both phases would not alter significantly the results since the update phase represents a small fraction of the computational complexity. The computational throughput of the GPU is more than 3 times higher than that of the CPU, on average. However, it is interesting to note that the minimum GPU throughput is significantly lower than the CPU. This is because of what was seen in previous sections, where the dataset complexity is too low for the overhead associated with using the GPU to outweigh the benefit of the parallel computation. Furthermore, it should be noted that the effective metrics of the GPU are well below the maximum theoretical presented in the device specifications, which are a bandwidth of 288 GB/s and a throughput of 4.29 TFLOP/s. This suggests that the GPU is underused on the presented test cases. The same reason for the lower speed-ups on higher dimensional problems may explain the GPU underuse.

Table 5.7: Effective bandwidth and computational throughput of labeling phase computed from results taken from running K-Means over datasets whose complexity ranged from 100 to $10\,000\,000$ patterns, from 2 to 1000 dimensions and from 2 to 2048 centroids.

	GPU bandwidth [GB/s]	GPU throughput [GFLOP/s]	CPU throughput [GFLOP/s]
mean	2.90	3.65	1.04
std	2.27	4.51	0.33
min	0.00	0.00	0.02
25% percentile	0.56	1.54	0.87
50% percentile	2.89	1.71	1.17
75% percentile	5.31	4.16	1.29
max	6.04	21.91	1.44

5.3.3 Influence of the number of points per thread

The number of patterns each thread processes (PPT) may influence performance as well. To evaluate this hypothesis, several runs over the datasets of $500\,000$ patterns with different points per thread were executed. A brief statistical analysis of the results is presented in Table 5.8. The average speed-up almost doubled when executing 2 PPT. For more than 2 PPT, the speed-up seemed to decrease with an increase of the number of PPT. Since the labeling kernel was not optimized for reducing the number of memory calls when processing more than one PTT, the increase in speed-up may be justified by the reduced overhead of calling less blocks of threads. The fraction of the threads that did not execute any patterns increased with the PPT, which may be the cause for the decrease of speed-up with an increase of PPT after 2.

Table 5.8: Speed-up obtained in the labeling phase for different number of patterns per thread (PPT).

	Speed-up				
	PPT = 1	PPT = 2	PPT = 4	PPT = 8	PPT = 16
mean	5.9	10.1	3.7	3.1	2.1
std	7.5	13.4	4.0	3.0	1.3
min	1.2	2.4	1.5	1.4	1.3
25% percentile	1.3	2.6	1.6	1.5	1.4
50% percentile	2.0	2.7	1.7	1.6	1.4
75% percentile	4.8	9.4	2.1	1.9	1.7
max	24.2	46.7	12.8	9.9	4.9

5.4 Building the co-association matrix with different sparse formats

The purpose of this section is to present brief results concerning the time that took to build a co-association matrix for different types of matrices. The ensemble from which the co-association matrices are built has 100 partitions and was produced from a mixture of 6 Gaussians with 5000 patterns. Only the upper triangular (condensed) matrix was built. The types of matrices under test are: fully allocated (a ”normal” matrix), LIL, DOK, CSR, an optimized fully allocated and the proposed EAC CSR. The SciPy's

LIL, DOK and CSR implementations were used. All tests were executed in machine Bravo.

The time that took to update the first partition and the total time were recorded for the different types of matrix. The results are presented in Table 5.9 and also in Fig. 5.3. For the CSR format only the first partition was updated, since it took a very long time to update just the first partition. A rough estimate for the time it would take to update the whole matrix is around 15 hours, 100 times the time it took to update the first partition. Observing the other timings, and for the exception of the EAC CSR matrix, this estimate should not be too far off. The reason that the first partition update of the EAC CSR matrix was so much faster is that it only requires a simple copy of the partition to the data structure.

It is clear from the results that the optimized versions are much faster than any of the others. These results focus on providing a justification for the design and implementation of a novel method of building the co-association matrix: a fully allocated matrix consumes too much memory but available sparse implementations are too slow. For this purpose a small dataset as the one used suffices to demonstrate this point. The difference between the two optimized versions will become clearer on future sections, where a more thorough study covering a wider spectrum of datasets is presented.

Table 5.9: Execution times for computing the condensed co-association matrix using different matrix strategies.

Matrix type (condensed)	Time 1st partition [s]	Time ensemble [s]
Optimzed Fully allocated	0.001	0.139
EAC CSR	0.004	1.470
Fully allocated	0.855	96.000
LIL	5.390	614.000
DOK	12.500	1535.000
CSR	548.000	-

5.5 GPU MST

To test the performance of the GPU MST algorithm, several graphs were used. Most of the graphs are United Stated road network graphs taken from the 9th DIMACS Implementation Challenge [1], the same used in the original source [49]. Furthermore, graphs taken from the co-association matrix of the second step of EAC were used. This is important because, as will become clear, the graphs within the EAC paradigm have different characteristics. All the tests were performed on machine Bravo. The average speed-up obtained by using the GPU version over the sequential one is presented in Table 5.10. Characteristics of the different graphs are also shown so as to illustrate what variables influence the speed-up obtained. It should be noted that a speed-up below 1 is actually a slow-down.

[1] http://www.dis.uniroma1.it/ challenge9/

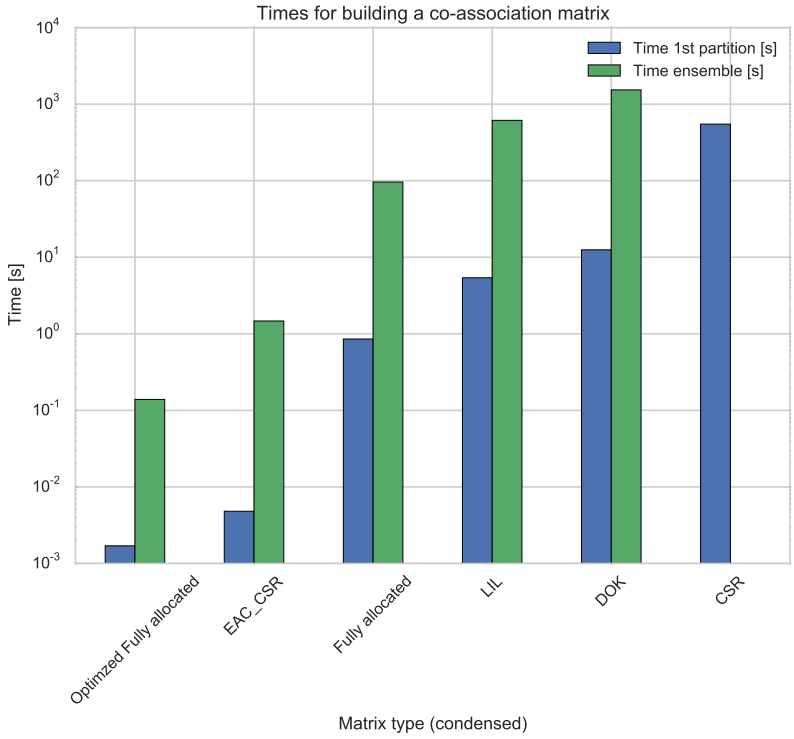

Figure 5.3: Execution times for computing the condensed co-association matrix using different matrix strategies.

Table 5.10: Average speed-up of the GPU MST algorithm for different data sets, sorted by number of edges.

Data set	No. vertices	No. edges	Speed-up [a]	No. edges / vertex	Memory [MBytes]
NY	264347	730100	0.77	2.76	7.59
BAY	321271	794830	0.79	2.47	8.52
COL	435667	1042400	0.99	2.39	11.28
FLA	1070377	2687902	1.39	2.51	28.67
NW	1207946	2820774	1.45	2.34	30.74
NE	1524454	3868020	1.56	2.54	41.14
CAL	1890816	4630444	1.58	2.45	49.75
LKS	2758120	6794808	1.69	2.46	72.88
E	3598624	8708058	1.80	2.42	93.89
W	6262105	15000000	1.94	2.39	163.13
Coassoc 50k [b]	50000	30296070	0.20	605.92	231.52
CTR	14000000	34000000	2.09	2.43	365.82

[a] Average speed-up from 10 rounds of executing the algorithm on each graph.
[b] Co-association matrix of a 100 partition ensemble produced from a mixture of 6 Gaussians with $50\,000$ patterns, using the rule sk=sqrt_2 th=30%.

Although all the graphs presented in Table 5.10 occupy significantly less memory than available in the used machine, the processing of bigger graphs is not possible. The reason for this is that between

each iteration two graphs have to be held in memory: the initial and the contracted. Moreover, the space occupied by the contracted graph will depend on the characteristics of the graph.

The results clearly show that it is possible to obtain speed-ups for computing a MST. This speed-up seems to increase with the size of the graph, with the notable exception of the graph from the EAC context. A note should be made here to bring to attention the contrast between these results and those presented by Da Silva Sousa et al. [49]. The speed-ups observed here are less than those reported by Da Silva Sousa et al. [49]. This is believed to be related with the technology stack used and this topic has been discussed in more depth in chapter 4. To understand how different parameters affect the speed-up of the algorithm, Table 5.11 presents the correlation matrix of these variables.

Table 5.11: Cross-correlation between several characteristics of the graphs and the average speed-up.

	No. vertices	No. edges	No. edges / vertex
Average speed-up	0.692	0.081	-0.654

The row corresponding to the average speed-up is of special relevance. One can observe that the parameters most correlated with the speed-up are the number of vertices and the number of edges per vertex (EPV). The correlation matrix suggests that as one increases the number of vertices, the speed-up will also increase. In fact, if no graphs from the EAC context were present in the results, the same would apply to the number of edges, since the EPV would be very similar. The reason for this is that speed-ups from parallelism are more salient when applied to big datasets, so that the speed-up of the computation itself outweighs the overhead associated with communication between host and device. The EPV is the other parameter that shows has highest (inverse) correlation with the speed-up. This suggests that the relationship between the number of edges and the number of vertices in the graph actually plays a big role in deciding if there will be a speed-up. In essence, this expresses the sparsity of the graph and results manifested speed-ups only for very sparse graphs.

The underlying reason for the poor performance of graphs with high EPV ratio is believed to be that, since the parallel computation is anchored to vertices, the workload per vertex is higher than if the graph had a low ratio. Accordingly, the workload per vertex is higher from the beginning and can increase significantly as the algorithm progresses. Besides, the workload can become highly unbalanced with some threads having to process hundreds of thousands of edges while others only a few thousands, which translates threads not doing any computation when waiting for the others.

The original source [49] of the algorithm doesn't address graphs with a EPV as high as presented here. In that sense, the results here complement those of the original source and suggest an increase in EPV translates in a decrease in speed-up. Still, this serves as motivation for more in-depth studies.

Within EAC paradigm, this algorithm is of little contribution for scaling to large datasets. The most obvious reason is that the EAC method would actually be slower if this algorithm was used. Still, even considering that speed-ups like those reported in literature were possible for EAC co-association graphs, the algorithm requires a double redundancy of edges (which effectively doubles the necessary memory to hold a graph) and at any iteration the device must be able to hold two distinct graphs (the initial and

the contracted). For these reasons, the device memory (which typically is smaller than the host memory) would confine the EAC method to small input datasets.

5.6 EAC Validation

The present section aims to provide results showing that the proposed methods do not alter the overall quality of the results. With this in mind, the results of the original version of EAC, implemented in Matlab, are compared with those of the proposed solution. Several small datasets, chosen from the datasets used by Lourenço et al. [32] and taken from the UCI Machine Learning repository [98], were processed by the two versions of EAC. Furthermore, since the generation of the ensemble is probabilistic and can change the results between runs, the proposed version is processed with the ensembles created by the original version as well. This guarantees that the combination and recovery phases of EAC, which are deterministic when using SL, are equivalent to the original. All data in this section refers to processing done in machine Alpha.

Table 5.12 presents the difference between the accuracies of the two versions. Analyzing these results, it is apparent that the difference is minimal. It should be noted at this point that the original implementation always maps the dissimilarities of the co-association matrix to the range $[0, 1]$. This forces the co-association matrix to have a floating point data type. However, since the number of partitions used is usually less than 255, the proposed version uses unsigned integers of 1 byte to reduce the used memory considerably. The differences in accuracy are thought to come from possible rounding differences and different implementations of core operations between Matlab and Python.

Table 5.12: Difference between accuracies from the two implementations of EAC, using the same ensemble. Accuracy was measured using the H-index.

	Difference between accuracies of implementations	
dataset	True number of clusters	Lifetime criteria
breast_cancer	4.94e-06	2.82e-06
ionosphere	1.65e-06	1.45e-06
iris	3.33e-06	3.33e-06
isolet	1.03e-07	4.08e-07
optdigits	3.79e-06	1.48e-06
pima	3.33e-06	3.33e-06
pima_norm	4.16e-07	4.16e-07
wine_norm	1.12e-07	1.91e-06

Table 5.13 presents the speed-up of the proposed version over the original one. It is clear that speed-up is obtained in all phases of EAC, often by an order of magnitude. This result, combined with the demonstration that the differences in accuracy are negligible, show that the proposed algorithm performs well in small datasets.

Table 5.13: Speed-ups obtained in the different phases of EAC, with independent production of ensembles.

dataset	No. patterns	No. features	No. classes	Production	Combination	Recovery
breast_cancer	683	10	2	50.4	7.5	15.8
ionosphere	351	34	2	21.9	11.3	19.9
iris	150	4	3	19.8	14.5	28.5
isolet	7797	617	26	7.0	6.2	206.3
optdigits	3823	64	10	17.3	10.2	53.0
pima	768	8	2	50.7	141.5	13.9
pima_norm	768	8	2	54.3	132.9	14.4
wine_norm	178	4	3	22.9	14.6	25.3

5.7 EAC

This section will present thorough results concerning several characteristics related to the EAC method. These were the timings of the different parts, how the number of patterns and the different K_{min} rules affected the sparsity of the co-association matrix, the typical number of associations per cluster in each rule, the growth of the number of associations with the different parameters, among others. Two 2-dimensional 10 million pattern mixtures of 6 Gaussians were generated. A variation of the number of dimensions has more interest in the performance characteristics of the production phase. Since the production of the ensemble uses K-Means, detailed results can be found in section 5.3. One mixture has overlapping Gaussians and the other has not. The results contained in this section refer to the dataset with overlapping Gaussians, but the same overall patterns can be found in the other and the same conclusions can be drawn.

Different rules for computing the K_{min}, different co-association matrix formats and different approaches for the final clustering will be mentioned. The different rules and their aliases are presented in Table 5.14. The different formats for the co-association matrix are the *full* (for fully allocated $n \times n$ matrix), *full condensed* (for a fully allocated $\frac{n(n-1)}{2}$ array to build the upper triangular matrix), *sparse complete* (for EAC CSR), *sparse condensed const* (for EAC CSR building only the upper triangular matrix) and *sparse condensed linear* (for EAC CSR condensed). The different approaches for the final clustering are *SLINK* [19], *SL-MST* (for using the Kruskal implementation in SciPy) and *SL-MST-Disk* for the modified version that performs an external memory sort.

Table 5.14: Different rules for computing K_{min} and K_{max}. n is the number of patterns and sk is the number of patterns per cluster.

Rule	K_{min}	K_{max}
sqrt	$\frac{\sqrt{n}}{2}$	$\sqrt{n}$
2sqrt	$\sqrt{n}$	$2\sqrt{n}$
sk=sqrt2	$sk = \frac{\sqrt{n}}{2}$	$1.3K_{min}$
sk=300	$sk = 300$	$1.3K_{min}$

The experiment that generated the results of these section was set up as follows. A large dataset was generated. The dataset was sampled uniformly to produce a smaller dataset with the desired

number of patterns. A clustering ensemble was produced (production phase) for each of these smaller datasets and for each of the rules, using K-Means. From each ensemble, co-association matrices of every applicable format were built (combination phase). A matrix format was not applicable when the dataset complexity would make its correspondent co-association matrix too big to fit in main memory. The final clustering (recovery phase) was also done for each of the matrix formats. SLINK was used with fully allocated formats and the MST-based SL (SL-MST) and MST-based SL on external memory (SL-MST-disk) were executed with sparse matrices. SL-MST was not executed if its space complexity was too big to fit in main memory. Furthermore, the combination and recovery phases were repeated several times for smaller datasets for statistical relevant of the execution times, so as to make the influence of any background process less salient. For big datasets, the execution times are big enough that the influence of background processes is negligible.

All results presented here originated from machine Bravo.

5.7.1 Performance of production and combination phases

The K_{min} parameter, whose evolution is presented in Fig. 5.4, influences several other EAC properties. Rules *sqrt*, *2sqrt* and *sk=sqrt2* never intersect with the increase if the number of patterns, but rule $sk = 300$ intersects the others, finishing with the highest K_{min}.

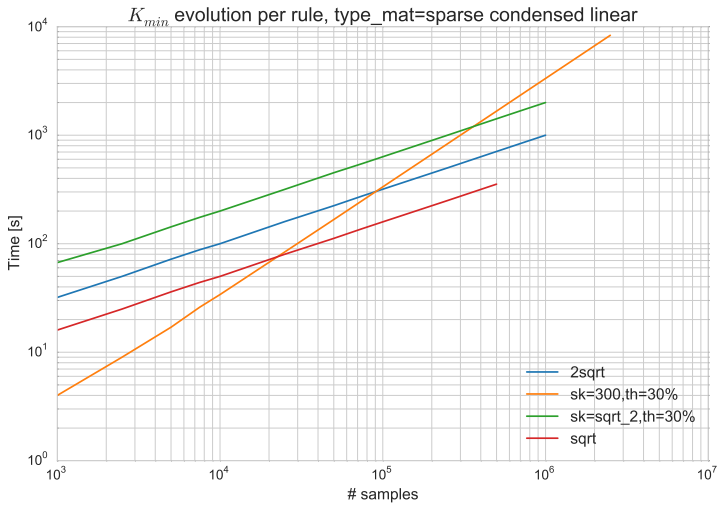

Figure 5.4: Evolution of K_{min} with cardinality for different rules.

The execution times for the production and combination phase can be observed in Figures 5.5, 5.6 and 5.7, which allow the comparison between the different rules and the different matrix formats, respectively. To avoid redundancy, only one matrix format is depicted to compare the execution times for the different rules and only one rule to compare the matrix formats. The results of the other cases follow the same pattern. Observing Fig. 5.6, one can see the tendency of the evolution ofK_{min} in the production execution time associated with the $sk = 300$ rule and the inverse in the combination time. A higher K_{min} means more centroids for K-Means to compute, so it is not surprising that the execution time for computing the ensemble increases as K_{min} increases. On the other hand, a higher K_{min}

translates in more condensed clusters and less associations per pattern. With less associations, the computation time for building the co-association matrix naturally decreases.

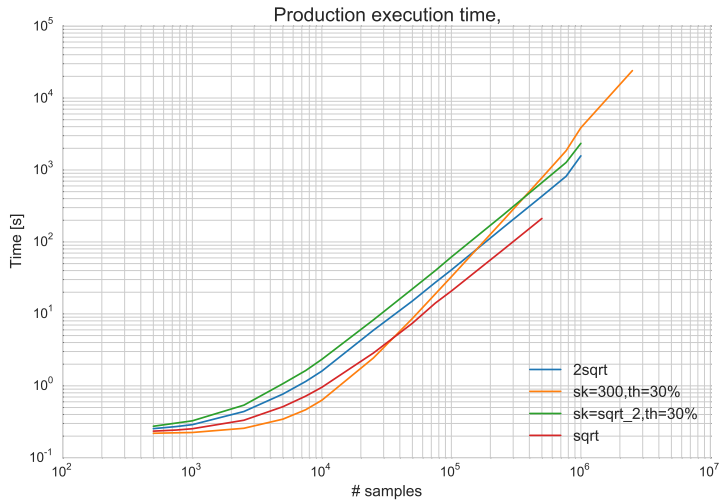

Figure 5.5: Execution time for the production of the clustering ensemble.

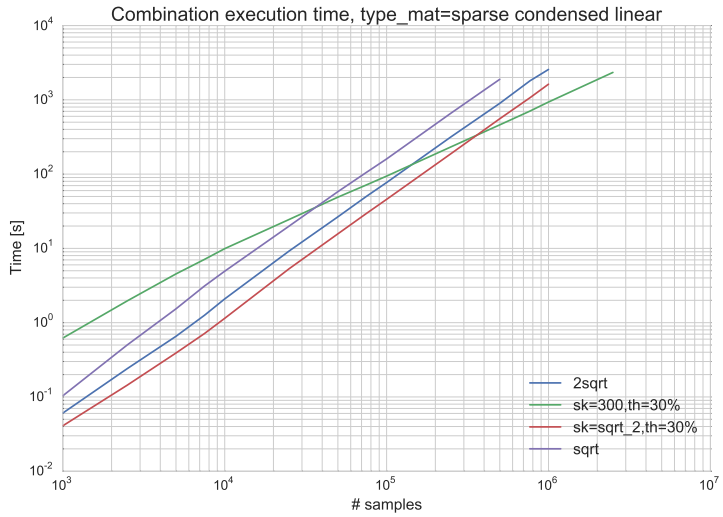

Figure 5.6: Execution time for building the co-association matrix from ensemble with different rules.

In a previous section, the execution times for the combination phase had already been briefly presented when comparing different sparse formats. Fig. 5.7 shows the execution times on a longitudinal study for optimized matrix formats. It is clear that the sparse formats are significantly slower than the fully allocated ones, specially for smaller datasets. The *full condensed* format usually takes close to half the time than the *full* format, which is natural given that it performs half the operations. Idem for the *sparse condensed* formats compared to the *sparse complete*. The big discrepancy between the sparse and full formats is due to the fact that the former needs to do a binary search at each association update and needs to keep the internal sparse data structure sorted.

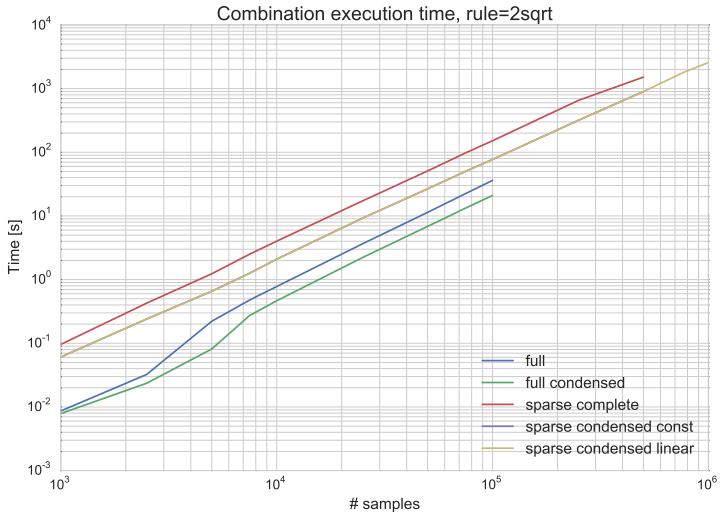

Figure 5.7: Execution time for building the co-association matrix with different matrix formats.

5.7.2 Performance comparison between SLINK, SL-MST and SL-MST-Disk

The clustering times of the different methods of SL discussed previously (SLINK, SL-MST and SL-MST-Disk) are presented in Figures 5.8, 5.9 and 5.10. The SL-MST-Disk method is significantly slower than any of the other methods. This is expected, since it uses the hard drive which has very slow access times compared to main memory. SL-MST is faster than SLINK, since it processes zero associations while SL-MST takes advantage of a graph representation and only processes the non-zero associations. In resemblance to what happened with combination times, the condensed variants take roughly half the time has their complete counterparts. This is expected, since SL-MST and SL-MST-Disk over condensed co-association matrices only process half the number of associations. SLINK takes roughly the same time for every rule, which means K_{min} has no influence, since SLINK processes the entire co-association matrix and K_{min} only influences the number of non-zero associations. The same rationale can be applied to SL-MST, where different rules can have significant influence over execution time, since they change the total number of associations. As with the combination phase, the execution time referent to the *sk=300* rule started with the greatest time and decreased with an increase in cardinality until it was the fastest.

5.7.3 Performance of all phases combined

The execution times of all phases combined are presented in Figures 5.11 and 5.12. The results are presented for the *sparse condensed linear* format but the remaining results follow the same tendency. It is interesting to note that, when using the SL-MST method in the recovery phase, the execution time for three of the rules do not differ much for large datasets. This is due to a sort of balancing between a slowing down of the production phase and a speeding up of the combination and recovery phases as the K_{min} increases at a higher rate for $sk = 300$ than for other rules. This is not observed for the $sqrt$ rule as K_{min} is always low enough that the total time is always dominated by the combination and recovery phases. The same does not happen when using the SL-MST-Disk method, as the total time is

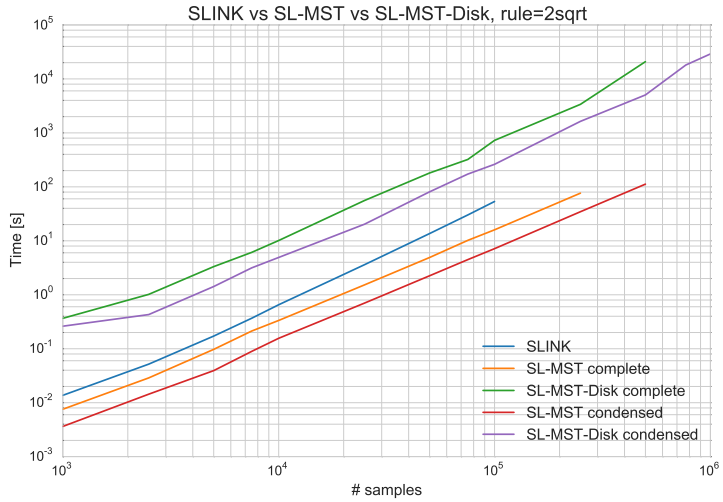

Figure 5.8: Comparison between the execution times of the three methods of SL. SLINK runs over fully allocated condensed matrix while SL-MST and SL-MST-Disk run over the condensed and complete sparse matrices.

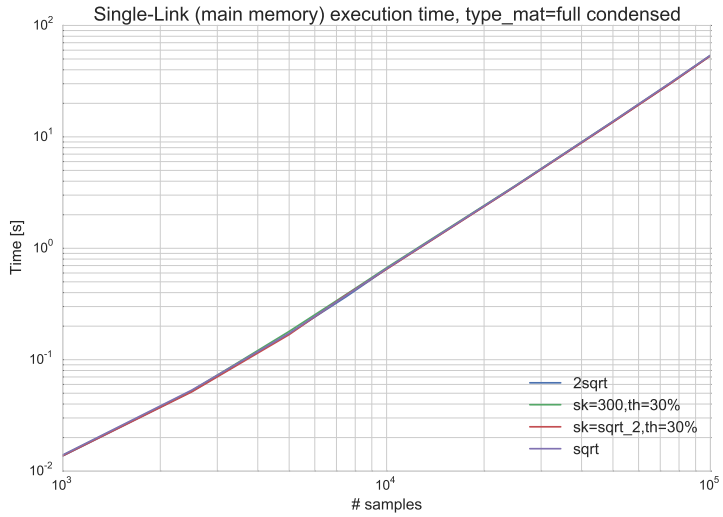

Figure 5.9: Comparison between the execution times of SLINK to different rules.

completely dominated by the recovery phase. This is clear, since the results in Fig. 5.12 follow a pattern similar to that presented in Fig. 5.10.

5.7.4 Analysis of the number of associations

The sparse nature of EAC has been pointed out before and is clearer in Fig. 5.13. This figure shows the association density, i.e. number of associations relative to the n^2 possible associations in a full matrix. The *full condensed* format maintains a density of roughly 50% and the density of *sparse complete* is two times that of the *sparse condensed* formats. The overall tendency is for the density to decrease as the number of patterns of the dataset increases. This is to be expected since the *full* matrix grows quadratically. Besides, it would be expected that the same associations would be grouped together more frequently in partitions and simply make previous connections stronger instead of creating new

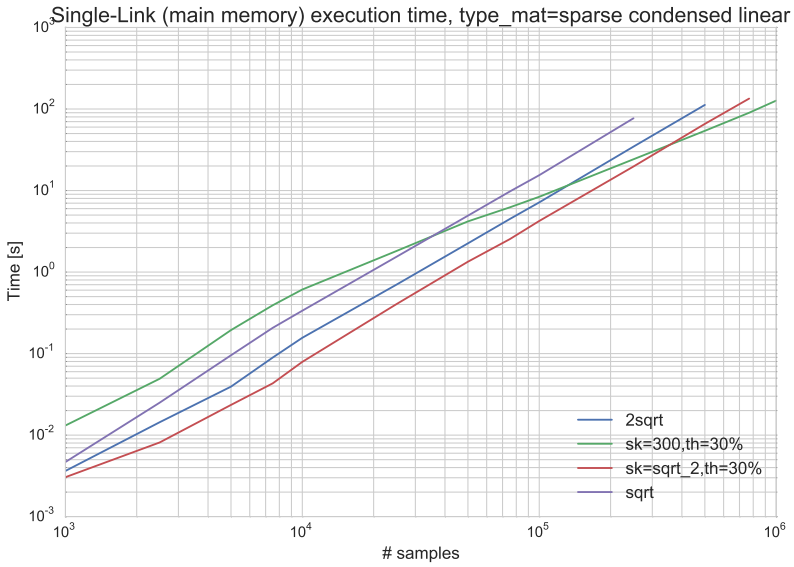

Figure 5.10: Comparison between the execution times of SL-MST for different rules.

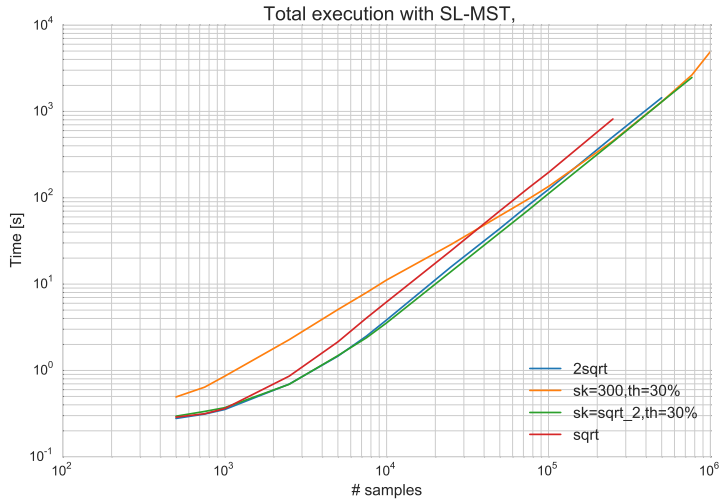

Figure 5.11: Execution times for all phases combined, using SL-MST in the recovery phase.

ones. Results presented in Fig. 5.14, which presents the number of associations per pattern, suggest that but it is only clear for the $sk = 300$ rule. The number of associations per pattern increases with the number of patterns of the dataset, with the notable exception of the *sk=300* rule which increases until it reaches a certain limit and then stabilizes. This is explained by the fact that this rule is based on setting a maximum constant number (300) of patterns in any given cluster, while in the other rules this number increases with the number of patterns. The number of associations per pattern is not 300 for the $sk = 300$ rule because a pattern will be clustered with different neighbors in different partitions. Still, the number of neighbors doesn't change enough that the number of associations per pattern increases boundlessly. In fact, Fig. 5.14 suggests that the number of associations per pattern is around 3 times the upper bound on the number of patterns per cluster (strictly related to K_{min}). This is clearer for $sk = 300$, but if one would trace the the number of patterns divided by K_{min} for each rule, a similar tendency would manifest. Lourenço et al. [32] reported that, on average, the overall contribution of the clustering

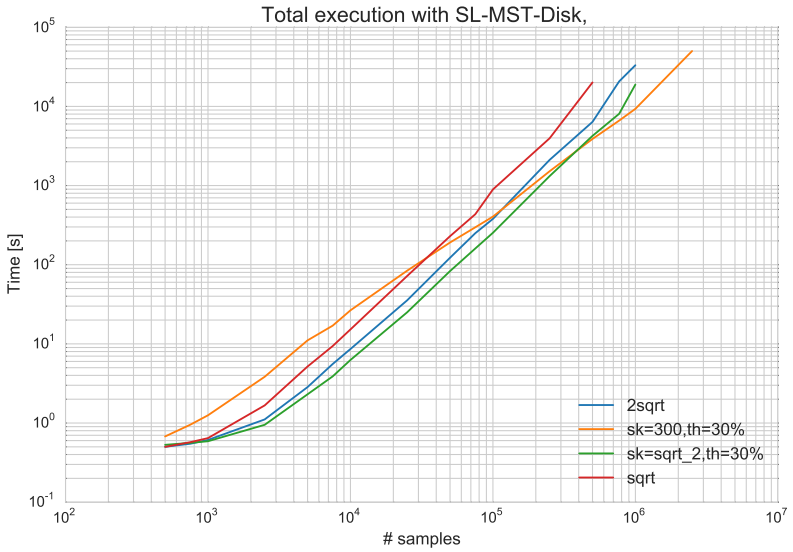

Figure 5.12: Execution times for all phases combined, using SL-MST-Disk in the recovery phase.

ensemble (including unbalanced clusters) duplicates the co-associations produced in a single balanced clustering with Kmin clusters. The spectrum of datasets evaluated regarding number of patterns was smaller than that evaluated in the present work. The present results suggest a slightly higher value. So, the decrease in density is more related with the quadratic growth of the *full* matrix in contrast with a linear growth of the number of associations.

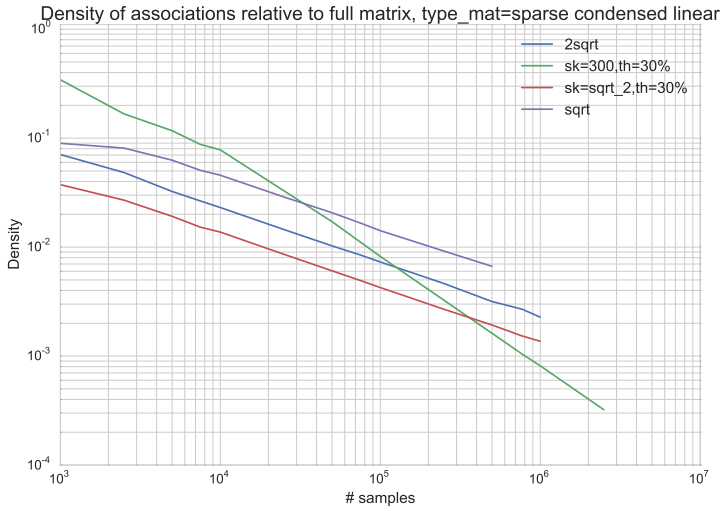

Figure 5.13: Density of associations relative to the full co-association matrix, which hold n^2 associations.

Predicting the number of associations before building the co-association matrix is useful for coming up with combination schemes that are both memory and speed efficient. It was stated before that the biggest cluster size in any partition of the ensemble is a good parameter for this end. Fig. 5.15 presents the relationship between the biggest cluster size and the maximum number of associations of any pattern. These ratio increases with the number of patterns in the beginning, but as the number of patterns increases it never goes over 3.

However, the number of features of the used datasets is rather reduced. It might be the case that this

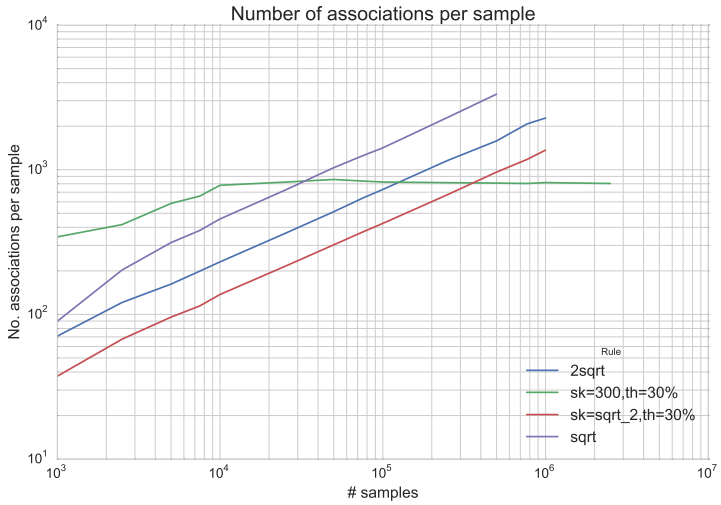

Figure 5.14: Evolution of the total number of associations divided by the number of patterns according to the different rules.

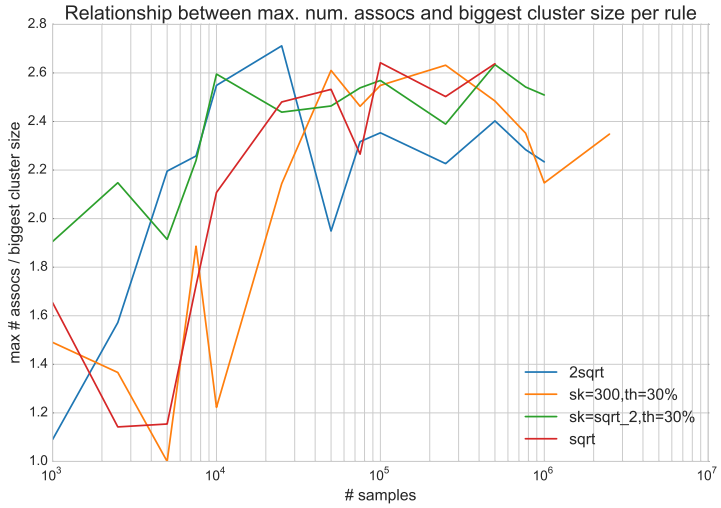

Figure 5.15: Maximum number of associations of any pattern divided by the number of patterns in the biggest cluster of the ensemble.

ratio would increase with the number of features, since there would be more degrees where the clusters might include other neighbors. With this in mind, further studies ranging a wider spectrum of datasets should yield more enlightening conclusions or reinforce those presented here.

5.7.5 Space complexity

The previous section analyzed results related to the number of associations. This is related to the space complexity of the different matrix formats, but does not present an accurate depiction of their complexity, mainly due to the data structures supporting the sparse formats. The true space complexity of the formats can be observed in Figures 5.16 and 5.17.

As explained previously, the allocated space for the space formats is based on a prediction that uses the biggest cluster size of the ensemble. This allocated space is usually more than what is necessary to store the total number of associations. Furthermore, the CSR sparse format, on which the EAC CSR

strategy is based, requires an array of the same size of the predicted number of associations. This overhead may in fact make the sparse format pre-allocate more associations than actually are possible for some rules, as can be seen in Fig. 5.16. Still, the allocated number of associations becomes a very small fraction compared to the *full* matrix as the dataset complexity increases, which is typical case for using a sparse format.

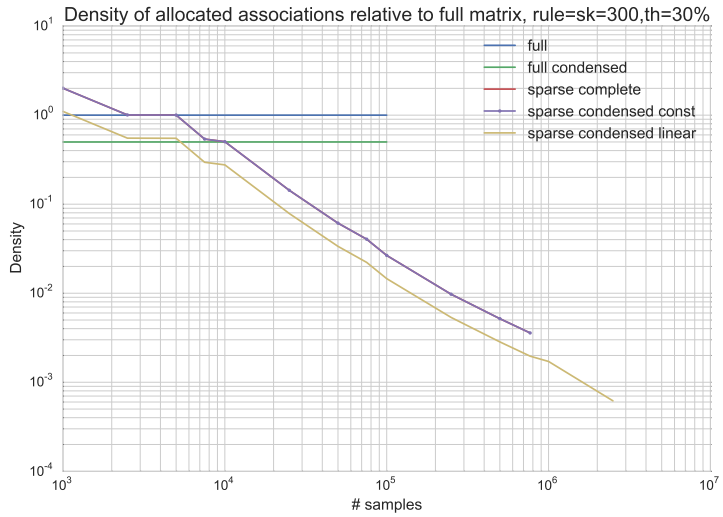

Figure 5.16: Allocated number of associations relative to the full n^2 matrix.

The actual memory used, presented in Fig. 5.17, follows roughly the same pattern. Here, the data types used play a big role in the amount of memory that is required. Each association was stored in a single byte, since the number of partitions was less than 255, as is usually the case. This means that the memory used by the fully allocated formats is n^2 and $\frac{n(n-1)}{2}$ Bytes for the fully allocated complete and condensed formats, respectively. In the sparse formats, the values of the associations were stored in an array of unsigned integers of 1 Byte. However, an array of integers of 4 Bytes of the same size existed to keep track of the destination pattern each association belongs to. Besides, one other array of integers of 8 Bytes is kept but it is negligible compared to the other two arrays. The impact of the data types can be seen for smaller datasets where the total memory used is actually significantly higher than that of the *full* matrix. It should be noted that this discrepancy is not as high for other rules as for $sk = 300$. Still, the sparse formats, and in particular the condensed sparse format, is preferred since the memory used for large datasets is a small fraction of would be necessary if using any of the fully allocated formats. The data types used depend on the problem at hand, since a user may choose to use a large ensemble or have a very large

5.7.6 Accuracy

Finally, the accuracy of each solution was measured and is presented in Fig. 5.18. The number of clusters of the final solutions was determined by the lifetime method. The accuracy was the same for all rules and for all matrix formats in each dataset, except in the beginning were the $sk = 300$ produces bad results due to the ensemble having partitions with a number of clusters inferior to the real number

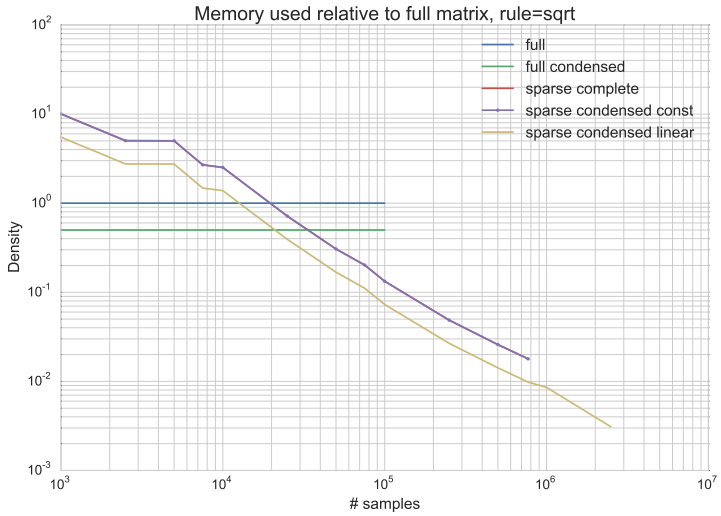

Figure 5.17: Memory used relative to the full n^2 matrix.

of clusters. Still, the $sk = 300$ rule is the one presented because it spans a wider spectrum of datasets. When two classes are overlapping, the lifetime method typically interprets them as being the same class. In the beginning, there are only two overlapping Gaussians, explaining the accuracy of roughly 84%. As more patterns are added to the datasets, the accuracy lowers to around 66%, since now 4 classes are overlapped in pairs. There are two lows in accuracy around the 50%. The first is due to a "bridge" between two classes by a couple of patterns that are not present in the surrounding datasets duo to sampling. The last is duo to the same reason, since now more patterns are included in the dataset.

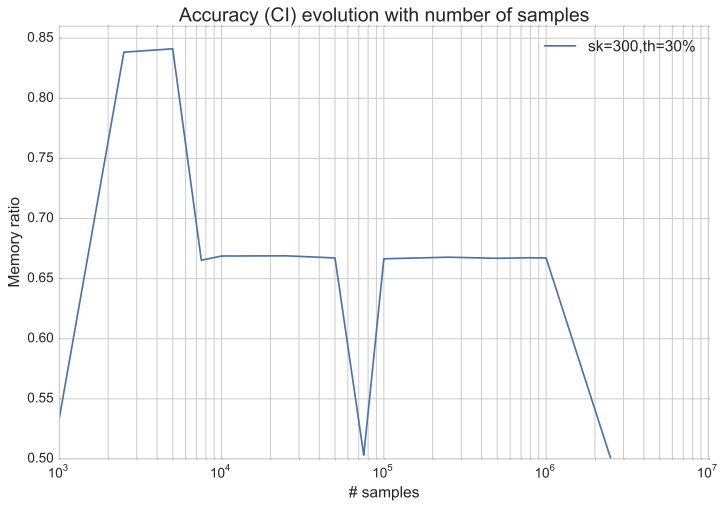

Figure 5.18: Accuracy of the final clusterings as measured with the Consistency Index.

5.8 Performance on real world datasets

The proposed EAC method was tested on real world datasets. Large real world datasets appropriate for clustering were hard to find freely available. The datasets used are aimed at other Machine Learning analysis, such as classification or regression. For this reason, the presented results are focused on

performance. Table 5.15 presents execution times for different phases of EAC on several real world datasets. The ensemble size was of 30, the combination phase used sparse condensed matrices and the *sk=300* rule and the recovery phase was done with SL based on main memory. No comparison is possible with the original implementation, since computation would not be possible. In most datasets the production phase took the longest. The reason for this is that clusters in the ensemble were small which led to fewer associations and, thus, more time spent in the production phase than in the others. Furthermore, the recovery phase was fast because SL was based on main memory. Although high, the computation times are acceptable for the processing of large datasets with a robust algorithm such as EAC in a typical workstation.

Table 5.15: Execution times for real-world large datasets. P and F refer to the number of patterns and features. P, C and R times refer to the production, combination and recovery times.

dataset alias	# P	# F	P time [s]	C time [s]	R time [s]
PHYACT 1 [98]	441568	30	2158.69	123.85	19.76
PHYACT 2 [98]	359170	30	1477.34	98.86	15.79
esopH [99]	136127	2	17.94	35.15	3.95
diabetes [100, 98]	101766	41	188.56	36.79	5.07

Chapter 6

Conclusions

6.1 Achievements

The main goal of this dissertation was scaling the EAC method for larger datasets than was previously possible and speeding it up for smaller datasets. The EAC method is composed by three steps and, to scale the whole method, each step was optimized separately while maintaining interoperability. During this process, a dichotomy between optimizing for speed or memory usage appeared repeatedly. An important lesson learn it that the right solution is not always obvious and one has to step back, ponder how the optimizations in one part affect the whole and choose wisely.

The first step was the production of clustering ensembles, which was originally done with K-Means. The space complexity was low compared to the whole algorithm, so the main focus was on speed optimization. For that end, algorithms in the young field of quantum clustering were researched and tested. Their computational complexity was shown to be prohibitive in the EAC context, which moved the research to parallel computation, more specifically, GPGPU. A GPU parallel K-Means was implemented and yielded positive results, effectively providing a speed-up over its sequential counterpart, ranging from as low as 1.25 for high dimensional datasets to close to 25 for bidimensional datasets. On low dimensional datasets the highest speed-up was observed with a high number of clusters, which is a desirable result since EAC usually deals with a very high number of clusters in the ensemble's partitions. Still, the speed-ups observed are lower that those reported in literature for problems of similar complexity. Since our results were produced from more modern machines, this shortcoming falls on the implementation itself. The burdens of the API and language used, along with the absence of possible optimizations, are the culprits for the sub-optimal performance.

In the combination step, the main problem for scaling was the space complexity. The clear solution here was exploiting the sparse nature of the co-association matrix of EAC. After implementations of sparse matrices in numerical libraries proved to be inadequate and literature lacked methods for efficiently building a sparse matrix, the next direction was designing a strategy for efficiently building the co-association matrix. This strategy, EAC CSR, was tested and shown to be much faster than other sparse matrix implementations tested. Besides, it provided the much needed space complexity reduc-

tion that allowed the processing of large datasets.

For the recovery step, the SL algorithm was identified as the best candidate for optimization. This was due to its relationship with MSTs, of which optimized implementations existed. GPU Boruvka was reported to have significant speed-ups and was identified has the best parallel GPU MST algorithm in literature. It was implemented but it showed to not be able to handle the lower sparsity of EAC co-associations graphs. This moved the focus of optimization of this step to external memory algorithms, which, although slower, were what ultimately allowed for the final processing of EAC in large datasets.

The main contributions to the EAC method, by step, were the GPU parallel K-Means in the production step, the EAC CSR strategy in the combination step and the SL-MST-Disk in the recovery step. New K_{min} rules for optimizing the sparsity of the co-association matrix were proposed and a deeper understanding of how they affect the properties of EAC are also relevant contributions. These contributions together allow for the application of the EAC method to datasets whose complexity was not handled by the original implementation. Furthermore, the proposed optimized version is also faster for smaller datasets.

6.2 Future Work

Naturally, during the research and development of the present work, divergent lines of research were deemed interesting. Occasionally, shortcomings in the present work were identified for which possible solutions were envisioned. Time restrictions have moved those possible solutions and lines of research from the main body of the present work to this section of recommendations for future work.

An obvious line of work is porting the work here presented to other technologies. As an example, the GPU algorithms could be implemented in OpenCL. This would bring major benefits in respect to portability since OpenCL supports most devices. Moreover, OpenCL's performance is becoming closer to CUDA's and since it's programming model was based on CUDA, it should be straightforward for a developers to make the switch.

The implementation of the GPU K-Means could be improved by using shared memory. Each block of threads would read centroids to this memory which would decrease the number of fetches to global memory significantly and therefore improve performance. A study of the optimal block size and a more thorough study of the optimal number of patterns to process in each thread are also relevant lines of research.

Dynamic Parallelism offers the ability of having a kernel call on other kernel without intervention from the host. This translates in the possibility of moving the control logic in the Borůvka variant to the device, effectively removing the memory transfer of values related with the control logic.

A possible way to further reducing the space complexity of the recovery step is threshold cut-off of associations, i.e. cutting associations in the co-association matrix that are weaker than a certain threshold. The underlying idea is that strong associations will have the bigger effect on the final clustering, while the weak will have little to no effect. This assumption could allow for the reduction of space complexity while keeping the final accuracy, or even improving it by cutting bad associations. This line of

research was briefly explored on small datasets and is in fact implemented, but robust testing was not possible. The main challenge here is to find safe thresholds that will not damage the overall quality of the results.

A good follow-up of the present work is to study the relationship between several metrics (e.g. sparsity, accuracy, maximum number of co-associations) and the complexity of the dataset. Several measures for describing the complexity of the dataset exist [101] and it would be interesting to profile several datasets of different complexities and structures and analyze the relationship between these complexity measures and EAC properties. On a performance perspective it could prove useful to deduce better rules to set the maximum number of associations in the sparse matrix. On a accuracy perspective it would be interesting to see if there are types of datasets that simply are not a good fit for EAC while other are, as well as perform automatic choosing of the K_{min} parameter. It would also be interesting to relate complexity with the threshold cut-off.

The WEAC algorithm, presented in chapter 2, is focused on improving accuracy. The underlying concept is to measure the quality of the partitions in the ensemble and allow the better ones to be more influential in the co-association matrix. The concept of measuring the quality of the partitions may prove useful for further decreasing the memory complexity with the EAC CSR scheme without compromising accuracy. The basic idea is to choose a max_assocs value that will likely be less than the number of associations many patterns will have, which will result in some associations being discarded. The associations that will be kept are the ones from the first partitions that were processed. With this in mind, one could order the partitions by quality and start the processing from those with better quality. This would increase the likelihood that the discarded associations are, in fact, weaker associations.

A possible extension to EAC CSR is allowing for bigger than main memory co-association matrices. An approach for this would be to divide the co-association matrix in several parts. The entire ensemble would then have to be processed for each of these parts, but it would allow for the processing of even larger datasets than is now possible.

Two ways of dealing with the space complexity of EAC were identified in literature: exploiting sparsity and using k-Nearest Neighbors. Building a k-Nearest Neighbors co-association matrix requires two matrices: one for holding the association values and another for holding the neighbors of each pattern. The mechanism for building this co-association matrix was implemented but it was not possible to make it inter-operable with the final step of EAC. However, this should be a straightforward process since its conversion to EAC CSR is can be done simply by linearizing both matrices. The values matrix would become the *data* array, the neighbors matrix would be the *indices* array and finally an *indptr* array would have to be created, which is straighforward, since the number of neighbors of each pattern is constant.

The *argsort* operation in the recovery step is one of the most computationally intensive. This operation is typically done by sorting chunks of the array in main memory and then merging them. The external algorithm used for this operation has a very low main memory profile. However, when it is executed most main memory is free. This means that a more efficient algorithm for performing this operation is possible simply by using more main memory, and therefore processing bigger chunks at a time. Besides, it is believed that a significant speed-up may be obtained by using GPUs for sorting these chunks.

Much effort was put into developing and testing co-association matrix building strategies. The schemes presented here provide a solid framework to work with large datasets in the middle step of EAC. As such, interesting directions for this work to take include researching and testing how state of the art algorithms designed for Big Data would complement EAC in the first and last steps.

Bibliography

[1] Anil K Jain. Data clustering: 50 years beyond K-means. *Pattern Recognition Letters*, 31(8): 651–666, 2010.

[2] a. K. Jain, M. N. Murty, and P. J. Flynn. Data clustering: a review. *ACM Computing Surveys*, 31 (3):264–323, 1999.

[3] Edgar Anderson. The species problem in Iris. *Annals of the Missouri Botanical Garden*, pages 457–509, 1936.

[4] Ronald A Fisher. The use of multiple measurements in taxonomic problems. *Annals of eugenics*, 7(2):179–188, 1936.

[5] Raymond A Jarvis and Edward A Patrick. Clustering using a similarity measure based on shared near neighbors. *Computers, IEEE Transactions on*, 100(11):1025–1034, 1973.

[6] Charu C Aggarwal and Chandan K Reddy. *Data clustering: algorithms and applications*. CRC Press, 2013.

[7] Ana Fred. Finding consistent clusters in data partitions. *Multiple classifier systems*, pages 309–318, 2001.

[8] Marina Meila. Comparing clusterings by the variation of information. *Learning theory and Kernel machines: 16th Annual Conference on Learning Theory and 7th Kernel Workshop, COLT/Kernel 2003, Washington, DC, USA, August 24-27, 2003: proceedings*, page 173, 2003.

[9] David L Davies and Donald W Bouldin. A cluster separation measure. *Pattern Analysis and Machine Intelligence, IEEE Transactions on*, (2):224–227, 1979.

[10] Daniel Boley. Principal Direction Divisive Partitioning. *Data Mining and Knowledge Discovery*, 2 (4):325–344, 1998.

[11] Michael Steinbach, George Karypis, Vipin Kumar, and Others. A comparison of document clustering techniques. *KDD workshop on text mining*, 400(1):525–526, 2000.

[12] Marie Chavent. A monothetic clustering method. *Pattern Recognition Letters*, 19(11):989–996, 1998.

[13] James C. Bezdek, Robert Ehrlich, and William Full. FCM: The Fuzzy C-Means Clustering Algorithm. *Computers & Geosciences*, 10(2–3):191–203, 1984.

[14] U Kang, Charalampos E Tsourakakis, and Christos Faloutsos. PEGASUS : Mining Peta-Scale Graphs. *Knowledge and Information Systems*, 27(2):303–325, 2011.

[15] J B MacQueen. Some Methods for classification and Analysis of Multivariate Observations. In *Proceedings of 5-th Berkeley Symposium on Mathematical Statistics and Probability, Berkeley, University of California Press*, volume 1, pages 281–297, 1967.

[16] D. Arthur, D. Arthur, S. Vassilvitskii, and S. Vassilvitskii. k-means++: The advantages of careful seeding. *Proceedings of the eighteenth annual ACM-SIAM symposium on Discrete algorithms*, 8: 1027–1035, 2007.

[17] Malay K Pakhira. A Modified k -means Algorithm to Avoid Empty Clusters. *International Journal of Recent Trends in Enineering*, 1(1), 2009.

[18] Peter H A Sneath and Robert R Sokal. Numerical taxonomy. *Nature*, 193(4818):855–860, 1962.

[19] R. Sibson. SLINK: an optimally efficient algorithm for the single-link cluster method. *The Computer Journal*, 16(1):30–34, 1973.

[20] J. C. Gower and G. J. S. Ross. Minimum Spanning Trees and Single Linkage Cluster Analysis. *Journal of the Royal Statistical Society*, 18(1):54–64, 1969.

[21] Daniel Müllner. Modern hierarchical, agglomerative clustering algorithms. *arXiv preprint arXiv:1109.2378*, 2011.

[22] J-L Starck and Fionn Murtagh. *Astronomical image and data analysis*. Springer Science & Business Media, 2007.

[23] Alexander Topchy, Anil K Jain, and William Punch. A mixture model for clustering ensembles. In *Society for Industrial and Applied Mathematics. Proceedings of the SIAM International Conference on Data Mining*, page 379. Society for Industrial and Applied Mathematics, 2004.

[24] Ana N L Fred and Anil K Jain. Combining multiple clusterings using evidence accumulation. *IEEE Transactions on Pattern Analysis and Machine Intelligence*, 27(6):835–850, 2005.

[25] Alexander Strehl and Joydeep Ghosh. Cluster Ensembles – A Knowledge Reuse Framework for Combining Multiple Partitions. *Journal of Machine Learning Research*, 3:583–617, 2002.

[26] Hongjun Wang, Hanhuai Shan, and Arindam Banerjee. Bayesian cluster ensembles. *Statistical Analysis and Data Mining: The ASA Data Science Journal*, 4(1):54–70, 2011.

[27] Sandrine Dudoit and Jane Fridlyand. Bagging to improve the accuracy of a clustering procedure. *Bioinformatics*, 19(9):1090–1099, 2003.

[28] Ana N L Fred and Anil K Jain. Data clustering using evidence accumulation. In *Pattern Recognition, 2002. Proceedings. 16th International Conference on*, volume 4, pages 276–280, 2002.

[29] André Lourenço and Ana Fred. Ensemble methods in the clustering of string patterns. *Proceedings - Seventh IEEE Workshop on Applications of Computer Vision, WACV 2005*, pages 143–148, 2007.

[30] Andre Lourenco, Carlos Carreiras, Samuel Rota Bulo, and Ana Fred. ECG analysis using consensus clustering. In *Signal Processing Conference (EUSIPCO), 2014 Proceedings of the 22nd European*, pages 511–515. IEEE, 2014.

[31] F.J. Duarte, a.L.N. Fred, a. Lourenco, and M.F. Rodrigues. Weighting Cluster Ensembles in Evidence Accumulation Clustering. *2005 Portuguese Conference on Artificial Intelligence*, 00:159–167, 2005.

[32] André Lourenço, Ana L N Fred, and Anil K. Jain. On the scalability of evidence accumulation clustering. *Proceedings - International Conference on Pattern Recognition*, 0:782–785, 2010.

[33] You Wen Qian, William Cukierski, Mona Osman, and Lauri Goodell. Combined multiple clusterings on flow cytometry data to automatically identify chronic lymphocytic leukemia. *ICBBT 2010 - 2010 International Conference on Bioinformatics and Biomedical Technology*, pages 305–309, 2010.

[34] L O'Callaghan, N Mishra, A Meyerson, S Guha, and R Motwani. Streaming-data algorithms for high-quality clustering. In *Data Engineering, 2002. Proceedings. 18th International Conference on*, pages 685–694, 2002.

[35] Raymond T Ng and Jiawei Han. Clarans: A method for clustering objects for spatial data mining. *Knowledge and Data Engineering, IEEE Transactions on*, 14(5):1003–1016, 2002.

[36] Tian Zhang, Raghu Ramakrishnan, and Miron Livny. BIRCH: an efficient data clustering method for very large databases. In *ACM SIGMOD Record*, volume 25, pages 103–114. ACM, 1996.

[37] Sudipto Guha, Rajeev Rastogi, and Kyuseok Shim. CURE: an efficient clustering algorithm for large databases. In *ACM SIGMOD Record*, volume 27, pages 73–84. ACM, 1998.

[38] Petros Drineas, Ravi Kannan, and Michael W Mahoney. Fast Monte Carlo algorithms for matrices III: Computing a compressed approximate matrix decomposition. *SIAM Journal on Computing*, 36 (1):184–206, 2006.

[39] Mario Zechner and Michael Granitzer. K-Means on the Graphics Processor: Design And Experimental Analysis. *International Journal on Advances in System and Measurements*, 2(2):224–235, 2009.

[40] Wen-Yen Chen, Yangqiu Song, Hongjie Bai, Chih-Jen Lin, and Edward Y Chang. Parallel spectral clustering in distributed systems. *Pattern Analysis and Machine Intelligence, IEEE Transactions on*, 33(3):568–586, 2011.

[41] Hong Tao Bai, Li Li He, Dan Tong Ouyang, Zhan Shan Li, and He Li. K-means on commodity GPUs with CUDA. *2009 WRI World Congress on Computer Science and Information Engineering, CSIE 2009*, 3:651–655, 2009.

[42] Jiadong Wu and Bo Hong. An efficient k-means algorithm on CUDA. *IEEE International Symposium on Parallel and Distributed Processing Workshops and Phd Forum*, pages 1740–1749, 2011.

[43] Mario Zechner and Michael Granitzer. Accelerating k-means on the graphics processor via CUDA. *Proceedings of the 1st International Conference on Intensive Applications and Services, INTENSIVE 2009*, pages 7–15, 2009.

[44] J Sirotkovi, H Dujmi, and V Papi. K-means image segmentation on massively parallel GPU architecture. In *MIPRO, 2012 Proceedings of the 35th International Convention*, pages 489–494, 2012.

[45] Reza Farivar, Daniel Rebolledo, and Ellick Chan. A parallel implementation of k-means clustering on GPUs. In *The 2008 International Conference on Parallel and Distributed Processing Techniques and Applications*, pages 340–345, 2008.

[46] Jeffrey DiMarco and Michela Taufer. Performance impact of dynamic parallelism on different clustering algorithms. In *Proc. SPIE 8752, Modeling and Simulation for Defense Systems and Applications VIII*, pages 87520E—-87520E, 2013.

[47] Vibhav Vineet, Pawan Harish, Suryakant Patidar, and P J Narayanan. Fast minimum spanning tree for large graphs on the GPU. In *Proceedings of the Conference on High Performance Graphics 2009*, pages 167–171. ACM, 2009.

[48] Scott Rostrup, Shweta Srivastava, and Kishore Singhal. Fast and memory-efficient minimum spanning tree on the GPU. *International Journal of Computational Science and Engineering*, 8(1): 21–33, 2013.

[49] C Da Silva Sousa, A Mariano, and A Proenca. A Generic and Highly Efficient Parallel Variant of Boruvka's Algorithm. In *Parallel, Distributed and Network-Based Processing (PDP), 2015 23rd Euromicro International Conference on*, pages 610–617, 2015.

[50] Joseph B Kruskal. On the shortest spanning subtree of a graph and the traveling salesman problem. *Proceedings of the American Mathematical society*, 7(1):48–50, 1956.

[51] Robert Clay Prim. Shortest connection networks and some generalizations. *Bell system technical journal*, 36(6):1389–1401, 1957.

[52] Otakar Borůvka. O jistém problému minimálním. *Práce Moravské Prirodovědecké Společnosti*, 3: 37–58, 1926.

[53] Wei Wang, Yongzhong Huang, and Shaozhong Guo. Design and Implementation of GPU-Based Prim ' s Algorithm. *International Journal of Modern Education and Computer Science*, 4(July): 55–62, 2011.

[54] Pawan Harish, Vibhav Vineet, and P J Narayanan. Large graph algorithms for massively multithreaded architectures. *International Institute of Information Technology Hyderabad, Tech. Rep. IIIT/TR/2009/74*, 2009.

[55] W. Daniel Hillis and Guy L. Steele. Data parallel algorithms. *Communications of the ACM*, 29(12): 1170–1183, 1986.

[56] Guy E Blelloch. *Prefix Sums and Their Applications*, chapter 1, pages 35–60. 1993.

[57] Mark Harris, Shubhabrata Sengupta, and John D. Owens. Parallel Prefix Sum (Scan) with CUDA Mark. *Gpu gems 3*, (April):1–24, 2007.

[58] Esma Aïmeur, Gilles Brassard, and Sébastien Gambs. Quantum speed-up for unsupervised learning. *Machine Learning*, 90(February 2012):261–287, 2013.

[59] Seth Lloyd, Masoud Mohseni, and Patrick Rebentrost. Quantum algorithms for supervised and unsupervised machine learning. *arXiv preprint arXiv:1307.0411*, 2013.

[60] Lov K Grover. A fast quantum mechanical algorithm for database search. In *Proceedings of the twenty-eighth annual ACM symposium on Theory of computing*, pages 212–219. ACM, 1996.

[61] Nathan Wiebe, Ashish Kapoor, and Krysta Svore. Quantum Algorithms for Nearest-Neighbor Methods for Supervised and Unsupervised Learning. *arXiv preprint arXiv:1401.2142*, page 31, 2014.

[62] Richard P. Feynman. Simulating physics with computers. *International Journal of Theoretical Physics*, 21(6-7):467–488, 1982.

[63] Peter Wittek. *Quantum Machine Learning: What Quantum Computing Means to Data Mining*. Academic Press, 2014.

[64] Ellis Casper and Chih-cheng Hung. Quantum Modeled Clustering Algorithms for Image Segmentation. *Progress in Intelligent Computing and Applications*, 2:1–21, 2013.

[65] Kuk-Hyun Han and Jong-Hwan Kim. Genetic quantum algorithm and its application to combinatorial optimization problem. *Proceedings of the 2000 Congress on Evolutionary Computation. CEC00 (Cat. No.00TH8512)*, 2, 2000.

[66] Wenjie Liu, Hanwu Chen, Qiaoqiao Yan, Zhihao Liu, Juan Xu, and Yu Zheng. A novel quantum-inspired evolutionary algorithm based on variable angle-distance rotation. *2010 IEEE World Congress on Computational Intelligence, WCCI 2010 - 2010 IEEE Congress on Evolutionary Computation, CEC 2010*, 2010.

[67] H Talbi, A Draa, and M Batouche. A new quantum-inspired genetic algorithm for solving the travelling salesman problem. In *Industrial Technology, 2004. IEEE ICIT '04. 2004 IEEE International Conference on*, volume 3, pages 1192–1197, 2004.

[68] Ellis Casper, Chih-Cheng Hung, Edward Jung, and Ming Yang. A Quantum-Modeled K-Means Clustering Algorithm for Multi-band Image Segmentation. In *Proceedings of the 2012 ACM Research in Applied Computation Symposium*, volume 1, pages 158–163, 2012.

[69] Jing Xiao, YuPing Yan, Jun Zhang, and Yong Tang. A quantum-inspired genetic algorithm for k-means clustering. *Expert Systems with Applications*, 37:4966–4973, 2010.

[70] Chih-Cheng Hung, Ellis Casper, Bor-chen Kuo, Wenping Liu, Edward Jung, Ming Yang, Xiaoyi Yu, Edward Jung, and Ming Yang. A Quantum-Modeled Artificial Bee Colony clustering algorithm for remotely sensed multi-band image segmentation. In *Geoscience and Remote Sensing Symposium (IGARSS), 2013 IEEE International*, pages 2501–2504. IEEE, 2013.

[71] Chih-Cheng Hung, Ellis Casper, Bor-Chen Kuo, Wenping Liu, Xiaoyi Yu, Edward Jung, and Ming Yang. A Quantum-Modeled Fuzzy C-Means clustering algorithm for remotely sensed multi-band image segmentation. In *Geoscience and Remote Sensing Symposium (IGARSS), 2013 IEEE International*, pages 2501–2504. IEEE, 2013.

[72] Shenshen Liang, Cheng Wang, Ying Liu, and Liheng Jian. CUKNN: A parallel implementation of K-nearest neighbor on CUDA-enabled GPU. *Proceedings - 2009 IEEE Youth Conference on Information, Computing and Telecommunication, YC-ICT2009*, pages 415–418, 2009.

[73] Yangyang Li, Nana Wu, Jingjing Ma, and Licheng Jiao. Quantum-inspired immune clonal clustering algorithm based on watershed. In *IEEE Congress on Evolutionary Computation*, pages 1–7. IEEE, jul 2010.

[74] Said M Mikki, Ahmed Kishk, and Others. Quantum particle swarm optimization for electromagnetics. *Antennas and Propagation, IEEE Transactions on*, 54(10):2764–2775, 2006.

[75] David Horn and Assaf Gottlieb. Algorithm for Data Clustering in Pattern Recognition Problems Based on Quantum Mechanics. *Physical Review Letters*, 88(1):1–4, 2001.

[76] Marvin Weinstein and David Horn. Dynamic quantum clustering: a method for visual exploration of structures in data. *Physical Review E - Statistical, Nonlinear, and Soft Matter Physics*, 80(6): 1–15, 2009.

[77] Zhi-Hua Li, Shi-Tong Wang, and Jiangsu Wuxi. Quantum Theory: The unified framework for FCM and QC algorithm. In *Wavelet Analysis and Pattern Recognition, 2007. ICWAPR'07. International Conference on*, volume 3, pages 1045–1048. IEEE, 2007.

[78] Hao Wang, Shiqin Yang, Wenbo Xu, and Jun Sun. Scalability of Hybrid Fuzzy C-Means Algorithm Based on Quantum-Behaved PSO. In *Fourth International Conference on Fuzzy Systems and Knowledge Discovery (FSKD 2007)*, volume 2, pages 261–265, 2007.

[79] Jun Sun, Bin Feng, and Wenbo Xu. Particle swarm optimization with particles having quantum behavior. In *Evolutionary Computation, 2004. CEC2004. Congress on*, volume 1, pages 325–331 Vol.1, 2004.

[80] a. Manju and M. J. Nigam. Applications of quantum inspired computational intelligence: A survey. *Artificial Intelligence Review*, 42:79–156, 2014.

[81] Marco Lanzagorta and Jeffrey Uhlmann. *Quantum Computer Science*, volume 1. 2008.

[82] David Rosenbaum and Aram W. Harrow. Uselessness for an Oracle Model with Internal Randomness. *arXiv:1111.1462*, pages 1–23, 2011.

[83] David Horn, Tel Aviv, Assaf Gottlieb, Hod HaSharon, Inon Axel, and Ramat Gan. Method and Apparatus for Quantum Clustring, 2010.

[84] David Horn and Assaf Gottlieb. The Method of Quantum Clustering. In *NIPS*, pages 769—-776, 2001.

[85] Peter Wittek. High-performance dynamic quantum clustering on graphics processors. *Journal of Computational Physics*, 233:262–271, 2013.

[86] Stéfan Van Der Walt, S. Chris Colbert, and Gaël Varoquaux. The NumPy array: A structure for efficient numerical computation. *Computing in Science and Engineering*, 13(2):22–30, 2011.

[87] Eric Jones, Travis Oliphant, Pearu Peterson, and Others. SciPy: Open source scientific tools for Python. URL `http://www.scipy.org/`.

[88] Travis E. Oliphant. Python for scientific computing. *Computing in Science and Engineering*, 9(3): 10–20, 2007.

[89] K. Jarrod Millman and Michael Aivazis. Python for scientists and engineers. *Computing in Science and Engineering*, 13(2):9–12, 2011.

[90] John D Hunter. Matplotlib: A 2D graphics environment. *Computing in science and engineering*, 9 (3):90–95, 2007.

[91] Wes McKinney. Data Structures for Statistical Computing in Python. *Proceedings of the 9th Python in Science Conference*, 1697900(Scipy):51–56, 2010.

[92] Fabian Pedregosa, Gaël Varoquaux, Alexandre Gramfort, Vincent Michel, Bertrand Thirion, Olivier Grisel, Mathieu Blondel, Peter Prettenhofer, Ron Weiss, Vincent Dubourg, Jake Vanderplas, Alexandre Passos, David Cournapeau, Matthieu Brucher, Matthieu Perrot, and Édouard Duchesnay. Scikit-learn: Machine Learning in Python. *Journal of Machine Learning Research*, 12 (Oct):2825–2830, 2011.

[93] Fernando Pérez and Brian E. Granger. IPython: A system for interactive scientific computing. *Computing in Science and Engineering*, 9(3):21–29, 2007.

[94] Numba Development Team. Numba, 2015. URL http://numba.pydata.org.

[95] Francesc Alted, Ivan Vilata, and Others. PyTables: Hierarchical Datasets in Python. URL http://www.pytables.org/.

[96] The HDF Group. Hierarchical Data Format, version 5.

[97] Francesc Altet i Abad and Ivan Vilata Balaguer. OPSI : The indexing system of PyTables 2 Professional Edition. Technical report, 2007. URL http://www.pytables.org/docs/OPSI-indexes.pdf.

[98] M Lichman. {UCI} Machine Learning Repository, 2013. URL http://archive.ics.uci.edu/ml.

[99] E S Yuksel, J C Slaughter, N Mukhtar, M Ochieng, G Sun, M Goutte, S Muddana, C Gaelyn Garrett, and M F Vaezi. An oropharyngeal pH monitoring device to evaluate patients with chronic laryngitis. *Neurogastroenterology and motility : the official journal of the European Gastrointestinal Motility Society*, 25(5), 2013.

[100] Beata Strack, Jonathan P DeShazo, Chris Gennings, Juan L Olmo, Sebastian Ventura, Krzysztof J Cios, and John N Clore. Impact of HbA1c measurement on hospital readmission rates: analysis of 70,000 clinical database patient records. *BioMed research international*, 2014, 2014.

[101] Tin K Ho and Mitra Basu. Complexity measures of supervised classification problems. *IEEE Transactions on Pattern Analysis and Machine Learning*, 24(3):289–300, 2002.

[102] Linchuan Chen and Gagan Agrawal. Optimizing MapReduce for GPUs with Effective Shared Memory Usage. *Proceedings of the 21st international symposium on High-Performance Parallel and Distributed Computing (HPDC'12)*, pages 199–210, 2012.

[103] Ren Wu, Bin Zhang, and Meichun Hsu. Clustering billions of data points using GPUs. *Proceedings of the combined workshops on UnConventional high performance computing workshop plus memory access workshop*, pages 1–5, 2009.

[104] S Shalom, Manoranjan Dash, Minh Tue, and Nithin Wilson. Hierarchical Agglomerative Clustering Using Graphics Processor with Compute Unified Device Architecture. In *2009 International Conference on Signal Processing Systems, ICSPS 2009*, pages 556–561, 2009.

[105] S Shalom and Manoranjan Dash. Efficient hierarchical agglomerative clustering algorithms on GPU using data partitioning. In *Parallel and Distributed Computing, Applications and Technologies (PDCAT), 2011 12th International Conference on*, pages 134–139, 2011.

[106] Yanjun Jiang, Enxing Li, and Zhanchun Gao. A GPU-based harmony k-means algorithm for document clustering. In *Information Science and Control Engineering 2012 (ICISCE 2012), IET International Conference on*, pages 1–4, 2012.

[107] Ranajoy Malakar and Naga Vydyanathan. A CUDA-enabled hadoop cluster for fast distributed image processing. *2013 National Conference on Parallel Computing Technologies, PARCOMPTECH 2013*, 2013.

[108] Max Grossman, Mauricio Breternitz, and Vivek Sarkar. HadoopCL: MapReduce on distributed heterogeneous platforms through seamless integration of hadoop and OpenCL. *Proceedings - IEEE 27th International Parallel and Distributed Processing Symposium Workshops and PhD Forum, IPDPSW 2013*, pages 1918–1927, 2013.

[109] Marko J Miši, M Ĉ, and Milo V Tomaševi. Evolution and Trends in GPU Computing. *MIPRO, 2012 Proceedings of the 35th International Convention*, pages 289–294, 2012.

[110] Feng Ji and Xiaosong Ma. Using Shared Memory to Accelerate MapReduce on Graphics Processing Units. *2011 IEEE International Parallel & Distributed Processing Symposium*, pages 805–816, 2011.

[111] Miao Xin and Hao Li. An implementation of GPU accelerated MapReduce: Using Hadoop with OpenCL for data- and compute-intensive jobs. In *Proceedings - 2012 International Joint Conference on Service Sciences, Service Innovation in Emerging Economy: Cross-Disciplinary and Cross-Cultural Perspective, IJCSS 2012*, pages 6–11, 2012.

[112] Bingsheng He, Weibin Fang, Qiong Luo, Naga K Govindaraju, and Tuyong Wang. Mars: a MapReduce framework on graphics processors. In *Proceedings of the 17th international conference on Parallel architectures and compilation techniques*, pages 260–269, 2008.

[113] Kamran Karimi, Neil G. Dickson, and Firas Hamze. A Performance Comparison of CUDA and OpenCL. *arXiv preprint arXiv:1005.2581*, 2010.

[114] Ching Lung Su, Po Yu Chen, Chun Chieh Lan, Long Sheng Huang, and Kuo Hsuan Wu. Overview and comparison of OpenCL and CUDA technology for GPGPU. *IEEE Asia-Pacific Conference on Circuits and Systems, Proceedings, APCCAS*, pages 448–451, 2012.

[115] Nvidia. CUDA C Programming Guide. *Programming Guides*, (August), 2015.

Appendix A

General Purpose computing on Graphical Processing Units

The original intended use for GPUs was graphics processing, hence its name. Recently, GPUs have been increasingly used for other purposes - a trend commonly known as General Purpose processing in Graphics Processing Units (GPGPU). GPU present a solution for ”extreme-scale, cost-effective, and power-efficient high performance computing” [102]. Furthermore, GPUs are common in consumer desktops and laptops, effectively bringing this computation power to the masses.

GPUs were typically useful for users that required high performance graphics computation. Other applications were soon explored as users from different fields realized the high parallel computation power of these devices. However, the architecture of the GPUs themselves has been strictly oriented toward the graphics computing until the appearance of specialized GPU models designed for data computation (e.g. NVIDIA Tesla).

GPGPU application on several fields and algorithms has been reported with significant performance increase, e.g. application on the K-Means algorithm [41, 42, 43, 103], hierarchical clustering [104, 105], document clustering [106], image segmentation [44], integration in Hadoop clusters [107, 108], among other applications.

Current GPUs pack hundreds of cores and have a better energy/area ratio than traditional infrastructure. GPU work under the SIMD framework, i.e. all the cores in the device execute the same code at the same time and only the data changes over time.

A.1 Programming GPUs

In the very beginning of GPGPU, programming was done directly through graphics APIs. Programming for GPUs was traditionally done within the paradigm of graphics processing, such as DirectX and OpenGL. If researchers and programmers wanted to tap into the computing power of a GPU they had to learn and use these APIs and frameworks, which is a challenging task since their general problems had to be modelled to the graphics-oriented primitives [109]. With the appearance of DirectX 9, shader pro-

gramming languages of higher level became available (e.g. C for graphics, DirectX High Level Shader Language, OpenGL Shading Language), but they were still inherently graphics programming languages, where computation must be expressed in graphics terms.

More recent programming models, such as CUDA and OpenCL, removed a lot of that burden by exposing the power of GPUs in a way closer to traditional programming. Currently, the major programming models used for computation in GPU are OpenCL and CUDA. While the first is widely available in most devices, the latter is only available for NVIDIA devices.

As Google's MapReduce computing model has increasingly become a standard for scalable and distributed computing over big data, attempts have been made to port the model to the GPU [110, 111, 112]. This translates in using the same programming model over a wide array of computing platforms.

A.2 OpenCL vs CUDA

Presently, the most mature programming models are CUDA and OpenCL. CUDA appeared first and is supported only by NVidia devices. It is also the most mature of the two and performs well since it was designed alongside with the hardware architecture of the supporting devices. OpenCL has the advantage of portability, but that comes with issues of performance portability. Both models are, in fact, very similar and literature suggests that porting the code from one to the other requires minimal changes [113, 114]. Literature also reports that CUDA performs better than OpenCL [114] for equivalent code.

A.3 Overview of CUDA

This section presents an overview of the CUDA programming model and its main concepts and characteristics. For a more thorough and extensive explanation of this topic, the CUDA C Programming Guides [115], the source of the present review, should be consulted. A GPU is comprised by one or several streaming processors (or multiprocessor). Each of these processors contains several simpler processors, each of which execute the same instruction at the same time at any given time. In the CUDA programming model, the basic unit of computation is a *thread*. Threads are grouped into *blocks* which are part of the block *grid*. The number of threads in a block is typically higher than the number of processors in a multiprocessor. For that reason, the hardware automatically divides the threads from a block into smaller batches, called *warps*. This hierarchy is represented in Figure A.1. The computation of one block is independent from other blocks and each block is scheduled to one multiprocessor, which means that more multiprocessors results in more blocks being processed at the same time, as represented in Figure A.2.

Block configuration can be multidimensional, up to and including 3 dimensions. Furthermore, there is a limit in the amount of threads in each dimension that varies with the GPU being used, e.g. for GPUs with CUDA compute capability 2.x the maximum number of threads is 1024 for the x- or y-dimensions, 64 for the z-dimension, an overall maximum number of threads of 1024 and a warp size of 32 threads.

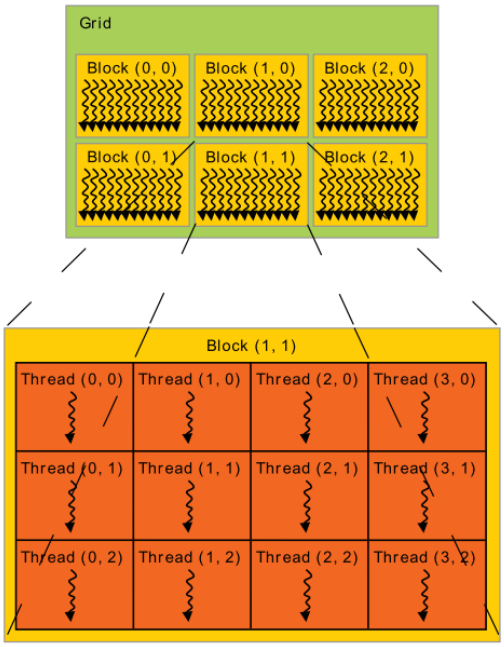

Figure A.1: Thread hierarchy [115].

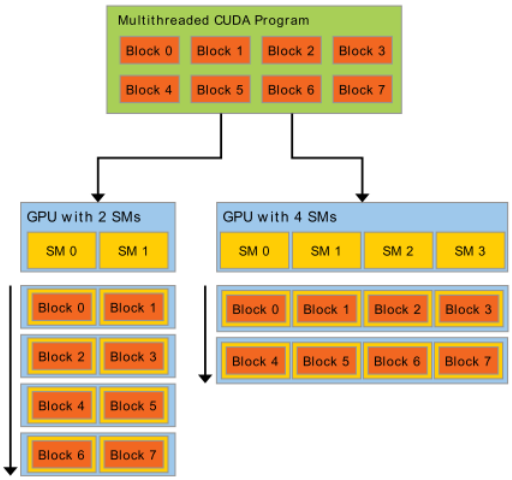

Figure A.2: Distribution of thread blocks is automatically scaled with the increase of the number of multiprocessors [115].

Instructions are issued per warp and registers and shared memory are allocated for an active block. A block will remain active until all threads have finished. When operands are not ready the warp is stalled and the context switches to another warp. Streaming processors have a limit to the maximum number of active warps, depending on the GPU. Choosing a block size is not trivial, as it is necessary to understand the characteristics of the kernel and the used GPU. The ratio between the number of active warps per multiprocessor and the maximum number of warps that can be active is called *occupancy* and a high occupancy is often used as a way to choose a good block size. The idea is to hide latency during global memory loads followed by thread synchronizations by maximizing the number of active warps, i.e. maximizing occupancy. Occupancy limiters include registers per thread, shared memory per block and threads per block. NVIDIA supplies a CUDA Occupancy Calculator to aid the programmer in tweaking block size, considering the other limiters.

Depending on the architecture, GPUs have several types of memories. Accessible to all cores (and threads) are the global memory, constant memory and texture memory, of which the last two are read-only. Blocks share a smaller but significantly faster memory called shared memory, which is a memory inside a multiprocessor to which all cores have access to, enabling inter-thread communication inside a block. Finally, each thread has access to local memory. Local memory resides in global memory space and has the same latency for read and write operations. However, if the thread is using only single variables or constant sized arrays, it uses register space, which is very fast. If the memory used exceeds the available register space the local memory used. This memory hierarchy is represented in Figure A.3.

The typical flow of a CUDA application (and, typically, any modern GPU application) is explained in this paragraph and can be observed in Figure A.4. First, the host CPU is responsible for several steps in the set-up phase. The host starts by transferring any necessary data to the device memory (global,

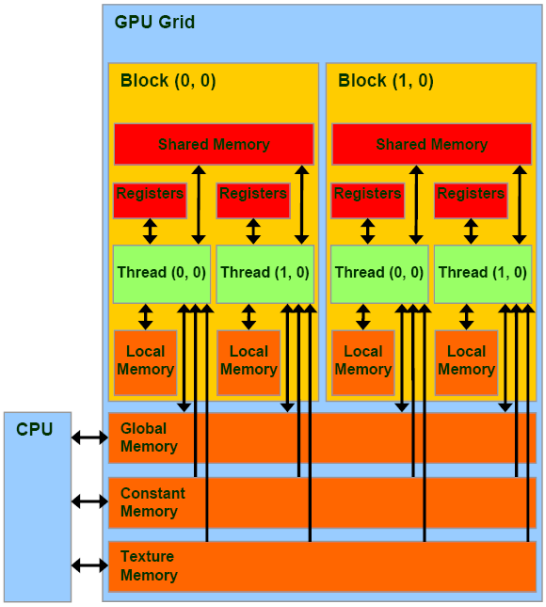

Figure A.3: Memory model used by CUDA [115].

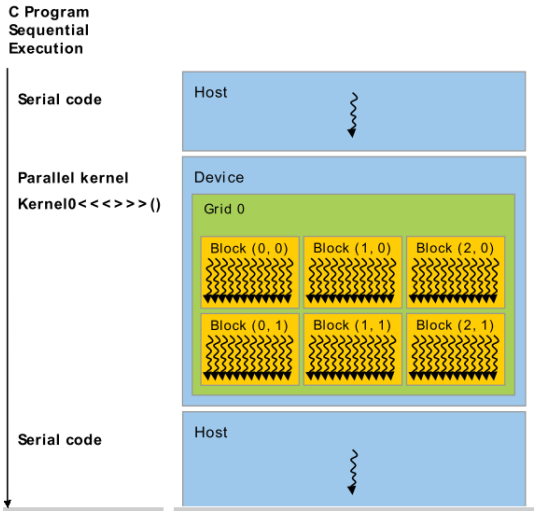

Figure A.4: Sample execution flow of a CUDA application [115].

texture or constant). The next step is selecting the *kernel* (the function that will run on the GPU) and the thread topology (configuration of threads in a block and blocks in the grid). The set-up phase is followed by the computation phase in the GPU. Finally, the host will transfer back the results from the device. It should be noted that the latest architectures support *Dynamic Parallelism*. This functionality allows the device to start other kernels without the intervention of the host CPU, which could alter the typical execution flow explained above. By using this functionality, kernels with data dependencies from other kernels would not require intervention from the host. Library calls and recursive parallel algorithms are also possible uses.